INSIGHTS INTO THE HUMAN FRAGILE X SYNDROME GENE FAMILY USING *DROSOPHILA MELANOGASTER*

By

Ronald Lane Coffee, Jr.

Dissertation

Submitted to the Faculty of the

Graduate School of Vanderbilt University

in partial fulfillment of the requirements

for the degree of

DOCTOR OF PHILOSOPHY

in

Biological Sciences

December, 2011

Nashville, Tennessee

Approved:

Professor Terry L. Page

Professor Kendal S. Broadie

Professor Joshua T. Gamse

Professor Laura A. Lee

Professor Donna J. Webb

To my amazing and infinitely supportive family

–

This work could not have been done without you

ACKNOWLEDGMENTS

I would first like to thank my advisor, Dr. Kendal Broadie, for his guidance and mentorship throughout my course of study. His unwavering enthusiasm for science and constant willingness to discuss and help guide my research endeavors have truly been an asset in completing this work. In addition to Dr. Broadie, I would like to especially thank Dr. Cheryl Gatto and Dr. Charles Tessier, post-doctoral research fellows in the laboratory, for all of their technical advice, guidance, and career brainstorming throughout the years. They both have served as fantastic co-mentors for me.

Next, I would like to thank the members of my dissertation committee for their helpful input and scientific advice: Drs. Terry Page, Joshua Gamse, Laura Lee, and Donna Webb. I appreciate their mentorship and insightful discussions throughout these past five years.

Throughout my graduate tenure, I have had the privilege of getting to know and working with exceptional people. I would like to thank all of the members of the Broadie Lab, both past and present, for their helpful advice and scientific training that they have provided in order to help me become a better scientist. It has not only been great working with these members, it has also been great spending time with them at dinners and social events. I would especially like to thank Neil Dani for his friendship. He has been a terrific support for the past two years as I have been physically separated from my partner due to our

relocation to Seattle. I have truly made a life-long friend. The complete list of great friends that I have made throughout my time in Nashville and at Vanderbilt is too numerous to all mention here. Know that I will remember all of you forever and appreciate you sharing your life with me.

Lastly, but certainly not least, I would like to thank the ever-abounding support and love of my family, including my mom (Robbie McAnally), step-father (Rudy McAnally), grandfather (Bob Campbell), and aunt (Donna Campbell). I would also like to thank my partner (Steve Cico) for his support and love. We initially met just prior to the start of my graduate school tenure. He has stood by my side throughout the entire busy and sometimes chaotic process/adventure. Words cannot express how much I appreciate and value him. Love you always, Steve.

TABLE OF CONTENTS

Page

DEDICATION ii

ACKNOWLEDGMENTS iii

LIST OF FIGURES vii

LIST OF ABBREVIATIONS ix

Chapter

I. INTRODUCTION 1

Mental Retardation 1
X-Linked Mental Retardation 2
Autism Spectrum Disorders 6
Synaptic Mechanisms Underlying Disease States 9
Fragile X Syndrome 14
The Fragile X Mental Retardation 1 (*FMR1*) Gene 15
Fragile X Mental Retardation Protein (FMRP) 18
Translational Control by Fragile X Mental Retardation Protein 23
Genetic Models of Fragile X Syndrome 25
Molecular Pathways Involved in Fragile X Syndrome 31
Hypothesis and Aims 33

II. FRAGILE X MENTAL RETARDATION PROTEIN HAS A UNIQUE, EVOLUTIONARILY CONSERVED NEURONAL FUNCTION NOT SHARED WITH FXR1P OR FXR2P 38

Abstract 38
Introduction 39
Results 45
Transgenic Constructs with Targeted Pan-Neuronal Expression 45
Only *FMR1* Restores Brain Protein Levels 48
Only *FMR1* Restores Brain Circuit Synaptic Architecture 51
Only *FMR1* Restores Neuromuscular Junction Synaptic Architecture 55
Human *FMR1*, *FXR1*, and *FXR2* All Restore Male Fecundity and Spermatogenesis 60
Discussion 65
Materials and Methods 73
Drosophila Stocks and Genetics 73

Molecular Techniques 73
Western Blot Analyses 76
Protein Extraction and Assay 76
Immunohistochemistry 77
Clock Neuron Analyses 78
Neuromuscular Junction Structural Analyses 78
Fecundity Measurements 79
Electron Microscopy 79
Statistics 80

III. IN VIVO NEURONAL FUNCTION OF THE FRAGILE X MENTAL RETARDATION PROTEIN IS REGULATED BY PHOSPHORYLATION ... 82

Abstract 82
Introduction 83
Results 87
Transgenic Constructs with Targeted Pan-Neuronal Expression 87
Only *S500D-hFMR1* Restores Brain Protein Translation Levels 90
Only *S500D-hFMR1* Restores Neuromuscular Junction Synaptic Architecture 94
Only *S500D-hFMR1* Restores Futsch/MAP1B Synaptic Cytoskeletal Loops 99
Only *S500D-hFMR1* Restores Brain Circuit Synaptic Architecture 102
Only *S500D-hFMR1* Restores Associative Learning 105
Discussion 107
Materials and Methods 116
Drosophila Stocks and Genetics 116
Generation of UAS-*hFMR1/S500A-hFMR1/S500D-hFMR1* 116
Western Blot Analyses 117
Protein Extraction and Assay 118
Immunocytochemistry 119
Neuromuscular Junction Analyses 120
Brain Circuit Analyses 120
Pavlovian Olfactory Learning 121
Statistics 123

IV. CONCLUSIONS AND FUTURE DIRECTIONS 124

REFERENCES 140

LIST OF FIGURES

Figure Page

1. Overview of Mental Retardation Causes 3
2. X Chromosome Causative MR Genes..... 5
3. Translational Regulation in Neurons..... 12
4. *FMR1* Gene and Its Product..... 17
5. dFMRP and hFMRP Protein Domain Comparisons..... 29
6. Model for FMRP Function..... 35
7. Generation of Transgenic Constructs with Targeted Neuronal Expression .. 46
8. Only *hFMR1* Rescues Elevated Protein Levels in the *dfmr1* Null Brain..... 50
9. Only *hFMR1* Rescues Clock Neuron Synapse Arbors in *dfmr1* Nulls..... 53
10. Only *hFMR1* Rescues Synapse Architecture in *dfmr1* Null Mutants..... 56
11. Only *hFMR1* Rescues Synapse Bouton Differentiation in *dfmr1* Nulls 58
12. All Three Human Genes Rescue *dfmr1* Mutant Male Fecundity..... 61
13. All Three Human Genes Rescue *dfmr1* Mutant Spermatogenesis Defects .. 63
14. Generation of Transgenic Constructs with Targeted Neuronal Expression .. 88
15. *S500D-hFMR1* Rescues Elevated Brain Protein Levels in *dfmr1* Null..... 92
16. *S500D-hFMR1* Rescues NMJ Synapse Architecture in *dfmr1* Null 96
17. *S500D-hFMR1* Rescues Synapse Bouton Differentiation in *dfmr1* Null 98
18. *S500D-hFMR1* Rescues Futsch/MAP1B Loops in *dfmr1* Null Synapse 101
19. *S500D-hFMR1* Rescues Central Brain Synapse Arbors in *dfmr1* Null 103
20. Only *S500D-hFMR1* Restores Olfactory Learning in *dfmr1* Null..... 106

21. Circadian Actograms of Control (w^{1118}) and *dfmr1* Null Animals..... 136

22. Polyribosomal Association Profile of w^{1118} Control Animals..... 138

LIST OF ABBREVIATIONS

AMPA	α-amino-3-hydroxy-5-methyl-4-isoxazole propionic acid
Arc	activity-regulated cytoskeleton associated protein
ASD	autism spectrum disorder
BC1	brain cytoplasmic RNA 1
BSA	bovine serum albumin
CaMKII	calcium-calmodulin-dependent protein kinase II
CC2	coiled-coil 2
cDNA	complementary DNA
CGG	cytosine-guanine-guanine repeat
CNV	copy number variant
CYFIP	cytoplasmic FMR1 interacting protein
dFMR1	*Drosophila* fragile X mental retardation gene 1
dFMRP	*Drosophila* fragile X mental retardation protein
Dicer	double-stranded RNA-specific RNase III
DLG	discs large
DmGluRA	*Drosophila* metabotropic glutamate receptor A
DNA	deoxyribonucleic acid
EM	electron microscopy
FMR1	fragile X mental retardation gene 1
FMRP	fragile X mental retardation protein

FXR1	fragile X-related gene 1
FXR2	fragile X-related gene 2
FXS	fragile X syndrome
FXTAS	fragile X tremor/ataxia syndrome
GFP	green fluorescent protein
GluR	glutamate receptor
hFMR1	human Fragile X mental retardation gene 1
hnRNP	heterogeneous nuclear ribonucleoprotein
HRP	horseradish peroxidase
I304N	isoleucine 304 asparagine
IQ	intelligence quotient
KH1/2	ribonucleoprotein K homology
KO	knockout
LI	learning index
LN_v	ventrolateral neurons
LTD	long-term depression
LTP	long-term potentiation
MAP1B	microtubule associated protein 1B
MB	mushroom body
MCH	4-methylcyclohexanol
mGluR	metabotropic glutamate receptor
MR	mental retardation
mRNA	messenger RNA

mRNP	messenger ribonucleoprotein
NES	nuclear export signal
NLS	nuclear localization signal
NMJ	neuromuscular junction
NP40	nonidet P40
NUFIP	nuclear FMRP-interacting protein
OCT	3-octanol
PBS	phosphate buffered saline
PDF	pigment dispersing factor
PSD95	post-synaptic density 95
RGG	arginine-glycine-glycine motif
RISC	RNA-induced silencing complex
RNA	ribonucleic acid
S500	serine 500
S500A	serine 500 alanine
S500D	serine 500 aspartic acid
S6K1	S6 kinase 1
SEM	standard error of the mean
sLNv	small ventrolateral neuron
UAS	upstream activation sequence
UTR	untranslated region
XLMR	X-linked mental retardation
ZT	zeitgeber time

CHAPTER I

INTRODUCTION

Mental Retardation

Determining the genetic causes of mental retardation (MR), and their intersection with environmental factors, is currently one of the greatest challenges in medical genetics. Recently, current practice has adopted using the euphemism “intellectual disability” when referring to MR (Rosa’s Law, 2010). However, intellectual disability is a much broader diagnosis and includes deficits that are too mild to qualify as mental retardation, or too specific, or acquired later in life due to injury or degenerative disease, rather than developmental delay. Therefore, I use the term MR [International Classification of Diseases, (ICD 317-319); Diagnostic and Statistical Manual of Mental Disorders, (DSM)] to define a developmental disability characterized by significant limitations in cognitive function and adaptive behavior, as expressed in conceptual, social, and practical adaptive skills, which manifests as a depressed developmental trajectory prior to 18 years of age (Chelly et al., 2006). MR consists of an intelligence quotient (IQ) <70, compared to the scaled average IQ in the general population of 100. The prevalence of MR in developed countries is 2-3% of the population (Leonard and Wen, 2002). On the basis of IQ, classification is divided into two main categories: mild MR with an IQ between 50-70 and severe MR with an IQ below 50. MR

causes are extremely heterogeneous and can result from environmental and genetic causes, or the intersection of the two factors (Fig. 1). MR environmental causes include prenatal exposure to toxic substances such as alcohol, environmental contaminants and infection. MR genetic factors include chromosomal abnormalities (numerical and partial chromosome duplications, and deletions) and monogenic disorders (autosomal dominant, autosomal recessive, X-linked) (Curry et al., 1997). Overall, however, the cause is known only in ~50% of cases with moderate to severe MR, and an even lower percentage of patients with mild MR. The higher prevalence of MR among male children is well known (Drews et al., 1995; Richardson et al., 1986). Males are 1.6 to 1.7 times more likely to experience both mild and severe forms of MR compared to their female cohorts. The relative risk in males for mild MR is 1.9 times greater than for severe MR (Croen et al., 2001). This sex differential shows that X-linked gene defects are a major cause of MR.

X-linked Mental Retardation

X-chromosome linked mental retardation (XLMR) is subdivided into syndromic (S-XLMR) and non-syndromic (NS-XLMR) forms, depending on whether further abnormalities (in addition to MR) occur in the patient (Lehrke, 1972; Ropers and Hamel, 2005). S-XLMR is amenable to conventional genetic mapping strategies because families sharing clinical symptoms can be pooled for linkage analysis to define candidate chromosomal intervals. In contrast, NS-XLMR is not associated with a specific set of clinical or metabolic symptoms and

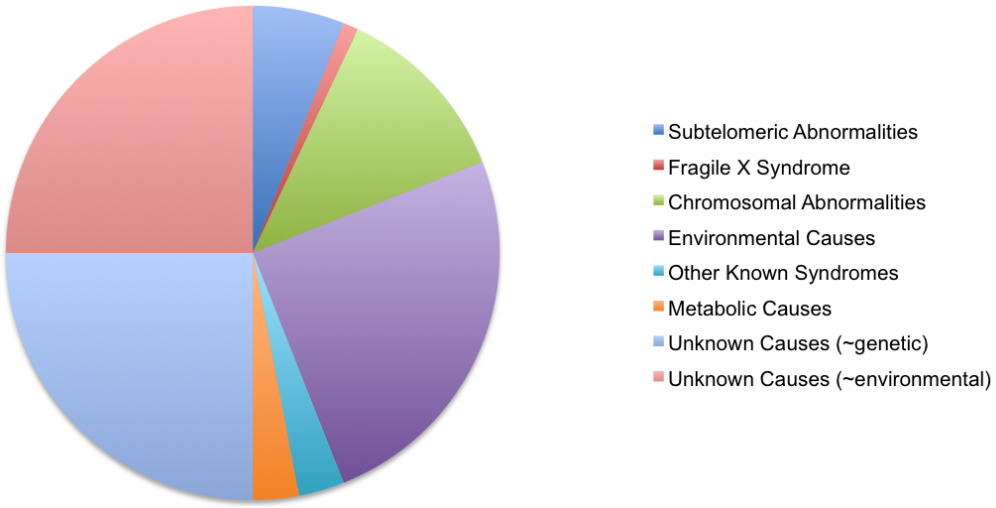

Figure 1. Overview of mental retardation causes. Chromosomal abnormalities (12%); Subtelomeric abnormalities (6%); Fragile X syndrome (1%); Other known syndromes (3%); Environmental causes (25%); Metabolic causes (3%); Unknown causes presumed to be genetic (25%); Unknown causes presumed to be environmental (25%). Figure adapted from (Winnepenninckx, et al., 2003).

generally exhibits high gene background heterogeneity (Chelly and Mandel, 2001). In this case, linkage results cannot be pooled, even from families in which MR genes map to overlapping regions, because these families might carry mutations in different genes. Around two-thirds of XLMR cases are thought to be non-syndromic (Fishburn et al., 1983) and therefore their molecular elucidation is extremely difficult. However, mutations in several XLMR genes can give rise to both non-syndromic and syndromic forms, indicating there is not a consistently reliable molecular basis for strictly distinguishing between S-XLMR and NS-XLMR (Ropers and Hamel, 2005). Genes implicated in NS-XLMR include *FMR2* (transcriptional regulator; long-term memory), *DLG3* (postsynaptic scaffolding protein) and *PAK3* (actin cytoskeleton regulator; neurite outgrowth) (Ropers, 2006). About 140 syndromic forms of XLMR have been described to date. In ~66 of these cases, the causative genetic defects have been identified, and in ~50 others, the underlying defect has been mapped to a specific region on the X chromosome (Ropers and Hamel, 2005). Genes involved in S-XLMR include *RSK2* (Coffin-Lowry syndrome; associated with mental impairment, cardiac and growth abnormalities), *MECP2* (Rett syndrome; Angelman and Prader-Willi-like phenotypes; associated with cognitive and developmental delay; jerky movements; hand-flapping), and *FMR1* (Fragile X syndrome (FXS); associated with mental retardation and autism) (Ropers, 2006). A more thorough summary of XLMR genes is shown in Fig. 2.

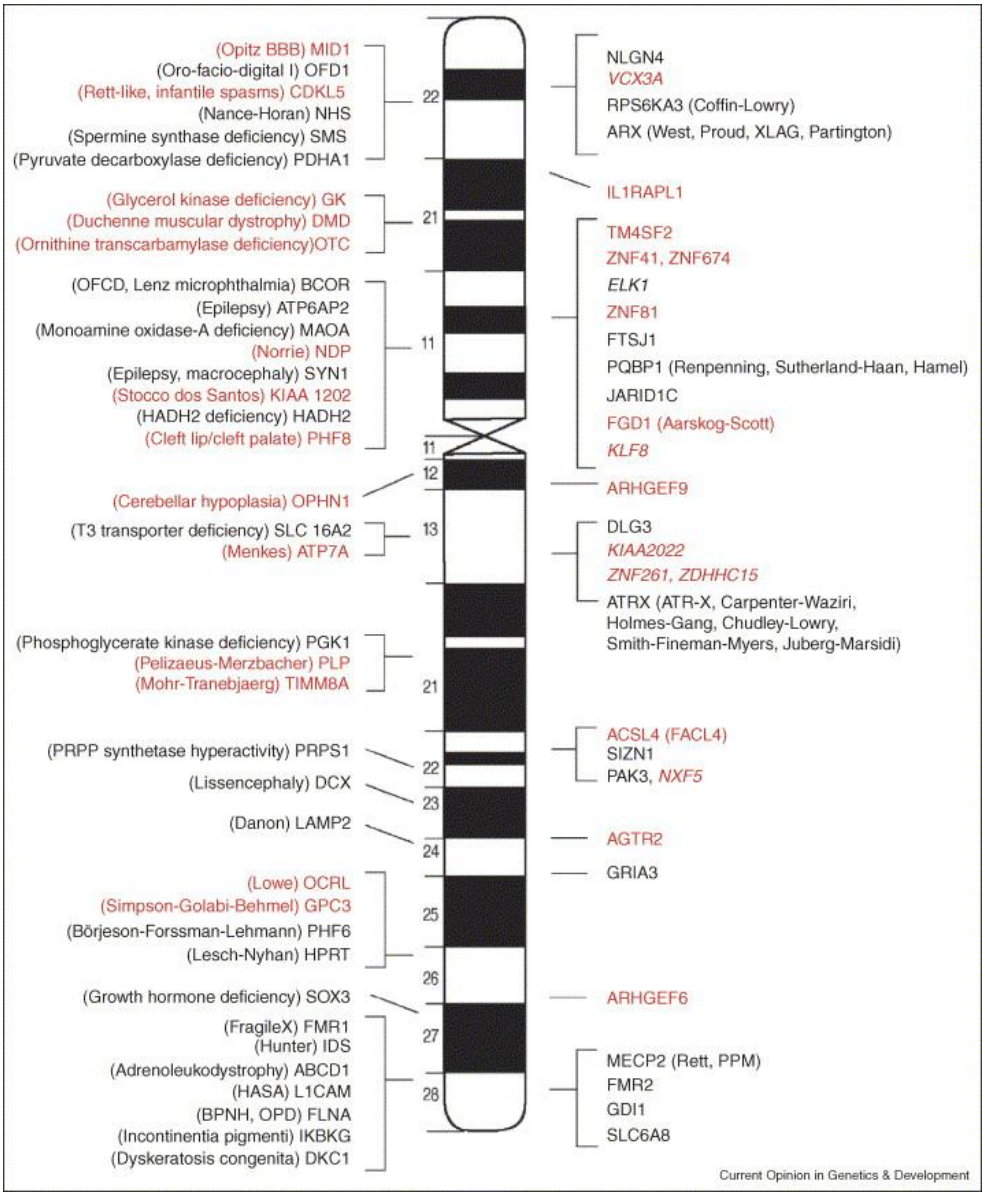

Figure 2. X chromosome causative MR genes. XLMR genes identified by mutation screening or by studying patients with chromosome rearrangements (in red). Italics denote candidate genes. Adapted from (Ropers, 2006).

Autism Spectrum Disorders

Autism spectrum disorder (ASD) was first described in the early 1940s by psychiatrists Kanner in the United States, reviewed in (Kanner, 1971) and Asperger in Austria (Asperger, 1944). ASD is a highly heterogeneous genetic disorder with heritability indices of 0.85-0.92 (Monaco and Bailey, 2001; Smalley et al., 1988). Findings from a comprehensive genetics evaluation have previously reported that a Mendelian chromosomal cause, or at least pre-disposition, occurs in 15-40% of children who fit the ASD behavioral diagnostic criteria (Schaefer and Mendelsohn, 2008). The Centers for Disease Control and Prevention have reported ASD diagnosis in the United States in 1/91 for 3-17 year old children (Kogan et al., 2009). Most epidemiological analyses indicate that the apparent 'autism epidemic' does not reflect a true increase in ASD incidence, but rather an increased awareness by both the public and medical establishment, leading to more complete case findings together with broadening of the diagnostic criteria (Shattuck, 2006a; Shattuck, 2006b).

ASD is clinically defined on the basis of three behavioral symptoms: 1) impairment in social interactions, 2) lack of communication and 3) the propensity for repetitive behavior (American Psychiatric Association. *Diagnostic and Statistical Manual of Mental Disorders*). Typically, autistic children do not seek or provide comfort to others, often ignoring others around them. Children with autism fail to develop friendships with peers and siblings, and reciprocal communication, through speech, gestures, or facial expressions, is impaired. Children usually do not recognize the concept that speech can be used to name

objects, request a toy or to engage others (Miles, 2011). ASD typically develops before the age of 3, and most ASD children are not diagnosed until after their second year of age when language delays become obvious. However, ASD onset is typically gradual: ~30% of ASD children have a 'regressive' onset in which they gradually lose language and become more distant (Miles, 2011). There is much debate on whether these children are normal and then become abnormal by some exogenous environmental exposure. However, the best evidence, including retrospective analysis, suggests the regressive course is genetically determined (Anderson et al., 2007; Lord et al., 2004; Stefanatos, 2008). Approximately 25% of children who fit the ASD diagnostic criteria between the ages of 2-3 subsequently begin to talk and communicate by the age of 7 and are able to function, at some level, in the regular school population. For the remainder, most have limited improvement with age, and continue to require parent, school and societal support throughout life (Seltzer et al., 2004).

Using medical genetic evaluation techniques, a genetic cause can be identified in 20-25% of children on the autism spectrum (Miles, 2011). For the remaining 75-80% of cases, there is no identified cause. Genetic causes of autism are classified as cytogenetically visible chromosomal abnormalities (~5%), copy number variations (CNVs) (10-20%), and single-gene disorders (~5%). Maternally derived 15q duplications of the imprinted Prader Willi/Angelman region are the most commonly observed chromosomal abnormalities associated with autism; detected in 1-3% of cases. These duplication events are mediated by unequal homologous recombination involving

clustered low copy repeats (Wang et al., 2008). The most common CNVs related to autism are 15q11.2-11.3 duplications and reciprocal 16p11.2 microdeletions and duplications, which are located at a hot spot of genomic instability caused by duplicated blocks of DNA, leading to unequal crossing over during meiosis (Fernandez et al., 2010; Shinawi et al., 2010). Most CNVs arise *de novo* and therefore cannot account for familiality. Often, when CNVs are inherited, they may be present in family members who are unaffected by autism, thus the causative effect is difficult to determine (Rutter). Surprisingly, many CNVs seem to be different in different families (Pinto et al., 2010). A number of single-gene disorders have been extensively studied and are used as ASD models, prominently including Fragile X, Rett and Timothy syndromes.

Fragile X syndrome (FXS) is the leading cause of both inherited MR and ASD (Heulens and Kooy, 2011). It is caused by expansion of a CGG trinucleotide repeat in the promoter region of the *FMR1* gene leading to hypermethylation and subsequent gene silencing (Verkerk et al., 1991). ~30% of Fragile X patients have autism co-morbidity (Bailey et al., 2008; Hagerman et al., 1986). Rett syndrome is one of the original DSM-designated pervasive developmental disorders, and the only one for which there is specific genetic etiology (Amir et al., 1999). Approximately 96% of Rett syndrome patients have mutations in the X-lined *MECP2* gene. Children often have a period of normal development followed by loss of language with stereotypic hand movements (Miles, 2011). Timothy syndrome is an autosomal dominant disorder caused by a mutation in

the *CACNA1C* calcium channel gene at 12p13.3, and is characterized by cardiac defects as well as autistic symptoms (Splawski et al., 2004).

Synaptic Mechanisms Underlying Disease States

At the junction between two neurons is a small gap, about 20 nm wide, which serves as a contact barrier between nerve cells. This physical gap, termed a “synapse”, is the site of communication from one neuron to another through secreted chemical signals, termed neurotransmitters. Synapse formation (synaptogenesis) is a critical stage in neural circuit assembly and synapse elimination (pruning) is a critical stage in neural circuit refinement. Synapses undergo both short- and long-lasting changes in structure/function (synaptic plasticity) that are critical for learning and memory (Steward and Schuman, 2001). Defects in synaptogenesis and synaptic plasticity are considered to be the leading causes of MR and autism (Costa-Mattioli et al., 2009). The role of synapses in these developmental brain disorders has been studied extensively in FXS (absence of FMRP; neurons develop abnormally long and immature dendritic spines; impaired functional plasticity) (Dolen et al., 2007), Rett syndrome (excess MeCP2 leads to excess synapses) (Chao et al., 2007) and tuberous sclerosis (mutated *TSC1/2* leads to excessive protein that alters synaptic cell signaling) (Ehninger et al., 2008). In ASD, mutations within the neuroligin gene family are associated with impaired synaptogenesis (Jamain et al., 2003).

One important aspect of synapse biology is local protein translation, with developmental signals, electrical activity and behavioral experience all inducing synthesis of specific proteins necessary for enduring synaptic modifications (Steward and Schuman, 2001). Proteins that are newly synthesized must be made from mRNAs that are synthesized as a consequence of new transcriptional activation or from mRNAs that are constitutively present (local translation control). For the former, signaling must occur from the distant synapse to the neuronal nucleus transcriptional machinery and back again (Steward and Schuman, 2001), a very challenging proposition. For the latter, there must be a mechanism for regulating translation locally via synaptic activity, which includes maintained repression of translation until the activity-dependent trigger occurs. Studies using protein synthesis inhibitors have revealed that transient periods of synaptic development/pruning, long-lasting forms of synaptic plasticity and behavioral regulation all require tight control of protein synthesis (Bailey et al., 1996; Davis and Squire, 1984; Schuman, 1999).

Synaptic plasticity, defined as alterations in the efficacy of synaptic transmission, has long been proposed to be the cellular basis for learning and memory (Bredt and Nicoll, 2003). Persistent changes in synaptic efficacy involve at least two phases; 1) an early phase (<1 hour) that is independent of new protein synthesis, and 2) a long-lasting late phase (hours to years) that is dependent on new protein synthesis (Richter and Klann, 2009). Long-term potentiation (LTP) and depression (LTD) refer to persistent increases or decreases in synaptic strength, respectively (Kandel, 2001). Most of the work on

LTP and LTD has been conducted in the hippocampus – the brain structure required for spatial memory consolidation (Richter and Klann, 2009). Ribosomes, translation factors and mRNA are present not only in neuronal cell bodies, but also in dendrites, dendritic spines, axonal growth cones and (debatably) mature axons, suggesting that local protein synthesis could aid in long-lasting synaptic plasticity and thus long-term behavior modifications without engaging transcriptional machinery (Steward and Schuman, 2001). Inhibition of translation initiation results in the abrogation of late LTP earlier than when transcription is inhibited, as induced by application of protein synthesis inhibitors (Banko et al., 2005; Bradshaw et al., 2003). These data suggest that local protein synthesis is a critically important component of multiple forms of long-lasting hippocampal synaptic plasticity.

Spatial control of translation is an important task that neurons must be able to accomplish due to their inherent architectural complexity and network of disperse synaptic connections (Darnell, 2011). Synapses must be able to locally alter and regulate their ‘strength’ in response to local cues using mechanisms of new protein synthesis. In order to locally regulate protein synthesis, mRNAs must be transported to the neuronal processes, and be translationally repressed during transport localization (Darnell, 2011; Martin and Ephrussi, 2009) (Fig. 3). It is thought that such mRNAs are recognized through *cis*-acting RNA elements, which are mainly found in untranslated regions (UTRs), primarily in the 3′-UTR (Andreassi and Riccio, 2009). These elements are variable in length and sequence and fold into distinct secondary structures that work as recognition

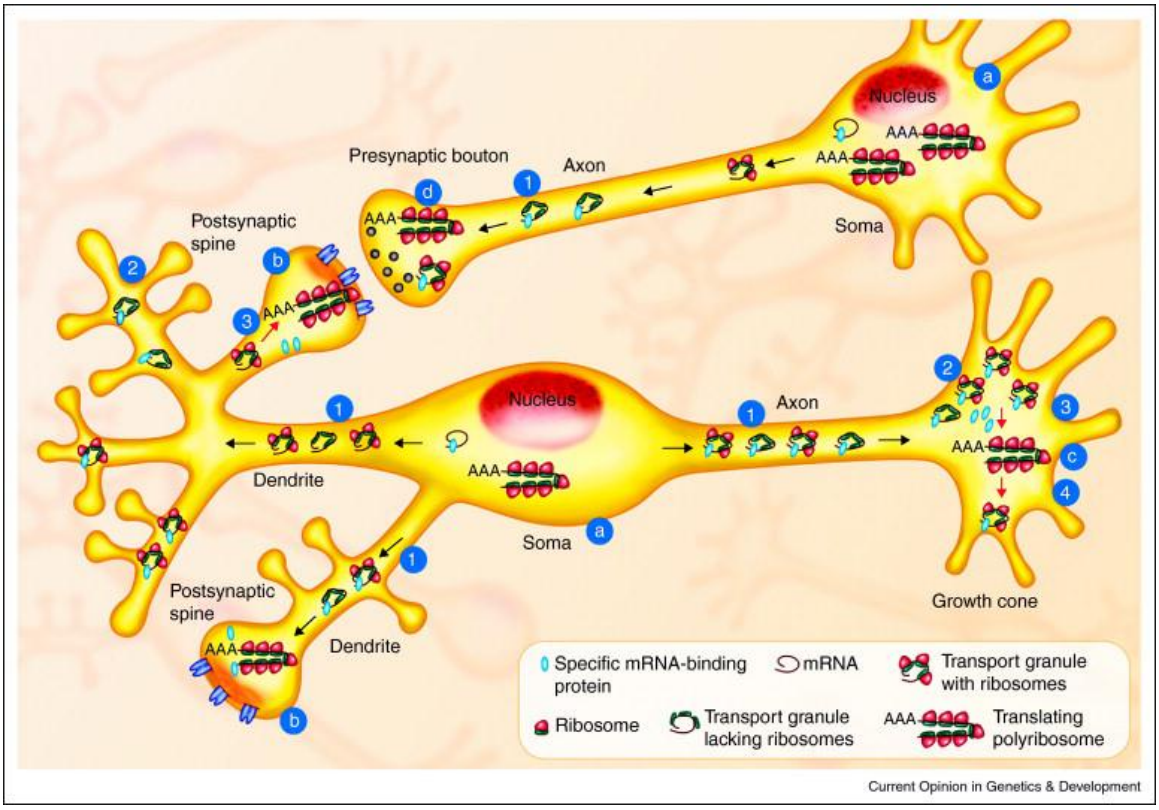

Figure 3. Translational regulation in neurons. While the soma was originally believed to be the site of all protein synthesis in the neuron **(a)** it is now clear that actively translating polyribosomes are present in and near the dendritic spines (the sites of postsynaptic excitatory input), **(b)**, in growth cones during development and regeneration after injury **(c)** and arguably on the presynaptic side of synapses **(d)**. Localized protein synthesis permits rapid changes in the local proteome but requires delivery of mRNA (black spirals) and synthetic machinery to the distant sites in the form of transport granules, with or without ribosomes (40S and 60S subunits are blue and red dots, respectively). The prevailing theory is that specific mRNA-binding proteins (light blue ovals) repress translation during transport **(1)** and maintain the mRNA in a repressed state until new protein synthesis is needed **(2)**. Mechanisms exist to activate the synthesis of specific proteins in the dendrites and growth cones **(3)**, and specific mechanisms halt their translation as well **(4)**. Adapted from (Darnell, 2011).

platforms for *trans*-acting RNA-binding proteins. Among the best-studied RNA-binding proteins is ZBP1, which binds the 3′-UTR of β-actin mRNA to drive its localization to axonal growth cones and dendrites (Zhang et al., 2001a). Other RNA-binding proteins with similar functions include Staufen (Mikl et al., 2011) and Fragile X Mental Retardation Protein (FMRP) (Zhang et al., 2001b). Following delivery to dendrites or axons, mRNAs are thought to be maintained in a repressed state until synaptic stimulation triggers activation of translation (Darnell, 2011). Translational regulatory initiation and elongation factors are regulated by phosphorylation, sequence-specific RNA binding proteins (RNABPs), and small non-coding RNAs (such as miRNAs) that regulate translation of a specific subset of mRNAs (Darnell, 2011).

The two primary pathways for signal transduction from neuronal receptors to these translation regulatory factors are the PI3K/Akt/mTOR and MAPK/ERK kinase cascades (Costa-Mattioli et al., 2009; English and Sweatt, 1997; Hoeffer and Klann, 2010; Lin et al., 2001). Both pathways affect initiation by phosphorylation of translation factor eIF4E binding proteins (4EBPs), causing their release from eIF4E to increase initiation. Inhibition of translation initiation can result from stimuli that cause eIF2α phosphorylation through kinase activation. Inhibition can also occur through the elongation phase, for example through synaptic glutamate receptor activation leading to eEF2 phosphorylation (Sutton et al., 2007). In addition to this critical translation control, remodeling of the synaptic environment can also be accomplished by the regulated degradation of proteins (Cajigas et al., 2010). Selective protein degradation provides a

mechanism to relieve inhibition and promote synaptic strengthening. Several reports have highlighted functions for the ubiquitin proteasome system (UPS) in synaptic development and plasticity (Haas and Broadie, 2008; Patrick, 2006; Patrick et al., 2003). The UPS attaches ubiquitin to lysine residues of specific protein substrates, which then triggers subsequent degradation of the ubiquitinated protein by the 26S proteasome. Thus, protein synthesis and degradation together provide a mechanism for fine-tuning protein availability locally in synapses, and this, in turn, leads to regulation of synaptic development and plasticity.

Fragile X Syndrome

In 1943, Martin and Bell first described a new form of X-linked MR, and two decades later, Lubs in 1969 chanced upon a chromosomal test identifying a fragile site on the X chromosome (Lubs, 1969). More than two decades after that, in 1991, the disease-causing *FMR1* gene was identified (Verkerk et al., 1991), followed quickly thereafter by a mouse model of the FXS disease (Bakker et al., 1994). Not long afterwards, in 2000, the *Drosophila* homolog to *FMR1* (*dFMR1*) was identified (Wan et al., 2000) and a fruit fly disease model generated by the Broadie Lab (Zhang et al., 2001b). FXS was initially described as non-syndromic but is now considered the most common type of syndromic XLMR (Ropers, 2006). FXS is a wide spectrum neurological disorder, and the most common inherited cause of MR and ASD (Hagerman, 2008). The prevalence for the population as a whole is ~1:5000 (Coffee et al., 2009). Approximately 33% of

FXS patients are co-morbid for ASD, while ~2-3% of autistic patients have co-morbidity with FXS (Rogers et al., 2001). Apart from the cognitive deficit hallmark, typical facial features such as an elongated face, protruding jaw line and enlarged ears characterize the syndrome. Elevation of birth weight in newborns, as well as macrocephaly in males commonly occur (Terracciano et al., 2005). These non-neurological signs testify that the FMRP also functions in non-neuronal tissues. The range of behavioral symptoms includes hyperactivity, obsessive-compulsive behaviors, sleep disorders, anxiety, and aggressive behavior (Chonchaiya et al., 2009). In about 20% of patients, epileptic seizures occur; however, typically decreasing with age (Musumeci et al., 1999). Mild to severe MR is the major phenotype of FXS. IQ in affected males ranges from 20-60, but MR symptoms in females tend to be milder (Terracciano et al., 2005; Visootsak et al., 2005). Post-mortem neuropathological studies have shown longer, immature postsynaptic dendritic spines in both temporal and visual cortical areas (Irwin et al., 2001). Compared with the normal mushroom-shaped mature dendritic spines, FXS patients display more elongated dendritic spines as well as increased spine density (Irwin et al., 2000). Multiple neural circuits must be impacted in order to contribute to the spectrum of FXS disease symptoms.

The Fragile X Mental Retardation 1 (*FMR1*) Gene

FXS normally arises as a consequence of a large expansion of a CGG trinucleotide repeat in the 5′ untranslated region of the *FMR1* gene (Oberle et al., 1991). In the general population, normal individuals carry a polymorphic CGG

triplet ranging from 5-54 (mean=30) repeats upstream of the *FMR1* gene. The abnormally high repeats (>200) in FXS patients lead to genomic hypermethylation and subsequent transcriptional silencing of the *FMR1* gene (Fig. 4). At the cytogenetic level, the expansion can be seen as a gap/break on the X chromosome at Xq27.3 (the “FRAXA site”) when fragile X cells are grown under folate-depleted conditions (Sutherland, 1977). Intermediate numbers of CGG repeats (50-200), referred to as the ‘premutation condition’, occur in disease carriers who are asymptomatic in regards to FXS, but can show at low frequency an unassociated late-onset ataxia (Hagerman and Hagerman, 2002). Transmission of premutated alleles to the next generation may result in changes in the number of repeats, either decreasing or increasing. In the case of transmission by the mother, an expansion to full mutation will occur in ~80% of the cases when the premutation repeat number is between 50-110 (Heitz et al., 1992; Yu et al., 1992). Repeat expansion from a premutation to a full-sized syndrome-causing mutation (>200) occurs in all tissues except the male germline (Bardoni et al., 2000). The rate of expansion into a full mutation depends on the size of the premutation; the smaller the premutation, the lower the chance of expansion. Males with the full mutation are always affected, whereas females carrying the mutation vary in phenotypic outcomes due to X-linked inactivation causing mosaicism (Wohrle and Steinbach, 1991). Male premutation carriers can develop a late-onset neurodegenerative syndrome called fragile X tremor/ataxia syndrome (FXTAS) (Hagerman et al., 2001). Conversely, female premutation carriers can develop fragile X-associated primary ovarian insufficiency (FXPOI)

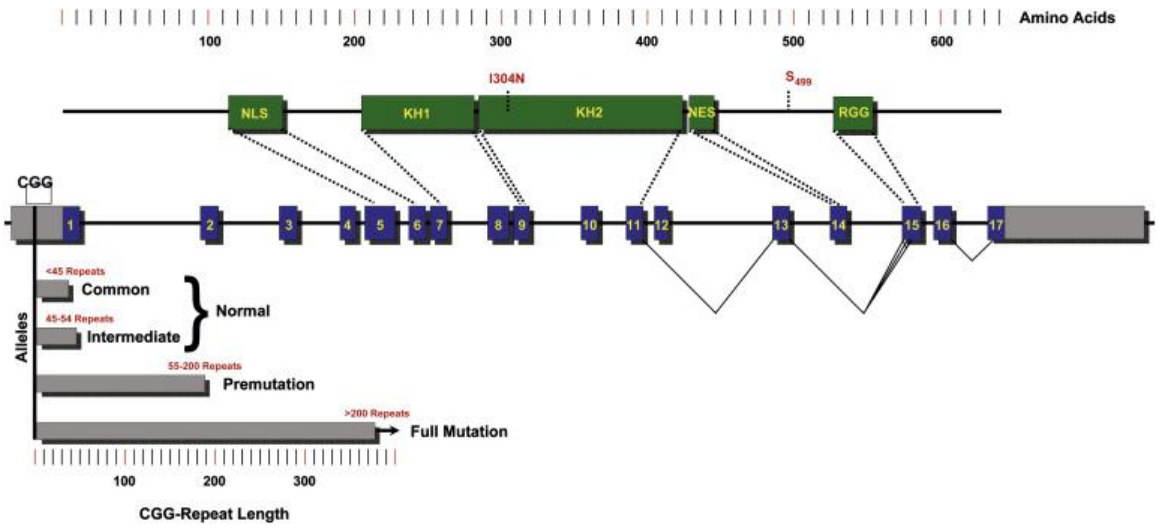

Figure 4. *FMR1* gene and its product. (Top) FMRP protein domains (green) and key residues (red). NLS, nuclear localization signal; KH1 and KH2, RNA-binding domains; NES, nuclear export signal; RGG, RGG box, RNA-binding domain. I304N is a naturally occurring FXS mutation abrogating polysome association; murine S499 is the primary phosphorylated serine. (Middle) *FMR1* gene, coding exons (blue) and untranslated regions (gray). Exons coding for major protein domains are indicated, as well as alternative splicing. (Bottom) 5′ untranslated CGG-repeat alleles. The common and intermediate normal alleles (<55 repeats) are indicated, as are the premutation carrier alleles (55–200 repeats) and the full-mutation FXS alleles (>200 repeats). Adapted from (Bassell and Warren, 2008).

(Vianna-Morgante et al., 1996). Only a few cases of sporadic FXS, without the CGG repeat expansion, have been reported (de Vries et al., 1998). In all these cases, either deletion within or around the *FMR1* locus, or missense point mutations in the *FMR1* coding sequence, confirm a causative role for loss of the *FMR1* gene in FXS. Available treatments inadequately target only a subset of disease symptoms, so there is a pressing need for research into the genetic and neurobiological basis of this disease.

Fragile X Mental Retardation Protein (FMRP)

FMRP appears fairly ubiquitously expressed in all tissues, albeit with particularly high expression in neurons (Verheij et al., 1993). The gene spans ~40 kb and encodes a full length mRNA of 3.9 kb. The gene is composed of 17 exons and its transcript is subjected to extensive alternative splicing (Ashley et al., 1993) (Fig. 4). *FMR1* gene expression has been studied by *in situ* RNA hybridization in a variety of human and murine tissues. Widespread and strong expression was observed in early mouse embryos, while in successive stages of development, the levels of expression diminished and became more localized in tissues (Bakker et al., 1994). FMRP can be up to 632 amino acids long and has five defined functional domains: three types of RNA-binding domains (Siomi et al., 1993; Zanotti et al., 2006), namely two K Homology (KH) domains in the middle region of the protein (KH1, KH2; KH=heterogeneous nuclear ribonucleoprotein K homology) and an RGG box in the C-terminal region (containing repeats of an Arg-Gly-Gly motif); a non-classical nuclear localization

signal (NLS); and a nuclear export signal (NES) (Eberhart et al., 1996). FMRP also has two predicted coiled-coil domains important for protein-protein interactions.

Only three pathological point mutations have been reported in the *FMR1* gene. An I304N missense mutation affecting the KH2 RNA binding domain was found in a single patient with unusually severe FXS symptoms (De Boulle et al., 1993). KH domain functions in other proteins range from mRNA splicing to mRNA localization to translational control. It was suggested that this mutation might cause a dominant negative effect, by affecting the structure of the messenger ribonucleoprotein (mRNP) complexes containing FMRP (Darnell et al., 2005). Two truncating mutations resulting in absence of FMRP were detected in another study (Coffee et al., 2008). The RGG box binds a G-quartet structure present in many FMRP mRNA targets (Darnell et al., 2001). In other proteins, RGG boxes have been shown to mediate RNP formation. FMRP also binds non-coding adaptor RNAs, microRNAs and components of the RNA-induced silencing complex (RISC) (Jin et al., 2004; Zalfa et al., 2005). In the brain, FMRP mRNP complexes associate in an mRNA-dependent manner with actively translating polyribosomes (Khandjian et al., 1996; Tamanini et al., 1996), where FMRP acts as a negative translational regulator of target mRNAs (Laggerbauer et al., 2001; Sung et al., 2003). In mouse microarray screens, immunoprecipitated FMRP associates with ~4% of total brain mRNAs (Darnell et al., 2001), although there is growing evidence that this number is likely a gross exaggeration of the number of *in vivo* targets. Recent work to define FMRP RNA targets has been conducted

using high-throughput sequencing of RNAs isolated by crosslinking immunoprecipitation (HITS-CLIP) from the mouse brain (Darnell et al., 2011). The brain polyribosome-programmed translation system developed in this study reveals that FMRP reversibly stalls ribosomes during translation elongation of target mRNAs. The results suggest that loss of the FMRP translational “brake” on the synthesis of a subset of synaptic proteins is the causative defect in FXS (Darnell et al., 2011). Overlap between the FMRP targets identified and the current list of autism susceptibility genes and loci sheds light on common pathways between the two disease states, supporting the hypothesis that synaptic dysfunction is critical to the development of autistic features common to FXS and ASD (Kelleher and Bear, 2008).

FMRP has been predicted to shuttle between the nucleus and cytoplasm. However, conventional methods do not usually show any detectable FMRP in the nucleus, although faint nuclear localization has been reported using both light and electron microscopy (Feng et al., 1997; Verheij et al., 1993). These reports conclude that <5% of the total FMRP is localized in the nucleus under normal conditions. Cells that have been treated with leptomycin B, which blocks mRNA export, reportedly weakly retain FMRP in the nucleoplasm; however, in all cases, the vast majority of FMRP protein is still localized in the cytoplasm (Tamanini et al., 1999). Supporting nuclear localization, FMRP reportedly interacts with a distinct set of nuclear proteins including nucleolin and the nuclear FMRP-interacting protein (NUFIP) (Bardoni et al., 1999). In the nucleus, one role of FMRP could be to associate with target mRNAs and escort them out of the

nucleus (Eberhart et al., 1996). A mutated form of FMRP, I304N in the KH2 domain, reportedly shuttles more frequently between the nucleus and the cytoplasm, which may indicate either that many domains are involved in nuclear import and export, or that bound mRNA slows the transport/shuttling process or makes re-entry into the nucleus more difficult (Tamanini et al., 1999). A second possible role for FMRP in the nucleus could be chromatin remodeling. *In vitro*, FMRP strongly binds single-stranded DNA (Dejgaard and Leffers, 1996). Mammalian FMRP has been shown to interact with a mammalian Argonaute protein (eIF2C2), and three components bound together (FMRP, Argonaute, and miRNAs) have also been detected where RNAi-mediated pathways operate (Matzke and Birchler, 2005).

Translation in neurons involves the transport of some mRNAs away from the cell body and local protein synthesis in dendrites and possibly axons (Steward and Schuman, 2003). Several lines of evidence suggest that FMRP has an active role in this mRNA transport, although there is no direct evidence that it is required for the transport process *per se*. FMRP and its mRNA are found in both the cell body and, at a much lower level, bound in a detectable granule in dendritic processes, including dendritic spines. In dendrites and spines, FMRP and *FMR1* target mRNA co-localize in large, mobile granules (Zalfa et al., 2006), and the movement of these granules into dendrites is enhanced by neuronal signaling through metabotropic glutamate receptors (mGluRs). One target of *FMR1* regulation is its own message, forming an activity-regulated negative feedback loop (Bagni and Greenough, 2005). FMRP is translated in unstimulated

synaptoneurosomes (a synaptic fraction containing pre- and postsynaptic termini; the presynaptic compartment contains the synaptic vesicles and the postsynaptic compartment contains the translational machinery) as well as in response to mGluR stimulation (Weiler et al., 1997). It is feasible to hypothesize that FMRP is translated locally at the synapse and not during the transport process. In the end, both *FMR1* message and FMRP are transported in granules to locations throughout the dendrite, where translation of mRNA is regulated by synaptic activation. In the absence of FMRP, mGluR activation does not trigger increased protein synthesis in synaptoneurosomes (Weiler et al., 1997).

Using immunoprecipitation, two-hybrid screens and mass spectrometry analysis, several groups have identified proteins that interact with FMRP (Darnell et al., 2005; Darnell et al., 2011; Reeve et al., 2008). A few examples of these interactors include nucleolin, 82-FIP, RanBPM, Dicer, FXR1P/2P, and eIF2C2/AGO1. Most of the interacting proteins bind with the amino terminal portion of FMRP. The only protein that has been found to interact with the FMRP C terminus is RanBPM (Menon et al., 2004; Nakamura et al., 1998). The 82 kDa FMRP-interacting protein (82-FIP) is found in both the nucleus and cytoplasm (Bardoni et al., 2003). It shows no homology to proteins of known function, and contains no defined functional domains. It is found in most neurons and its subcellular distribution is cell-cycle dependent in COS cells, indicating that the composition of some FMRP-containing mRNP complexes might be cell cycle modulated. Interestingly, none of the proteins that interact with FMRP have yet to be associated with a disease state, and none of the genes that encode FMRP-

interacting proteins have, so far, been linked to hereditary MR. FMRP binds to RNA homopolymers and to a subset of transcripts found in the brain (Brown et al., 2001; Chen et al., 2003; Zalfa et al., 2003). Four mechanisms of RNA target recognition have been suggested: i) recognition of G-quartet secondary RNA structure (Darnell et al., 2001), or ii) a poly (U) stretch in the mRNA (Brown et al., 1998); iii) FMRP binding indirectly to the mRNA through either a small non-coding RNA brain cytoplasmic RNA 1 (BC1) (Iacoangeli et al., 2008) or iv) through miRNAs (Edbauer et al., 2010). BC1 RNA is predicted to base pair to neuronal mRNAs that encode molecules that are important for synaptic structure and function, such as MAP1B (microtubule associated protein 1B) mRNA (Iacoangeli et al., 2008). It has been shown that human FMRP associates with miRNAs, which inhibit mRNA expression (Duan and Jin, 2006). FMRP could contribute to this regulatory pathway by stabilizing the specific annealing between miRNAs and the complementary region in the 3′ untranslated region of the target mRNAs. The learning and memory difficulties that are found in patients with FXS are widely attributed to alterations in mRNA metabolism regulating synapse structure and function.

Translational Control by Fragile X Mental Retardation Protein

FMRP is an RNA-binding protein that associates with many mRNAs encoding proteins important for synaptic development and plasticity (Darnell et al., 2001). FMRP controls dendritic mRNA localization (Dictenberg et al., 2008), stability (D'Hulst et al., 2006) and translational efficiency of dendritic mRNAs in

response to stimulation of mGluRs (group 1 metabotropic glutamate receptor) (Napoli et al., 2008), and likely other cell surface receptors. In neurons, FMRP is packaged into messenger ribonucleoprotein (mRNP) particles that contain several other proteins involved in translation control (Staufen, eIF4E, ribosomal proteins), as well as cytoskeleton dynamics (tubulin, Rac1, CYFIP) and motor transport (dynein, kinesins) (Brendel et al., 2004; Kanai et al., 2004; Napoli et al., 2008). The range of FMRP regulatory targets is famously uncertain, however some consensus targets have emerged in recent years. αCaMKII (Ca^{2+}/calmodulin-dependent protein kinase and Arc (activity-regulated cytoskeleton-associated protein) are proposed FMRP translation regulatory targets, synthesized *de novo* in response to neuronal activity and critical for synaptic plasticity (Kanai et al., 2004; Kao et al., 2010; Krueger et al., 2011; Park et al., 2008).

The molecular mechanism by which FMRP controls translation has been investigated by assessing the polysome/mRNP distribution of the FMRP-containing complex (Ceman et al., 2003). FMRP has been shown to co-sediment with polyribosomes (Stefani et al., 2004), and its phosphorylation state is a critical determinant of polyribosome association (Ceman et al., 2003). FMRP has also been shown to co-sediment equally between polyribosomes and non-translating mRNP fractions (Brown et al., 2001). Yet other findings suggest that FMRP primarily associates with the mRNP fraction (Napoli et al., 2008; Zalfa et al., 2003), perhaps indicating repression at the initiation step. FMRP may inhibit translation at initiation through an interacting factor, CYFIP1 (cytoplasmic FMRP-

interacting protein 1) (Napoli et al., 2008), which associates the cap-binding factor eIF in mRNP fractions. The same study also suggested that CYFIP1 is important in the FMRP-regulatory circuit: an increased level of proteins encoded by known FMRP target mRNAs was seen upon reduction of CYFIP1 in neurons. An alternative model for how FMRP represses translation suggests that CYFIP1 would be tethered to FMRP as well as to eIF4E (Napoli et al., 2008). By binding eIF4E, CYFIP1 would exclude eIF4G and, indirectly, the 40S ribosomal subunit from associating with mRNA. In this model, a synaptic activity trigger would release CYFIP1 from eIF4E to allow translation initiation (Napoli et al., 2008). Another FMRP binding partner, brain cytoplasmic RNA 1 (BC1), a non-coding RNA, increases the affinity of FMRP for the CYFIP1-eIF4E complex in brain (Napoli et al., 2008). It has been clearly demonstrated that FMRP negatively regulates translation both in the mouse and in the *Drosophila* models of FXS (Coffee et al., 2010; Qin et al., 2005).

Genetic Models of Fragile X Syndrome

There are two well-established animal models of FXS: in the mouse and the fruit fly. The *FMR1* knockout (KO) mouse (Bakker et al., 1994) was reported first in 1994, while the *Drosophila* KO model was reported in 2001 (Zhang et al., 2001b). The mouse *FMR1* KO model displays relatively very mild learning/memory impairments, but better recapitulates other FXS behavioral symptoms including hyperactivity and seizures in response to audiogenic stimuli (Qin et al., 2011). Neither FXS patients nor *FMR1* KO mice have gross brain

defects; however, individual neuronal structure displays aberrant dendritic structural phenotypes, e.g. expanded dendritic arbors and immature dendritic spines in both patients and model (Hinton et al., 1991). In normal development, an overproduction of spines is followed by a period of activity-dependent pruning. One possibility is that *FMR1* KO mice fail to normally prune these synaptic processes. Such defects in dendritic spine pruning vs. maturation may indicate that FMRP regulates experience-dependent synaptogenesis and synapse stabilization (Braun and Segal, 2000; McKinney et al., 2005). While basal synaptic function appears relatively normal in mutant mice, hippocampal long-term depression (LTD) dependent on activation of mGluRs is selectively enhanced (Bear et al., 2004). LTD is one of the mechanisms that contribute to learning and memory in the brain by triggering long lasting synaptic modifications, especially activity-guided synapse elimination (Costa-Mattioli et al., 2009). Mouse studies also show a clear role for FMRP in the axonal growth cone, presynaptic terminal and in presynaptic signaling (Christie et al., 2009; Deng et al., 2011). Mouse *FMR1* KO brains have reduced overall levels of mRNA granules, interpreted as a reduced number of translationally silent polyribosomes (Aschrafi et al., 2005).

A CGG trinucleotide repeat mouse has also been generated in an attempt to better understand the timing and mechanism involved in the *FMR1* CGG repeat instability, expansion and methylation state (Bontekoe et al., 2001). The endogenous repeat was replaced with a human CGG repeat carrying 98 units. Showing mild instability upon maternal transmission, the length has since been

expanded to 230 repeats. Disappointedly, methylation of the CpG islands still remains absent even though the repeat number is >200, as in the full mutation human disease condition (Bontekoe et al., 2001). This mouse model does not exhibit FXS phenotypes, but rather FXTAS, with levels of mRNA elevated and FMRP levels decreased, just as in the FXTAS premutation condition (Brouwer et al., 2008; Brouwer et al., 2007). Therefore, either more repeats or other genetic manipulation are necessary in order to model FXS with a CGG full mutation expansion in mouse. One very recent body of work investigates the effects of FMRP ablation in adult neural stem cells and demonstrates the disruption of hippocampus-dependent learning (Guo et al., 2011). This work investigated the function of FMRP expression in neural stem and progenitor cells and its role in adult neurogenesis (Deng et al., 2010b). Removal of FMRP in these cells by inducible gene recombination leads to reduced hippocampal neurogenesis *in vitro* and *in vivo*, as well as impaired hippocampal-dependent learning in mice. Restoration of FMRP expression specifically in these neural stem cells rescues learning defects in FMRP-deficient mice. Therefore, this work suggests that adult neurogenesis may contribute to the learning impairment seen in FXS, and these learning deficits can be corrected by delayed restoration of FMRP specifically in the neural stem and progenitor cells (Guo et al., 2011).

The *Drosophila* FXS model was established by an imprecise P-element excision to produce a series of *dfmr1* null mutants (Zhang et al., 2001b). Since then, an array of additional *dfmr1* alleles and transgenes has been created to facilitate FXS research in this model (Lee et al., 2003; Morales et al., 2002).

Drosophila FMRP (dFMRP) displays close homology with mammalian FMRP, including conserved structure, RNA-binding properties, tissue and subcellular expression patterns, and a conserved functional role as a negative translational regulator (Wan et al., 2000; Zhang et al., 2001b) (Fig. 5). Importantly, however, the *Drosophila* genome contains only a single *FMR1* gene, whereas vertebrate genomes contain three highly related genes: *FMR1* and two associated paralogs (Fragile X-related genes 1 and 2; *FXR1*, *FXR2*). dFMRP may regulate translation via the miRNA pathway: dFMRP associates with the RISC complex (Caudy et al., 2002; Ishizuka et al., 2002), and *dfmr1* mutants interact genetically with the RISC pathway (Jin et al., 2004), which modulates synaptic protein synthesis required for memory formation in *Drosophila* (Ashraf et al., 2006). Null *dfmr1* mutants exhibit reduced motor coordination (Xu et al., 2004; Zhang et al., 2001b), irregular circadian activity levels (Dockendorff et al., 2002; Inoue et al., 2002), and defective learning and memory (Bolduc et al., 2008; Dockendorff et al., 2002). Male *dfmr1* flies also display enlarged testes, and spermatogenesis and fecundity defects (Coffee et al., 2010; Zhang et al., 2004), while females display oogenesis defects (Costa et al., 2005), as in the human disease state. dFMRP is a negative regulator of growth, branching and synaptic differentiation in many neural circuits including motoneurons at the neuromuscular junction (NMJ) (Coffee et al., 2010; Gatto and Broadie, 2008; Zhang et al., 2001b), peripheral sensory neurons (Lee et al., 2003) and multiple classes of central brain interneurons (Michel et al., 2004). In the mushroom body (MB) learning and memory brain center, individual Kenyon Cell neurons display over-elaborated

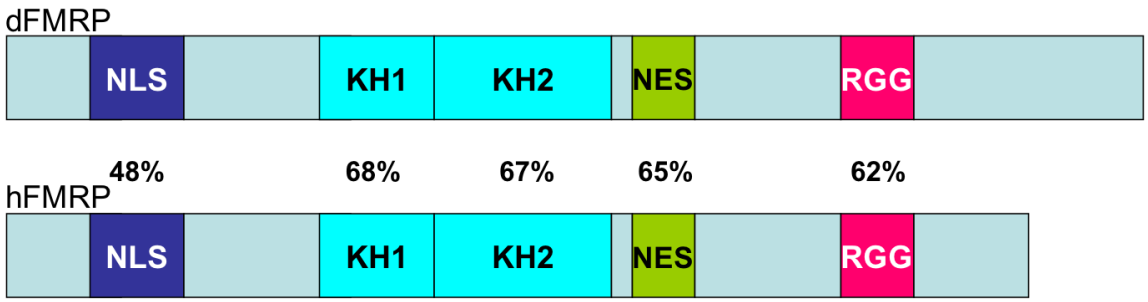

Figure 5. Protein domain comparisons. *Drosophila* FMRP (dFMRP; top) shares functional domain conservation and a high level of homology with human FMRP (hFMRP; bottom). Overall there is 56% peptide similarity. dFMRP is 681 amino acids in length while hFMRP is 632 amino acids in length.

axonal and dendritic structural development (Michel et al., 2004). In addition, circadian activity is controlled by the well-defined clock circuitry, in which the small ventrolateral (sLN_v) neurons are sufficient for pacemaker activity (Grima et al., 2004). In these cells, null *dfmr1* mutants display an over-elaborated synaptic bouton array that extends well beyond the normal termination points (Coffee et al., 2010; Gatto and Broadie, 2009).

Molecular mechanisms of dFMRP function have been dissected by dFMRP immunoprecipitation and genetic interaction studies (Broadie and Pan, 2005). To date, dFMRP is known to regulate six mRNAs: i) *futsch*, encoding MAP1B, which regulates microtubule dynamics (Zhang et al., 2001b). Genetic studies demonstrate that misregulation of *futsch* translation is a primary cause of synaptic structure-function defects in *dFMR1* mutants. ii) Rac1 (Ras-related C3 botulinum toxin substrate); genetic evidence suggests that dFMRP down-regulates Rac1 translation. Through regulation of Rac1 and cytoplasmic FMRP interacting protein (CYFIP/Sra-1), dFMRP plays a key role in modulating the actin cytoskeleton during neuronal morphogenesis (Schenck et al., 2003). iii) *chickadee*, encoding actin-binding profilin (Reeve et al., 2005). Profilin regulates actin dynamics/stability and its misregulation in *dfmr1* mutants is a primary cause for structural defects (Tessier and Broadie, 2008). iv) *pickpocket1*, encoding a Degenerin/Epithelial Sodium Channel (DEG/ENaC) subunit; genetic evidence suggests dFMRP represses Pickpocket1 expression in an argonaute1-dependent mechanism, confirming a role in the miRNA pathway (Xu et al., 2004). More recently, work from our laboratory has shown that dFMRP regulates mRNA

expression of several calcium-binding proteins, including Frequenin 1/2, Calmodulin and Calbindin (Tessier and Broadie, 2011). Taken together, these RNA targets strongly suggest that actin/microtubule cytoskeleton regulation, in addition to calcium signaling regulation, are primary components of dFMRP function mediating synaptic processes.

Molecular Pathways Involved in Fragile X Syndrome

Huber and Bear famously first reported that hippocampal postsynaptic group 1 class 5 metabotropic glutamate receptor (mGluR)-mediated LTD, a specific form of protein synthesis-dependent synaptic plasticity, is elevated in *Fmr1* KO mice (Huber et al., 2002). LTP remains normal in the hippocampus, but defective in the neocortex (Wilson and Cox, 2007). mGluR-LTD requires rapid translation of pre-existing mRNA and stimulates loss of surface expressed synaptic AMPA and NMDA receptors via recycling pathways. Activation of $mGluR_5$ also regulates trafficking of AMPA GluRs (Nosyreva and Huber, 2005). Thus, the mGluR theory of FXS states that dysregulated $mGluR_5$ centrally contributes to the pathology of FXS (Bear et al., 2004). The theory further suggests that mGluR activation normally stimulates synthesis of proteins involved in stabilization of LTD, and FMRP functions as a negative translational regulator that puts a brake on LTD.

It has also been proposed that the phosphorylation of FMRP on a specific serine residue switches the protein to an activated state (association with stalled polyribosomes) in which it can then proceed as a translational repressor (Ceman

et al., 2003). Subsequent release from stalled polyribosomes onto actively translating polyribosomes has been proposed to occur through a switch to the dephosphorylated state. Further reports demonstrate that dephosphorylation of FMRP leads to synapse loss through acute postsynaptic translational regulation (Pfeiffer and Huber, 2007). Induction of mGluR-LTD is proposed to be caused by an increase in synaptic stimulation as well as iontotropic glutamate receptor (GluA) endocytosis (Gladding et al., 2009). Reduced levels of FMRP lead to increased $mGluR_5$-mediated GluA endocytosis in rat hippocampal neurons (Nakamoto et al., 2007). Treating *Fmr1* KO mice with the $mGluR_5$ antagonist, MPEP (blocks $mGluR_5$ activity), can increase habituation in open field tests, decrease sensitivity to audiogenic seizures (Yan et al., 2005), and rescue courtship learning and memory defects in *Drosophila* (McBride et al., 2005). Work in *Drosophila* demonstrates that dFMRP protein expression is upregulated in *DmGluRA* mutants, removing the sole *Drosophila* mGluR (Pan et al., 2008). Conversely, DmGluRA is upregulated in *dfmr1* mutants, demonstrating mutual negative feedback. This work further shows that *DmGluRA* nulls display defects in coordinated movement, which are rescued by the removal of dFMRP. Further, blocking of mGluR signaling alleviates the NMJ structural overgrowth and the elevation of presynaptic vesicle pools in the *dfmr1* mutant (Pan et al., 2008). The data in this study suggest that DmGluRA and dFMRP convergently regulate neuronal presynaptic properties. Therefore, development of antagonistic drugs targeting mGluRs could prove to be a promising therapeutic strategy for the

treatment of FXS and is currently being investigated by pharmaceutical companies.

Another synapse class suggested to be dysregulated in FXS is the GABAergic inhibitory pathway (Centonze et al., 2007). *Fmr1* KO mice show loss of GABAergic inhibition (Gross et al., 2011). Impaired GABAergic signaling in FXS might be caused by decreased expression of GABA receptors (D'Hulst et al., 2006). $GABA_AR$ subunit mRNA and protein levels are decreased in both mouse and *Drosophila* FXS models, thus suggesting that FMRP contributes to the stability and/or translation of $GABA_AR$ transcripts (D'Hulst et al., 2009; Gantois et al., 2006). GABA administration in the *Drosophila* FXS model blocks glutamate toxicity, and rescues Futsch over-expression, neuronal overgrowth defects and memory impairment (Chang et al., 2008), as well as neuronal hyper-excitability (Olmos-Serrano et al., 2010). Impaired GABAergic signaling could also be the result of the dysregulation of mGluRs, as there is crosstalk between these two receptor types in several different brain regions (Deng et al., 2010a; Hirono et al., 2001). Targeted therapeutic treatments and development of agonistic drugs for GABARs are currently being generated and investigated.

Hypothesis and Aims

The long-term goal of this thesis work was to better understand the molecular and synaptic mechanisms of behavioral dysfunction in the FXS disease state. The *FMR1* gene was cloned 20 years ago, but the molecular and neurobiological basis of the disease remains surprisingly elusive. I have used the

established *Drosophila* FXS model to test the functional conservation between *dFMR1* and its three human homologs. I have also conducted a structure-function analysis of FMRP, targeting a well-conserved phosphorylation residue involved in regulation and signaling. This was the first study of FMRP protein domain requirements *in vivo*. My hypothesis is that FMRP shuttles to the nucleus where it binds specific mRNA targets via the synergistic interaction of multiple RNA-binding domains, then escorts these mRNAs to their final cellular destinations, and finally regulates their translation downstream of phosphorylation-dependent signaling event (Fig. 6). I further hypothesize that this mechanism has been evolutionarily conserved from *Drosophila* to man, albeit with evolutionarily derived, message-specific functions sub-served by the three-member protein family in human.

The first aim of this work was to test the functional conservation of *dFMR1* and the human three-gene family (*hFMR1*/*hFXR1*/*hFXR2*) (Coffee et al., 2010). First, I show that human *FMR1* replaces all *Drosophila FMR1* functions just as well as the native gene, indicating complete functional conservation. Second, I show that *FMR1* has a unique function in *Drosophila* neurons as a translational regulator sculpting synaptic connections, which cannot be compensated for by *FXR1* or *FXR2*. Lastly, I show that the entire human gene family can fully replace each other's function in the non-neuronal setting of the *Drosophila* testes, demonstrating a fundamentally different mechanistic requirement in non-neuronal cells that can be fulfilled by any of the three family members.

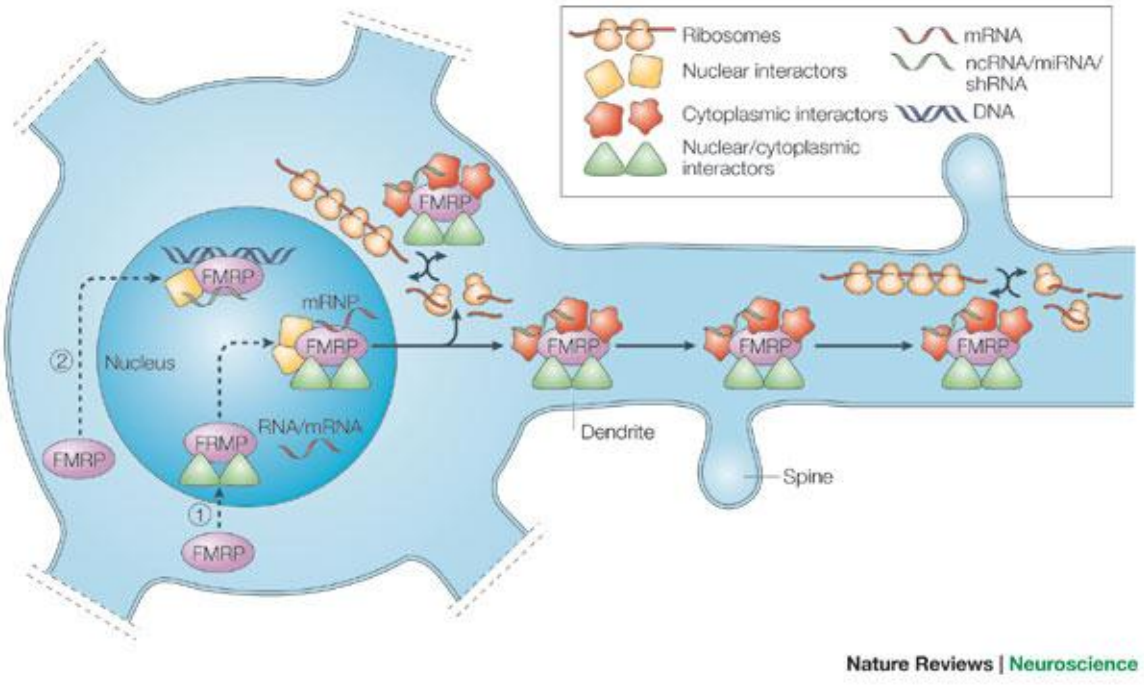

Figure 6. Model for FMRP function. FMRP enters the nucleus and could function through two possible mechanisms. In the first (1), FMRP could interact with other proteins, with itself (for example, the FMRP paralogs FXR1P and FXR2P), and with RNA/mRNA to form a ribonucleocomplex that may be involved in mRNA export from the nucleus to the cytoplasm. Once in the cytoplasm, a 'core' complex, containing FMRP and some of its nuclear partners, would interact with cytoplasm-specific proteins (such as cytoplasmic FMRP-interacting protein 1 (CYFIP1), CYFIP2 and Staufen) and move along processes to the synapses, transporting RNA/mRNA and, later, regulating synaptic protein synthesis. In the second mechanism (2), FMRP could be involved in the nuclear RNA interference pathway that is associated with small, non-coding RNAs (short hairpin RNAs or shRNAs) and specific nuclear partners (that is, nucleolin and Y-box binding protein 1 (YB1)). miRNA, microRNA; ncRNA, non-coding RNA. Adapted from (Bagni and Greenough, 2005).

The second aim of this work was to test *in vivo* requirements of *FMR1* phosphorylation state of a specific serine residue. Here, I study the effects of the phosphorylation state of a serine residue (S500) previously reported to serve as a 'switch' from an activated (phospho-FMRP) to deactivated (dephospho-FMRP) state (Ceman et al., 2003; Narayanan et al., 2008). I used transgenic expression of a phospho- and dephosphomimetic (*S500D-hFMR1* and *S500A-hFMR1*, respectively) in the *dfmr1* null mutant background to test *in vivo* requirements. Prior *in vitro* work has shown that the mouse FMRP phosphorylation is necessary for the regulation of FMRP's role as a negative translational regulator (Narayanan et al., 2008). My *in vivo* work here demonstrates that the *S500D-hFMR1* phosphomimetic can restore wildtype FMRP function, while the *S500A-hFMR1* dephosphomimetic is unable to restore function in all molecular, cellular and behavioral assays. I conclude that human FMRP S500 phosphorylation is necessary for its *in vivo* function as a neuronal translational repressor and regulator of synaptic architecture, and for the manifestation of FMRP-dependent learning behavior.

Taken together, my studies show that *FMR1* function has been evolutionarily conserved from *Drosophila* to man, and that the human paralogs (*FXR1* and *FXR2*), probably rising through a duplication event, are only able to compensate for lack of *FMR1* in a non-neuronal tissue. Further, I demonstrate that S500 phosphorylation is critically important for FMRP function as the phosphomimetic, *S500D-hFMR1*, is able to phenocopy wildtype protein function, while the dephosphomimetic, *S500A-hFMR1*, is unable to provide any function

and so resembles the null mutant condition. These studies provide strong evidence that the *Drosophila* FXS model is an extraordinarily beneficial system in which to study FXS and to gain insight into its causative molecular, cellular, and behavioral mechanisms of the disease state.

CHAPTER II

FRAGILE X MENTAL RETARDATION PROTEIN HAS A UNIQUE, EVOLUTIONARILY CONSERVED NEURONAL FUNCTION NOT SHARED WITH FXR1P OR FXR2P

This paper has been published under the same title in *Disease Models & Mechanisms*, 2010

R. Lane Coffee, Jr., Charles R. Tessier, Elvin A. Woodruff, III, and Kendal Broadie

Department of Biological Sciences, Vanderbilt Brain Institute, Kennedy Center for Research on Human Development, Vanderbilt University, Nashville, TN

Abstract

Fragile X syndrome (FXS), resulting solely from loss of function of the human *Fragile X Mental Retardation 1* (*hFMR1*) gene, is the most common heritable cause of mental retardation and autism disorders, with syndromic defects also in non-neuronal tissues. The human genome additionally encodes two closely related *hFMR1* paralogs: *hFXR1* and *hFXR2*. The *Drosophila* genome, in contrast, encodes a single *dFMR1* gene with similar close sequence homology to all three human genes. Null *dfmr1* mutants recapitulate FXS-associated molecular, cellular and behavioral phenotypes, suggesting *FMR1* function has been conserved, albeit with specific functions possibly sub-served by the expanded human gene family. To test evolutionary conservation, we used tissue-targeted transgenic expression of all three human genes in the *Drosophila*

disease model to investigate function at 1) molecular, 2) neuronal and 3) non-neuronal levels. In neurons, *dfmr1*-null mutants exhibit elevated protein levels altering central brain and neuromuscular junction (NMJ) synaptic architecture, including increased synapse area, branching, and bouton numbers. Importantly, *hFMR1* can fully rescue both the molecular and cellular defects in neurons, comparably to *dFMR1*, whereas *hFXR1* and *hFXR2* provide absolutely no rescue. For non-neuronal requirements, we assayed male fecundity and testes function. Null *dfmr1* mutants are effectively sterile due to disruption of the 9+2 microtubule organization in the sperm tail. Importantly, all three human genes fully and equally rescue mutant fecundity and spermatogenesis defects. These results indicate that *FMR1* gene function is evolutionarily conserved in neural mechanisms and cannot be compensated by either *FXR1* or *FXR2*, but that all three proteins can substitute for each other in non-neuronal requirements. We conclude that *FMR1* has a neural-specific function distinct from its paralogs, and that the unique *FMR1* function is responsible for regulating neuronal protein expression and synaptic connectivity.

Introduction

Fragile X syndrome (FXS) is the most common cause of inherited mental retardation and the leading known genetic cause of autism (Clifford et al., 2007; Cohen et al., 2005; Fisch et al., 2002; Hagerman et al., 2005; Rogers et al., 2001). The X-chromosome linked disorder is caused by loss of a single gene function, *fragile X mental retardation 1* (*FMR1*), most frequently by expansion of

CGG repeats (>200 repeats) in the 5′ regulatory region causing hypermethylation that results in transcriptional silencing (Heitz et al., 1992; Oberle et al., 1991; Pieretti et al., 1991). In addition to mental impairment, FXS patients also display a wide range of social interaction problems characterized by poor eye contact, hyperactivity, attention deficit and obsessive-compulsive behaviors (Boccia and Roberts, 2000; Cornish et al., 2001; Fryns et al., 1984; Torrioli et al., 2008), and hypersensitivity to sensory stimuli (Fryns, 1984; Hessl et al., 2001). Other physical anomalies include elongated face, prominent ears and enlarged male testes (Chudley and Hagerman, 1987; Giangreco et al., 1996; Moore et al., 1982). These non-neurological symptoms testify that the *FMR1* gene performs important functions in non-neuronal tissues. Indeed, the *FMR1* product (FMRP) is ubiquitously expressed, albeit with elevated expression in brain and testes (Agulhon et al., 1999; Devys et al., 1993). Although FXS is a monogenic disease, the wide range of clinical symptoms strongly indicates that FMRP is involved in the regulation of multiple modulatory factors.

FXS has been extensively investigated in both vertebrate and invertebrate genetic model systems (Bassell and Warren, 2008; Gatto and Broadie, 2009b). In all systems, FMRP has five well-defined functional domains: two RNA-binding KH domains in the middle region (KH1, KH2; KH = heterogeneous nuclear ribonucleoprotein K homology)(Siomi et al., 1993), an RNA-binding RGG box in the C-terminal region (containing repeats of an Arg-Gly-Gly motif) (Darnell et al., 2001), a non-classical nuclear localization signal (NLS) and a nuclear export signal (NES) (Eberhart et al., 1996; Zhang and Broadie, 2005). Consistent with

its ability to bind RNA, FMRP regulates transcript trafficking and functions as a negative regulator of translation (Dictenberg et al., 2008; Estes et al., 2008; Laggerbauer et al., 2001; Mazroui et al., 2002). In vertebrates, FMRP is part of a 3-member family that includes two other similar proteins: Fragile X-related protein 1 (FXR1P) and 2 (FXR2P). The autosomally-encoded paralogs express in a very similar tissue and cellular profile to FMRP, including the subcellular distribution in neurons, with only slight differences (Agulhon et al., 1999; Bakker et al., 2000). For example, FXR1P is more abundantly expressed in cardiac and skeletal muscle compared to FMRP and FXR2P (Bakker et al., 2000; Mientjes et al., 2004). Moreover, all three proteins show ultrastructurally overlapping expression, can be co-immunoprecipitated and can associate with the same protein partners (Bakker et al., 2000; Ceman et al., 1999; Christie et al., 2009; Schenck et al., 2001; Zhang et al., 1995). Both hetero- and homo-dimerization of the FMRP/FXR1P/FXR2P family has been proposed to occur (Ceman et al., 1999; Christie et al., 2009; Tamanini et al., 1999b; Zhang et al., 1995).

Only loss of *FMR1* causes FXS, and loss of *FXR1* or *FXR2* has not been linked to any disease state. However, the mouse *FXR1* knockout is lethal shortly after birth due to defects in cardiac and skeletal muscle development (Mientjes et al., 2004), whereas both *FMR1* and *FXR2* knockouts, as well as double knockouts, are adult viable. At least some FXS-like phenotypes are exhibited in *FXR2* knockout mice (Bontekoe et al., 2002), while *FMR1* knockouts recapitulate many FXS symptoms including learning defects, hyperactivity, sensory hypersensitivity, social deficits and macroorchidism (Chen and Toth, 2001;

Dobkin et al., 2000; McNaughton et al., 2008; Slegtenhorst-Eegdeman et al., 1998). At a cellular level, *FMR1* knockouts exhibit elevated brain protein synthesis levels (Qin et al., 2005) and accumulation of developmentally arrested postsynaptic spines (Comery et al., 1997; Nimchinsky et al., 2001). Interestingly, double knockout of *FMR1* and *FXR2* results in augmented defects, including exaggerated behavioral phenotypes in open-field activity, prepulse inhibition of acoustic startle response, contextual fear conditioning and circadian arrhythmicity (Spencer et al., 2006; Zhang et al., 2008), and worsened cellular phenotypes, including further enhanced long-term depression (LTD) (Zhang et al., 2009). These data predict that the paralogs have overlapping functions and/or compensate for each other. However, expression levels of *FXR1/2* are unaltered in *FMR1* null mice and, similarly, levels of FMRP and FXR1P are unaltered in *FXR2* null mice (Bakker et al., 2000; Bontekoe et al., 2002). Recent work has shown that kissing-complex RNA (kcRNA) interference with the KH2 domain is able to displace FXR1P and FXR2P from polyribosomes as it does for FMRP (Darnell et al., 2009); however, FMRP has a unique ability to recognize G-quadruplexes, suggesting that the FMRP RGG box domain function may not be duplicated in the two paralogs. Thus, despite co-expression, co-molecular complex formation and phenotypic interactions between these three gene family members, evidence of their distinctive versus overlapping roles remains elusive.

The single *Drosophila FMR1* gene (*dFMR1*) product is nearly identically homologous overall to all three human family members: 35% identity/56% similarity compared to hFMRP, 37% identity/65% similarity compared to hFXR1P

and 36% identity/65% similarity compared to hFXR2P. The N-terminal region has a higher homology (dFMRP:hFMRP 50% identity, 84% similarity), with the C-terminal being relatively divergent (Zhang et al., 2001). Importantly, dFMRP displays highly conserved structure in all defined functional domains: KH1, 68% identity; KH2, 67% identity; RGG box, 62% identity; NLS, 48% identity; NES, 65% identity (compared to hFMRP). With the exception of *FMR1* exons 11/12, for which there are no corresponding *FXR1/2* sequences, exon 1-10 and 13 sizes are nearly identical in *FMR1*, *FXR1* and *FXR2* (Kirkpatrick et al., 2001). Non-mammalian *FMR1* orthologs similarly lack exons 11 and 12. These comparisons imply that the mammalian gene family likely arose by duplication from a common ancestor similar to the *Drosophila FMR1* gene. Consistently, dFMRP displays conserved RNA-binding domains, tissue and subcellular expression patterns, and functional roles in mRNA trafficking and negative translational regulation (Banerjee et al., 2007; Epstein et al., 2009; Estes et al., 2008; Reeve et al., 2005; Zhang et al., 2001; Zhang et al., 2005). Moreover, *dFMR1* knockout closely recapitulates FXS symptoms in a wide range of molecular, cellular, and behavioral phenotypes (Bolduc et al., 2008; Dockendorff et al., 2002; Gatto and Broadie, 2009a; McBride et al., 2005; Pan et al., 2004). These striking similarities between *Drosophila* and mammalian FMRP suggest well-conserved function, but beg the question of why mammals have an expanded three-member protein family.

In this study, we investigate the functional conservation of the entire Fragile X gene family by expressing each of the three human genes in the

Drosophila FXS model with tissue-specific drivers. A wide-ranging series of phenotypic tests at the molecular, cellular and ultrastructural levels were selected to survey function in nervous system and non-neuronal tissue. A wild-type *dFMR1* transgene was used as the positive control and each human gene was investigated in two independent transgenic lines, all with targeted expression driven in either neurons or germ cells within the *dfmr1* null mutant background. The results show that *FMR1* has an evolutionarily conserved function in the *Drosophila* central and peripheral nervous system that is not possessed by either *FXR1* or *FXR2*. When all three human genes are targeted to *Drosophila* neurons, only human *FMR1* is able to restore brain protein levels in the *dfmr1* null mutant, and it is just as effective as the native *Drosophila FMR1*. Similarly, only human *FMR1* is able to restore normal synaptic architecture in *dfmr1* null neurons. *FXR1* and *FXR2* completely lack this ability to compensate. In contrast, in non-neuronal tissue all three human genes are equally competent at replacing *dFMR1* function. When each gene is targeted to the testes, they all fully restore male fecundity and rescue testes spermatid axoneme defects. These results indicate a unique, evolutionarily conserved role for *FMR1* in neuronal mechanisms and a broader, shared role for *FMR1, FXR1* and *FXR2* in non-neuronal tissue.

Results

Transgenic constructs with targeted pan-neuronal expression

Humans have a 3-member gene family composed of the highly similar *hFMR1, hFXR1* and *hFXR2* genes (Zhang et al., 1995). The three gene products associate with ribosomes in large complexes thought to cooperatively mediate transport of neural mRNAs to specific intracellular locations and inhibit their translation until signaled (Ceman et al., 1999; Christie et al., 2009; Dictenberg et al., 2008; Khandjian et al., 2004; Siomi et al., 1996; Zhang et al., 1995). In *Drosophila*, the single *FMR1* gene (*dFMR1*) likely represents an ortholog of the common ancestor of *hFMR1* and its two paralogs. This speculation suggests that the functions of the 3-member gene family may subdivide the roles of *dFMR1*, in addition to any newly-evolved functions each gene may serve. The *dFMR1* gene has a similar sequence homology to all three human genes, so it is not clear which, if any, may be the true homolog. To address these questions, we engineered transgenic human cDNA constructs for *hFMR1, hFXR1* and *hFXR2*, as well as wildtype *dFMR1* as a positive control, and expressed each with tissue-specific drivers in the *Drosophila* FXS model (*dfmr1* null mutant). The generation and testing of these transgenic tools is illustrated in Figure 7.

cDNA constructs engineered for *dFMR1* and each human family gene member were sub-cloned downstream of the UAS promoter sequence (5X UAS; Fig. 7A). A MYC epitope tag was added at the amino terminus of each transgene to track protein expression. The tagged transgenes could then be targeted to specific tissues using the pUAST/GAL4 expression system. Each construct was

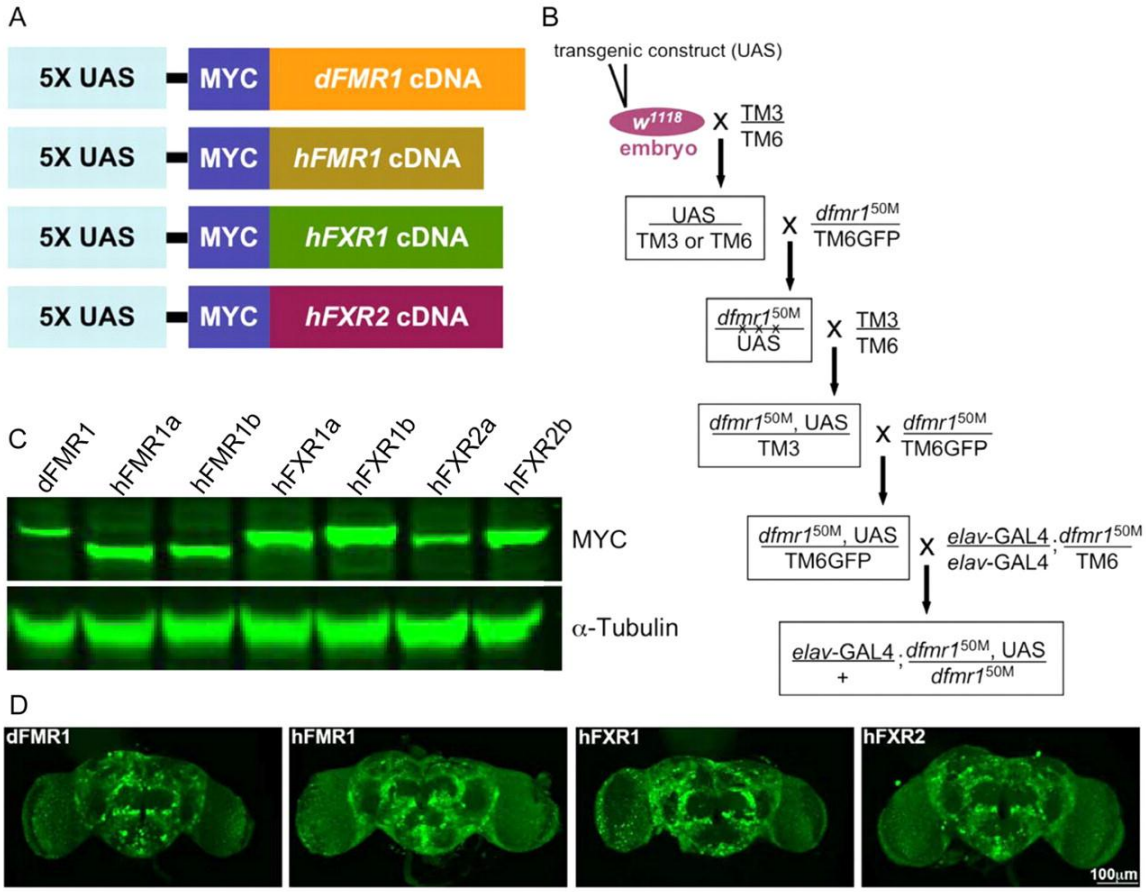

Figure 7. Generation of transgenic constructs with targeted neuronal expression. (A) The four UAS transgenic constructs generated and tested in this study. The positive control is wild-type *dFMR1*, and the three human genes are *hFMR1*, *hFXR1* and *hFXR2*. All cDNA transgenic constructs are tagged with a MYC epitope in the pUAST (5X UAS) expression vector to follow protein expression. In all assays, two independent transgenic lines for each human transgenic construct were analyzed. (B) The embryonic transformation and genetic crossing scheme that was used to introduce each stably integrated UAS transgene into the *dfmr1* null mutant background and then drive expression with the pan-neuronal GAL4 driver *elav*-GAL4. (C) Western blot analyses of transgenic protein expression for the *dFMR1* line (control) and two independent lines of *hFMR1*, *hFXR1* and *hFXR2* (denoted as a/b). Expression from brain extracts (1–2-day-old adults) was tested with an anti-MYC antibody against the epitope tag common to all four transgenes (see A). Lines were selected for comparable transgene expression. The loading control is α-tubulin. (D) Brain immunohistochemistry for transgene expression of the *dFMR1* line (control) and the three human lines (*hFMR1*, *hFXR1* and *hFXR2*). Drosophila adult brains (1–2 days old) were probed with anti-MYC to detect the transgene epitope tag. Comparable transgene expression occurs in all conditions. Bar, 100 μm.

microinjected into genetic background control w^{1118} embryos (Fig. 7B). Multiple stably integrated genomic lines for each transgene were isolated and self-perpetuating stocks generated. Third chromosome transformants were recombined into the *dfmr1*-null ($dfmr1^{50M}$) background and a stock produced with TM6-GFP serving to balance the recombined UAS transgene chromosome (Fig. 7B). In order to assay rescue of neuronal phenotypes, all transgenic lines were crossed with a stock line homozygous for the pan-neuronal driver *elav*-GAL4 and heterozygous for the $dfmr1^{50M}$ allele. The resulting experimental stocks were homozygous null for *dfmr1* with a single copy of the UAS transgene and a single copy of the *elav*-GAL4 driver (Fig. 7B). Two independent transgenic insertion lines for each human transgene were used in all experiments, compared to w^{1118} with *elav*-GAL4 driver alone (wild-type control), the *dfmr1*-null with *elav*-GAL4 driver alone (negative control) and UAS-*dFMR1* (positive control). Thus, nine genetic lines were compared in all subsequent experimental assays.

The expression of all transgenes was compared with a combination of brain Western blot and immunohistochemistry imaging for the common MYC epitope tag in order to select lines with comparable expression (Fig. 7C, D). Endogenous dFMRP expression is ubiquitous in neurons and relatively uniform between neurons throughout the wild-type *Drosophila* brain (Fig. 8A). We therefore selected *elav*-GAL4 as the best described pan-neuronal driver mimicking this expression (Gatto and Broadie, 2009a). Transgenic lines with high and low *elav*-GAL4 driven expression compared to the UAS-*dFMR1* positive control were discarded, and two independent insertion lines with comparable

expression for each transgene were selected for detailed analyses. Western blot analyses of brain protein extracts show comparable MYC epitope tag expression levels across all selected transgenic genotypes (Fig. 7C). The protein sizes of each transgene are roughly equivalent, albeit with *dFMR1* product slightly larger and *hFMR1* product slightly smaller than the other transgenes. We were careful to select lines that did not over-express the transgenes relative to endogenous dFMR1 (data not shown). We confirmed that *elav*-driven transgene expression is widespread throughout neurons (Fig. 7D). Anti-MYC labeling of brains from all four transgenic lines showed comparable transgene expression levels and distribution across genotypes. Importantly, the UAS-*dFMR1* positive control was indistinguishable from the three human transgenes in brain expression profile (Fig. 7D). These lines were therefore selected to systematically test their ability to rescue a wide range of *dfmr1*-null mutant phenotypes.

Only *FMR1* restores brain protein levels

In both rodents and *Drosophila*, FMRP/dFMRP acts as a negative regulator of protein synthesis in neurons (Lu et al., 2004; Reeve et al., 2005; Schutt et al., 2009; Zhang et al., 2001). Loss of this translational regulation is believed to be the root cause of all FXS impairments. In the absence of dFMRP, total brain protein levels are significantly elevated, particularly during key stages of synaptic development and refinement in the late-maturing brain (Tessier and Broadie, 2008). We therefore first examined whether this fundamental molecular defect was rescued by each of the three human transgenes. Importantly, the

dfmr1 null mutant brain is unaltered in size and gross architecture compared to wildtype and genetic controls (Fig. 8A). We therefore extracted total protein from brains to make a direct comparison of protein levels (Tessier and Broadie, 2008). Nine genetic lines were analyzed; the wild-type control, *dfmr1* null, UAS-*dFMR1* positive control and two independent lines each for the three human transgenes. Null *dfmr1* mutants with the *elav*-GAL4 driver alone (*elav*/+; $dfmr1^{50M}/dfmr1^{50M}$) have 22% higher levels of brain protein compared to controls (*elav*/+; w^{1118}) immediately post-eclosion (0-7 hours after eclosion (AE)) (Fig. 8B). Protein levels per animal were 16.6±0.45 μg in control compared to 20.2±0.47 μg in the null mutant ($P<0.01$, $n=8$). The positive transgenic control, *elav*-GAL4 driven UAS-*dFMR1* in the null mutant background, displayed brain protein levels of 16.4±0.61 μg, which was 23% lower than the *dfmr1* null and showed complete rescue to control levels ($P<0.01$, $n=8$; Fig. 8B). Two independent transgenic lines of all three human genes were assayed for brain protein levels. Both UAS-*hFMR1* lines (light and dark bars in Fig. 8B) showed exactly the same effect of lowering brain protein levels by 28% compared to the *dfmr1* null, restoring levels indistinguishable from wild-type control (15.83±0.56 μg, 15.8±0.4 μg; $n=8$, $P<0.001$). In contrast, *elav*-GAL4 driven neuronal expression of the two human paralogs, UAS-*hFXR1* and UAS-*hFXR2*, maintained brain protein levels comparable to *dfmr1* nulls, with no indication of rescue. For UAS-*hFXR1*, the two independent lines showed levels of 21.2±0.43 μg and 21.1±0.63 μg (Fig. 8B). For UAS-*hFXR2*, the protein levels were 19.34±0.61 μg and 20.1±0.66 μg. There

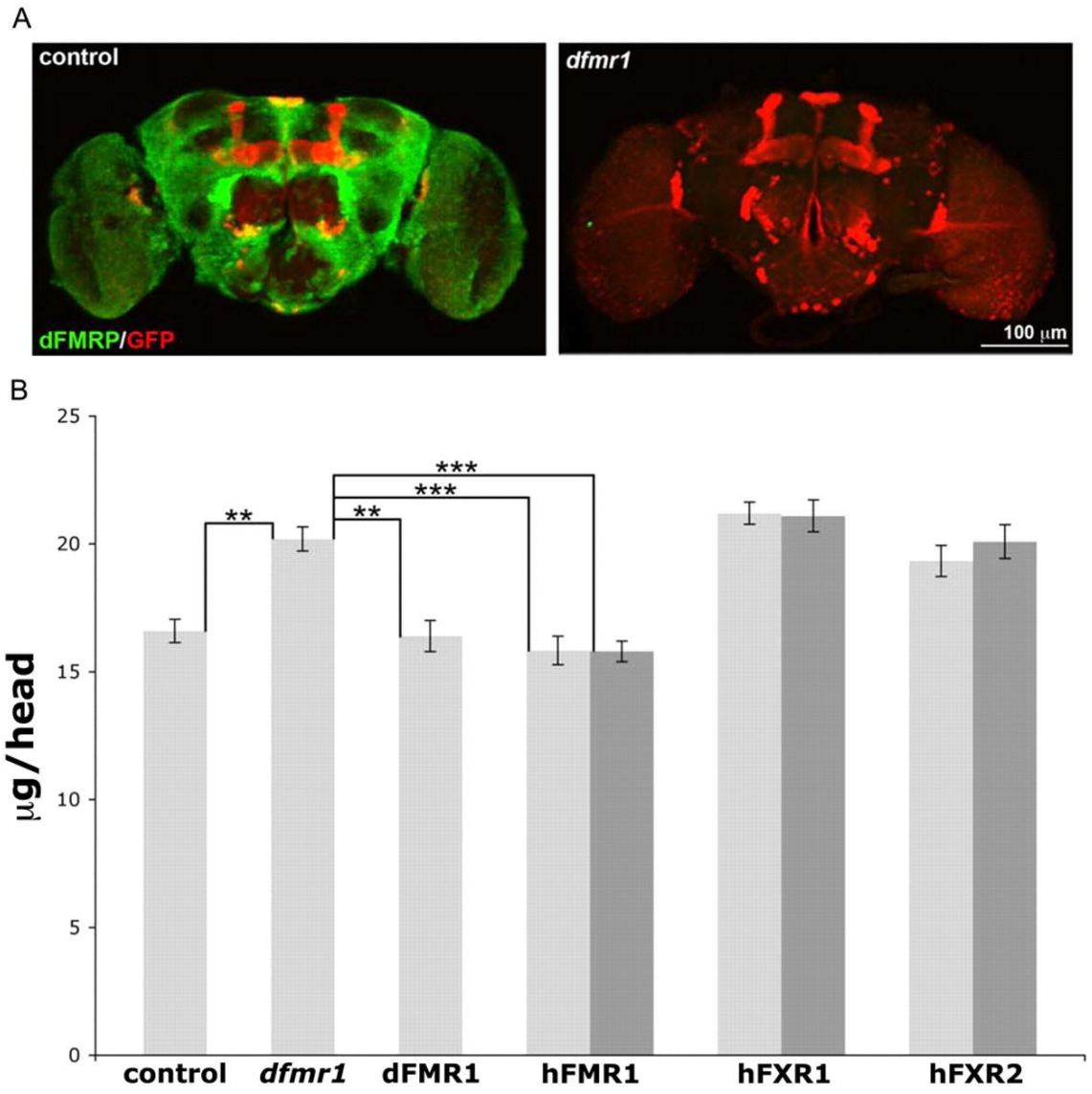

Figure 8. Only *hFMR1* rescues elevated protein levels in the *dfmr1* null brain. (A) Comparison of dFMRP expression in the wild-type control (w^{1118}) and the *dfmr1* null ($dfmr1^{50M}$) adult Drosophila brain, which were used as positive and negative controls in all assays. Acutely dissected brains (2 days old) were immunolabeled with anti-dFMRP (green) and anti-GFP (red) to reveal a transgene marker in the mushroom body learning/memory center. Note that the null mutant brain is of normal size with normal gross architecture. Bar, 100 μm. (B) Total brain protein was extracted from young adult (0–7 hours old) animals and quantified with a MicroBCA assay. The six genotypes that were compared are: w^{1118} control, *dfmr1* null ($dfmr1^{50M}$), *elav*-GAL4 driving UAS-*dFMR1* (positive control), and two independent lines each (light and dark gray bars) of UAS-*hFMR1*, UAS-*hFXR1* and UAS-*hFXR2* expression in the *dfmr1* null background. Each bar shows the average protein levels in μg per head. Sample size: 10–20 pooled heads per sample, n=8. Significance: $^{**}P<0.01$; $^{***}P<0.001$.

was no significant difference between any of these four lines relative to each other or compared to the *dfmr1* null condition. All four *hFXR1* and *hFXR2* transgenic lines maintained highly significantly ($P<0.001$) elevated brain protein levels compared to wildtype.

These results demonstrate that only human *FMR1* and not its paralogs, *hFXR1* and *hFXR2*, can rescue the hallmark elevation of brain protein levels in the *dfmr1* null back to the control state. Human *FMR1* was just as effective as *Drosophila FMR1* in restoring normal brain protein levels, indicating completely conserved function in this fundamental role. The fact that *hFXR1* and *hFXR2* lack this function may be predicted by the fact that these proteins have not been shown to act as negative translational regulators (Laggerbauer et al., 2001).

Only FMR1 restores brain circuit synaptic architecture

At a cellular level, the hallmark defect in FXS patients and disease models is inappropriate synaptic connectivity (Braun and Segal, 2000; Bureau et al., 2008; Comery et al., 1997; Gatto and Broadie, 2008; Hanson and Madison, 2007; Tessier and Broadie, 2008). In both mouse and *Drosophila* models, synapse architecture also appears immature or developmentally arrested. We first examined synapse connectivity in the central brain, based on well-established *dfmr1* phenotypes. Null *dfmr1* mutants exhibit strikingly abnormal circadian rhythm patterns, with a complete loss of rhythmicity in the absence of environmental entrainment (Bushey et al., 2009; Dockendorff et al., 2002; Inoue et al., 2002; Sofola et al., 2008). Although mouse *FMR1* knockouts show only

mild impairments, the *FMR1/FXR2* double knockout is likewise entirely arrhythmic (Zhang et al., 2008). In *Drosophila*, circadian activity is controlled by well-defined clock circuitry, in which the small ventrolateral (sLN_v) neurons are sufficient for pacemaker activity (Grima et al., 2004; Renn et al., 1999; Stoleru et al., 2004). These neurons express the neuropeptide Pigment Dispersing Factor (PDF) and exhibit a characteristic branching pattern with axonal processes projecting dorsally to a defasiculation point in the protocerebrum and then synaptic processes extending medially (Gatto and Broadie, 2009a; Helfrich-Forster, 1995; Helfrich-Forster, 2005). In *dfmr1*-null mutants, sLN_v processes are over-elaborated and extend beyond their normal termination points (Dockendorff et al., 2002; Gatto and Broadie, 2009a; Morales et al., 2002). Given the synergistic effect *FMR1* and *FXR2* on rhythmicity in mice (Zhang et al., 2008), it might be predicted that the proteins possess redundant or overlapping functions in the clock circuit. To test this hypothesis, we assayed the ability of each human transgene to rescue the *dfmr1* defects in the central clock circuit (Fig. 9).

Brains labeled with anti-PDF clearly display the dorsal sLN_v projections into the protocerebrum (Fig. 9A). At the point of axonal defasiculation, the processes split into a localized array of small synaptic projection at the dorsal horn and into the protocerebrum. These projections are bilaterally symmetrical on the two sides of the brain (Fig. 9A; middle and right). Null *dfmr1* animals exhibit a highly significant ($n \geq 10$; $P < 0.001$) increase in the number of PDF boutons compared to controls (Fig. 9B). Wild-type terminals contain a mean of 45.1 ± 1.3 boutons compared to 67.6 ± 2.0 in the *dfmr1* null. Thus, the mutant condition

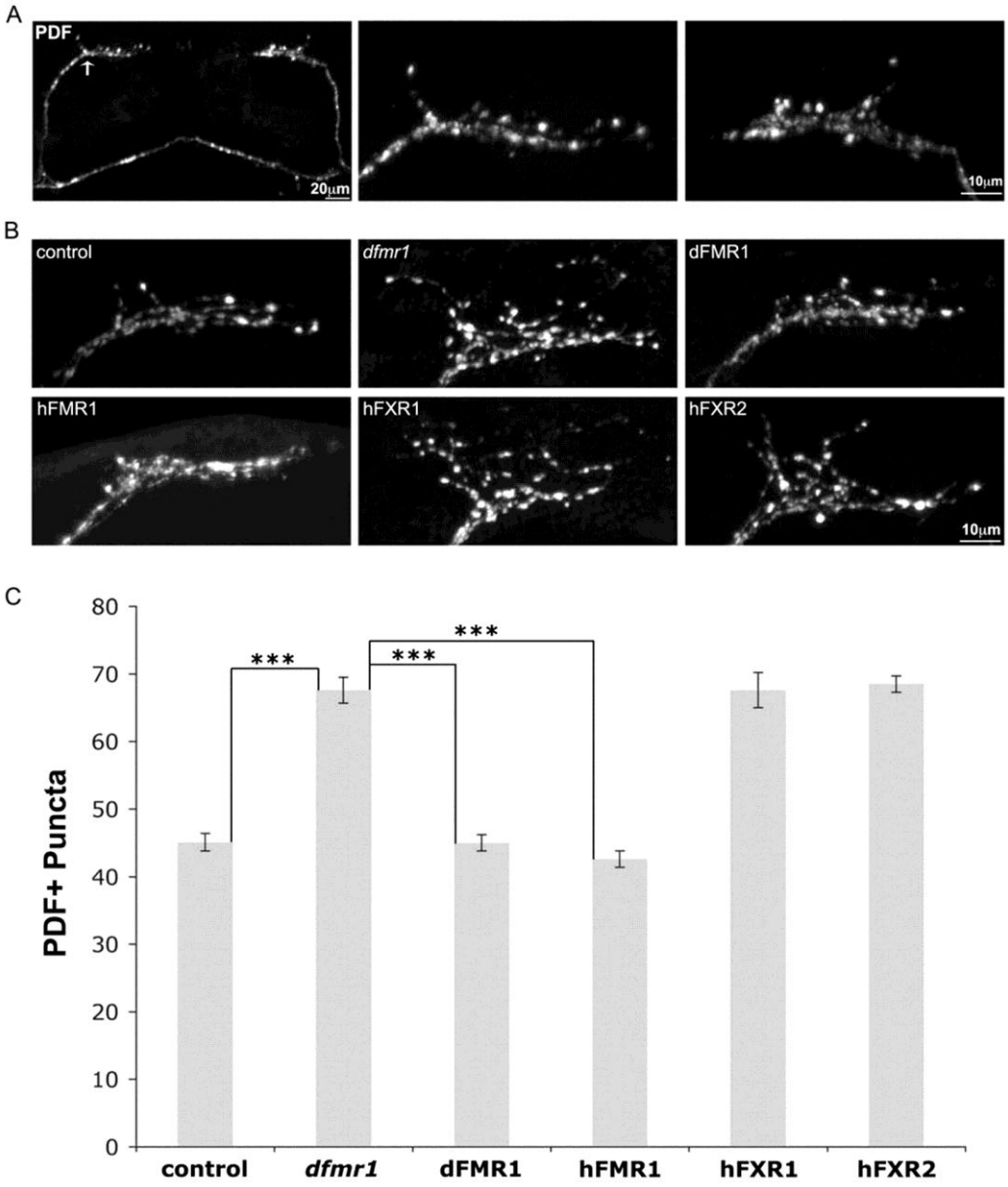

Figure 9. Only *hFMR1* rescues clock neuron synapse arbors in *dfmr1* null mutants. (A) Representative images of small ventrolateral (sLN_v) clock neurons in the adult brain labeled with anti-PDF. The low-magnification image on the left shows the bilaterally symmetrical sLN_v projections, terminating in synaptic arbor projections (arrow) in the dorsal protocerebrum. Note the PDF-positive punctae marking the synaptic boutons. Bars, 20 μm (A, left panel); 10 μm (A, middle and right panels). (B) Representative images of the sLN_v synaptic arbors from the six genotypes assayed: w^{1118} (control), $dfmr1^{50M}$ null (*dfmr1*), and the null background with *elav*-GAL4-driven UAS-*dFMR1*, UAS-*hFMR1*, UAS-*hFXR1* and UAS-*hFXR2*. Bar, 10 μm. (C) Quantification of the number of PDF-positive punctae per synaptic arbor in the six genotypes shown. Sample size: $n \geq 10$ animals for each genotype. Significance: ***$P<0.001$ for all comparisons.

shows a ~50% increase in PDF-positive synaptic boutons (Fig. 9C). Neuronal expression of wild-type *dFMR1* completely rescues the synaptic overgrowth characterizing the null mutant, and the terminals become clearly more restricted in extent and refined in number of synaptic boutons (Fig. 9B). The expression of wild-type *dFMR1* results in the differentiation of 45.0±1.2 boutons, a number indistinguishable from control and significantly ($n \geq 10$; $P < 0.001$) rescued compared to the *dfmr1*-null condition (Fig. 9C).

Each human transgene was next expressed in turn to evaluate rescue of the sLN_v synaptic arbor defect in *dfmr1* nulls. First, *hFMR1* expression in neurons was assayed, and showed complete rescue of the overgrowth defect (Fig. 9B). Targeted *hFMR1* resulted in 42.6±1.2 PDF-positive boutons in the sLN_v arbor, a rescue as complete as the native *Drosophila* gene (Fig. 9C). Next, the two paralogs were assayed in turn. At a qualitative level, sLN_v synaptic terminals appear as overgrown with *hFXR1* or *hFXR2* expression as in the purely null mutant state (Fig. 9B). Indeed, quantification of PDF bouton number fails to show any significant rescue by either of these transgenes. *hFXR1* expression resulted in 67.0±2.6 boutons, and *hFXR2* expression similarly resulted in 68.5±1.2 boutons (Fig. 9C). Neither value is significantly different from the *dfmr1* null (67.6±2.0), and both are very significantly elevated compared to the control (45.1±1.3; $n \geq 10$; $P < 0.001$). Thus, both *Drosophila* and human *FMR1* similarly and completely rescue the synaptic defect in the clock neurons, whereas neither human paralog exerts any detectable compensatory function.

Only *FMR1* restores neuromuscular junction synaptic architecture

In the *Drosophila* FXS model, the glutamatergic neuromuscular junction (NMJ) synapse is extremely well characterized (Gatto and Broadie, 2008; Pan et al., 2008; Zhang et al., 2001). The size and accessibility of this synaptic arbor, combined with the wealth of synaptic markers and structural information, make this terminal particularly suited to a systematic investigation. Null *dfmr1* mutants display defects on many levels of NMJ synaptic architecture, including grossly elevated synaptic area, increased synaptic branching and the formation of supernumerary synaptic boutons (Gatto and Broadie, 2008; Pan et al., 2008; Zhang et al., 2001). Most strikingly, developmentally arrested mini (or satellite) boutons accumulate in the absence of dFMRP function (Gatto and Broadie, 2008), which likely represent an early stage of normal bouton maturation (Beumer et al., 1999; Gorczyca et al., 2007; Ruiz-Canada et al., 2004). To compare synaptic development, we co-labeled junctions with presynaptic (HRP membrane marker) and postsynaptic (DLG scaffold marker) antibody probes to quantify all of these features in *dfmr1* null, wild-type control, *elav*-GAL4 (presynaptic) driven UAS-*dFMR1* positive control, and all three UAS human transgenes in the *dfmr1*-null mutant background.

Labeling for HRP delineates the innervating presynaptic neuron (red), and anti-DLG reveals the postsynaptic domain (green) of the target muscle (Fig. 10A). The positive transgenic control of *elav*-GAL4 driven UAS-*dFMR1* fully rescued both the enlarged junctional area and increased synaptic branching that characterizes the *dfmr1*-null condition (Fig. 10B, C). To quantify synaptic area,

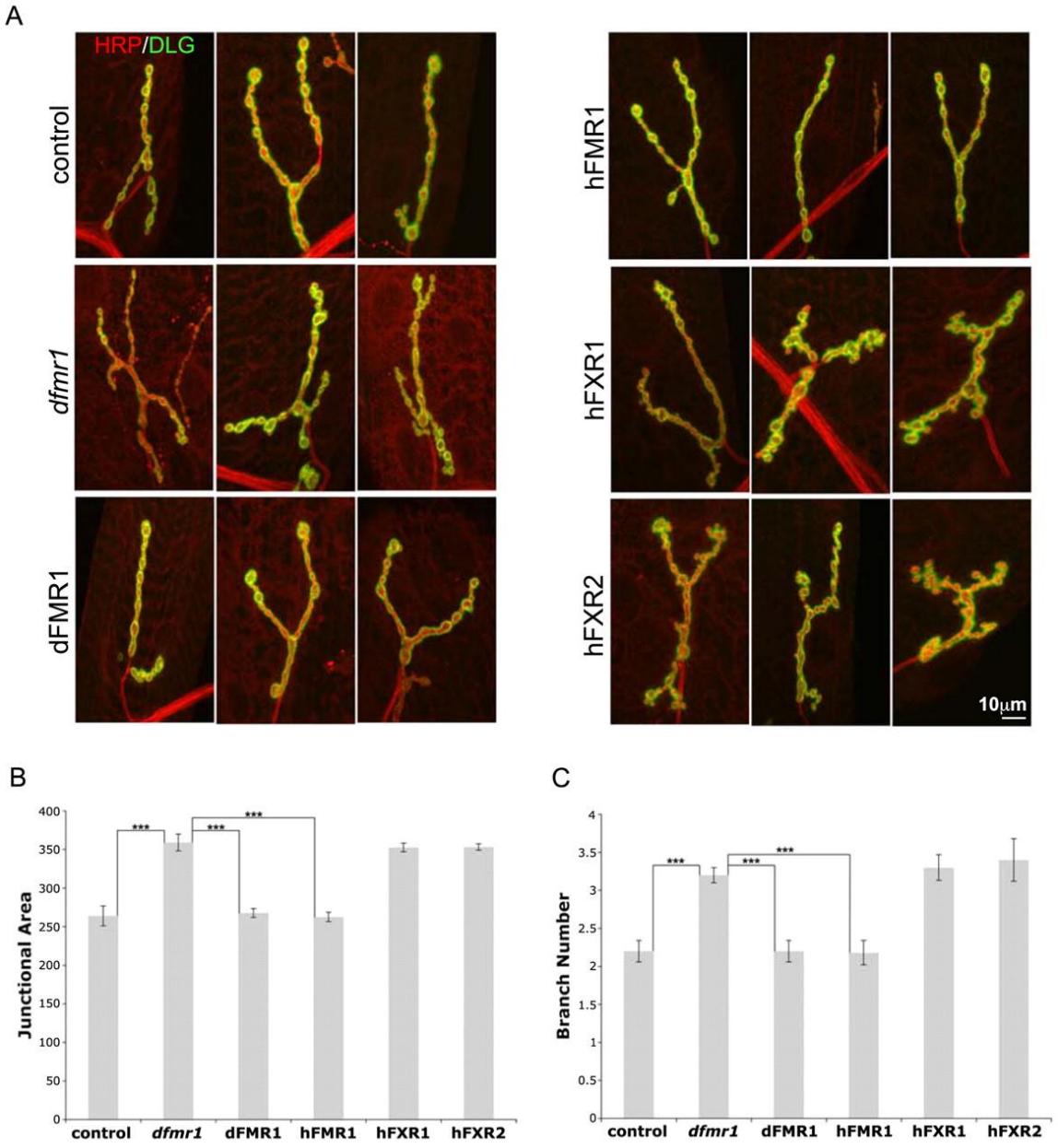

Figure 10. Only *hFMR1* rescues synapse architecture in *dfmr1* null mutants. The wandering third instar NMJ synapse was co-labeled with presynaptic and postsynaptic markers and compared between the six genotypes: wild-type control, *dfmr1* null mutants, and *elav*-GAL4-driven expression in the *dfmr1* null background of UAS-*dFMR1* (positive control) and two independent lines each of UAS-*hFMR1*, UAS-*hFXR1* and UAS-*hFXR2.* (A) Representative images of the muscle 4 NMJ labeled for presynaptic HRP (red) and postsynaptic DLG (green). Three example synaptic arbors are shown for each of the six genotypes. Bar, 10 μm. Quantification of junction area measured based on DLG domain expression (B) and the number of synaptic branches measured based on HRP labeling (C). Sample size: $n \geq 10$ animals for each genotype. Significance: ***$P<0.001$.

the junction delimited by DLG expression was measured (control, 264±13 μm^2; *dfmr1* null, 359±11 μm^2; $n \geq 10$, $P<0.001$; Fig. 10B). Presynaptic *dFMR1* expression completely restored junctional area to control levels (267±6 μm^2; $n \geq 10$, $P<0.001$). To quantify branching, HRP-labeled synaptic projections with more than two boutons were counted (control, 2.2±0.14; *dfmr1* null 3.2±0.1; $n \geq 10$, $P<0.001$; Fig. 10C). Presynaptic *dFMR1* expression completely restored synaptic branching from the elevated mutant levels (2.2±0.14 branches; $n \geq 10$, $P<0.001$). Strikingly, human *FMR1* was equally able to completely restore synaptic junctional area and arbor branching to wild-type levels (262±6 μm^2 area, 2.18±0.16 branches; $n \geq 10$, $P<0.001$; Fig. 10B,C). In sharp contrast, the two paralogs, *hFXR1* and *hFXR2*, were totally unable to restore synaptic area in the null mutant (*hFXR1*, 352±5.5 μm^2; *hFXR2*, 353±4.1 μm^2, $n \geq 10$; Fig. 10B). Similarly, both *hFXR1* and *hFXR2* failed to restore normal synaptic branch number in the mutant (3.3±0.17 branches and 3.4±0.28 branches, respectively; $n \geq 10$; Fig. 10C). Thus, only human *FMR1* has a conserved function in maintaining gross synaptic architecture, and *hFXR1* and *hFXR2* completely lack this ability.

dFMRP plays a key role in limiting synaptic bouton number and regulating the normal rate of bouton differentiation. To quantify mature type Ib bouton number, HRP/DLG co-labeled varicosities >2 μm in minimum diameter were counted within individual synaptic arbors (Fig. 11A). Null *dfmr1* mutants exhibit a very significantly increased number of synaptic boutons compared to controls (*dfmr1*, 29.1±0.7; control, 19.7±0.5; $n \geq 10$, $P<0.001$; Fig. 11B). Presynaptic *elav*-

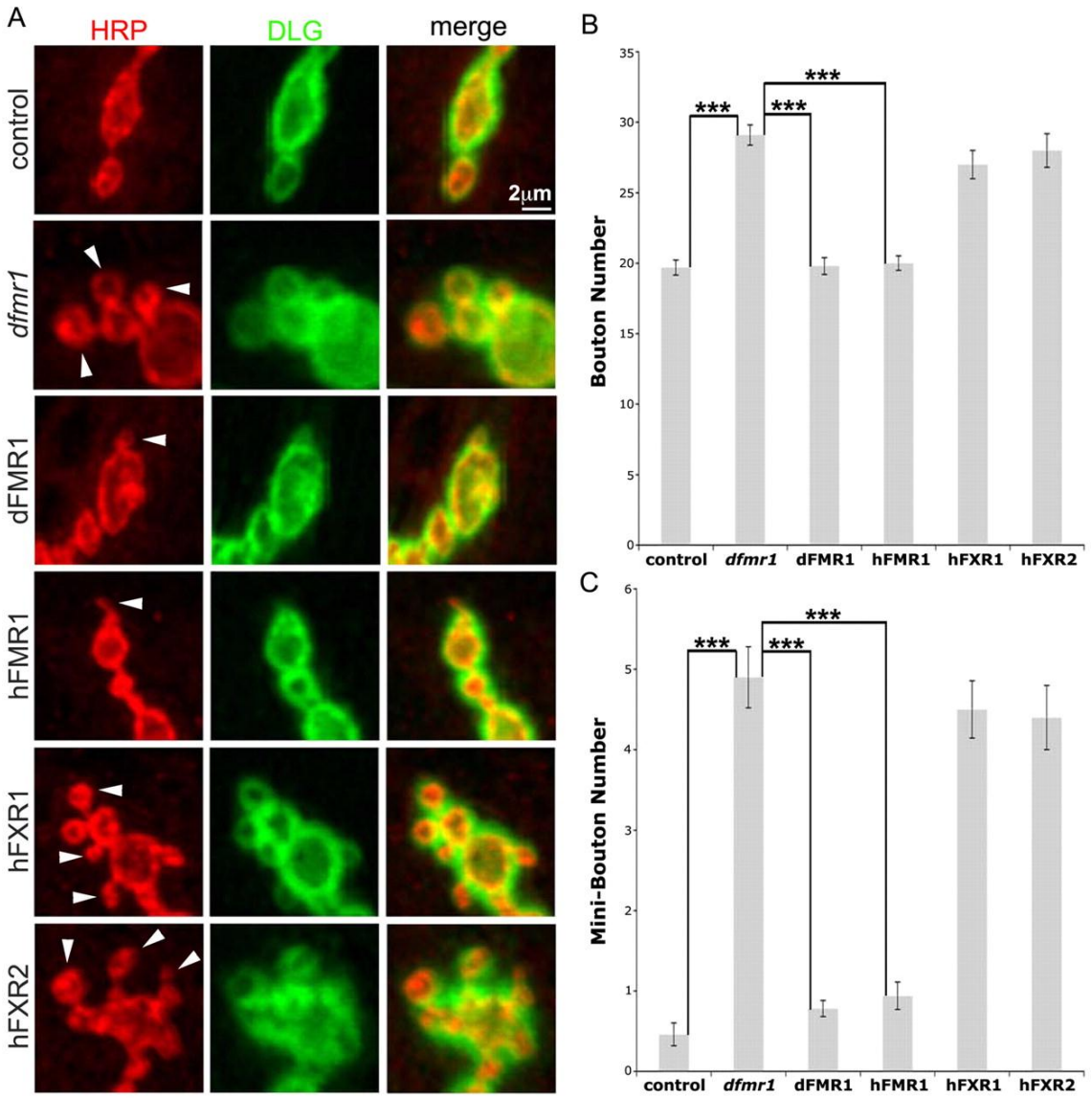

Figure 11. Only *hFMR1* rescues synapse bouton differentiation in *dfmr1* null mutants. (A) Representative high magnification images of synaptic boutons. Mature type 1b boutons were defined as boutons >2 μm in minimal diameter. Satellite mini-boutons, representing an early stage in bouton differentiation, are <2 μm in diameter and are directly attached to a mature type 1b bouton (arrows). Developmentally arrested mini-boutons accumulate in the *dfmr1* null mutant. Bar, 2 μm. Quantification of the number of mature boutons (B) and mini-boutons (C) per synaptic arbor in the six genotypes. The two independent lines for each human transgene were not significantly different, and were therefore pooled for these comparisons. Sample size: $n \geq 10$ animals for each genotype. Significance: ***$P<0.001$ for all comparisons.

GAL4 driven expression of the UAS-*dFMR1* positive control completely rescued bouton number back to control levels (19.8±0.6; $n \geq 10$, $P<0.001$; Fig. 11B). Strikingly, human *FMR1* was equally able to completely rescue synaptic bouton number to the wild-type array (20±0.5 boutons; $n \geq 10$, $P<0.001$; Fig. 11B). Conversely, the two paralogs, *hFXR1* and *hFXR2*, were totally incapable of restoring the elevated bouton number in the *dfmr1* null (27±1.0 and 28±1.2 boutons, respectively; $n \geq 10$, Fig. 11B). A particularly key feature of the null mutant phenotype is the accumulation of small, immature mini-boutons (Fig. 11A; arrows). These boutons were elevated 10-fold in the *dfmr1* null compared to genetic controls (*dfmr1*, 4.9±0.4; control, 0.46±0.14; $n \geq 10$, $P<0.001$; Fig. 11C). The positive control *dFMR1* was able to strongly rescue mini-bouton number back to wild-type levels (0.78±0.1; $n \geq 10$, $P<0.001$; Fig. 11C). With the same efficiency, human *FMR1* also restored mini-bouton numbers to control levels (0.94±0.17; $n \geq 10$, $P<0.001$; Fig. 11C). However, the two paralogs, *hFXR1* and *hFXR2*, were totally incapable of restoring the elevated mini-bouton number, which remain just as elevated as in the *dfmr1*-null mutant condition (4.5±0.36 mini-boutons and 4.4±0.4 mini-boutons, respectively; no significant difference from *dfmr1*; $n \geq 10$; Fig. 11C). These findings further delineate a specific role for *FMR1* in the control of synaptic architecture and bouton maturation that cannot be in the least compensated by its *FXR* paralogs.

Human *FMR1*, *FXR1* and *FXR2* all restore male fecundity and spermatogenesis

FXS patients display a range of non-neuronal symptoms, the most prominent of which is impaired testicular development in male patients (Lachiewicz and Dawson, 1994; Nistal et al., 1992; Turner et al., 1980). Both mouse and *Drosophila* disease models are similarly characterized by enlarged testes and reduced testicular function (Slegtenhorst-Eegdeman et al., 1998; Zhang et al., 2004). Null *dfmr1* males exhibit severely reduced fertility due to immotile sperm (Zhang et al., 2004). We utilized these defects as a sensitive assay for the non-neuronal roles of the three human genes. Each transgene was driven in the male germline with a *nanos* GAL4 driver line (*nos*-GAL4; Fig. 12A). Males of each genotype were mated to virgin wild-type females and the number of resulting progeny assessed. Nine male genotypes were tested: wild-type control, *dfmr1* null, and the UAS-*dFMR1* positive control and two independent lines each for the three human transgenes in the *dfmr1* null mutant background.

We first confirmed that *nanos*-GAL4 drives expression in the testes as previously described (Fig. 12C) (Schulz et al., 2004). Using the common MYC epitope tag on all 4 transgenes, similar transgene expression was present in all cases, with the highest expression in germline stem cells and lower expression throughout the spermatagonia, as expected (Fig. 12C). We then carried out male brooding tests with wildtype, *dfmr1* null and all 4 transgenic lines. All male genotypes where paired with three w^{1118} virgin females, allowed to mate for 9 days and progeny counted for a further 9 days. Wild-type control males produced an average of 138.5±1.3 progeny under these conditions (n=8 trials; Fig. 12B). In

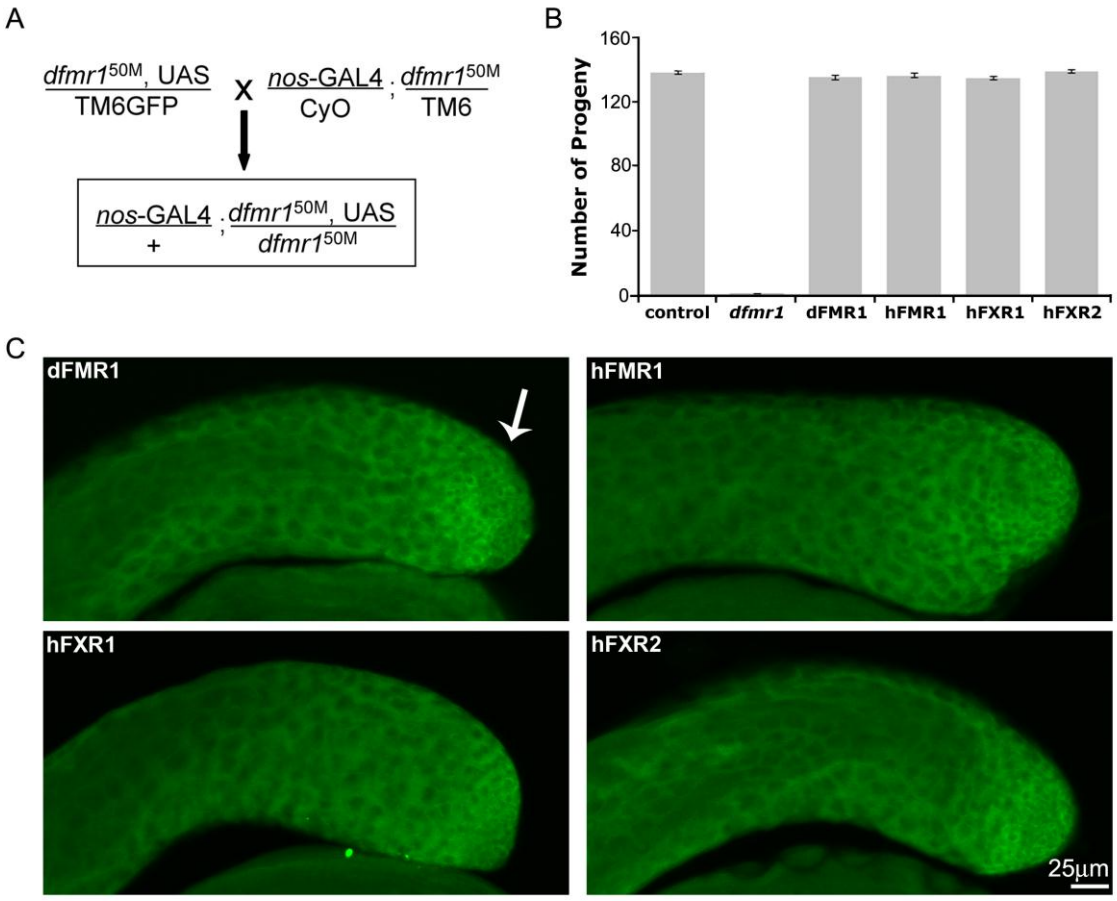

Figure 12. All three human genes rescue *dfmr1* mutant male fecundity. (A) The crossing scheme used to assay transgene function in the testes. The germline *nos*-GAL4 line was used to drive UAS-*dFMR1* (control) and the three human transgenes (UAS-*hFMR1*, UAS-*hFXR1* and UAS-*hFXR2*) in the *dfmr1* null mutant background. (B) Quantification of the number of progeny per male for all six genotypes. The *dfmr1* null mutant is effectively sterile owing to non-motile sperm. The two independent lines for each human transgene were not significantly different in any case, and were therefore pooled for these comparisons. (C) Representative images of adult male testes (<24 hours) with the *nos*-GAL4 line driving expression of the four MYC-tagged transgenes. Anti-MYC labeling was used to detect UAS-*dFMR1*, -*hFMR1*, -*hFXR1* and -*hFXR2*. Expression was highest in the germline stem cells (arrow) and early spermatid progeny, as expected for the *nos*-GAL4 driver. Bar, 25 µm.

sharp contrast, the *dfmr1* null was completely sterile in these trials, producing no viable progeny. The positive transgenic control of UAS-*dFMR1* driven by *nos*-GAL4 in the null background completely rescued the male fecundity defect (135.3±1.5 progeny, *n*=8 trials; Fig. 12B). To our surprise, all three human genes were similarly capable of completely rescuing mutant male performance to control levels. The human *FMR1* gene restored the number of progeny to 136.5±2.0 per male. The two paralogs, *hFXR1* and *hFXR2*, similarly restored the mutant male output to 135.1±1.0 and 139.3±1.1 progeny, respectively (Fig. 12B). Thus, all three human genes fully and equally compensate for the loss of dFMRP in the testes, indicating that they share the conserved function required for male fecundity.

Loss of male fecundity in the *Drosophila* FXS model is caused by defects in sperm tail microtubule organization, which renders the *dfmr1*-null sperm immotile (Zhang et al., 2004). In wild-type testes, the spermatid axoneme contains a 9+2 microtubule configuration of nine outer doublets and a single central pair (Fig. 13A). As the axoneme develops, accessory proteins are added to this core microtubule structure, giving the axoneme its characteristic pinwheel cross-section (see control inset). In *dfmr1* null spermatids, the central pair microtubules are routinely lost (Fig. 13A), while the outer ring microtubule doublets are often deranged (Fig. 13B). The central pair is required for the motility of the sperm tail. This microtubule defect is not caused by misregulation of the MAP1B homolog *futsch*, a key cause of microtubule defects in neurons (Hummel et al., 2000; Zhang et al., 2001), as *futsch* is not detectably expressed

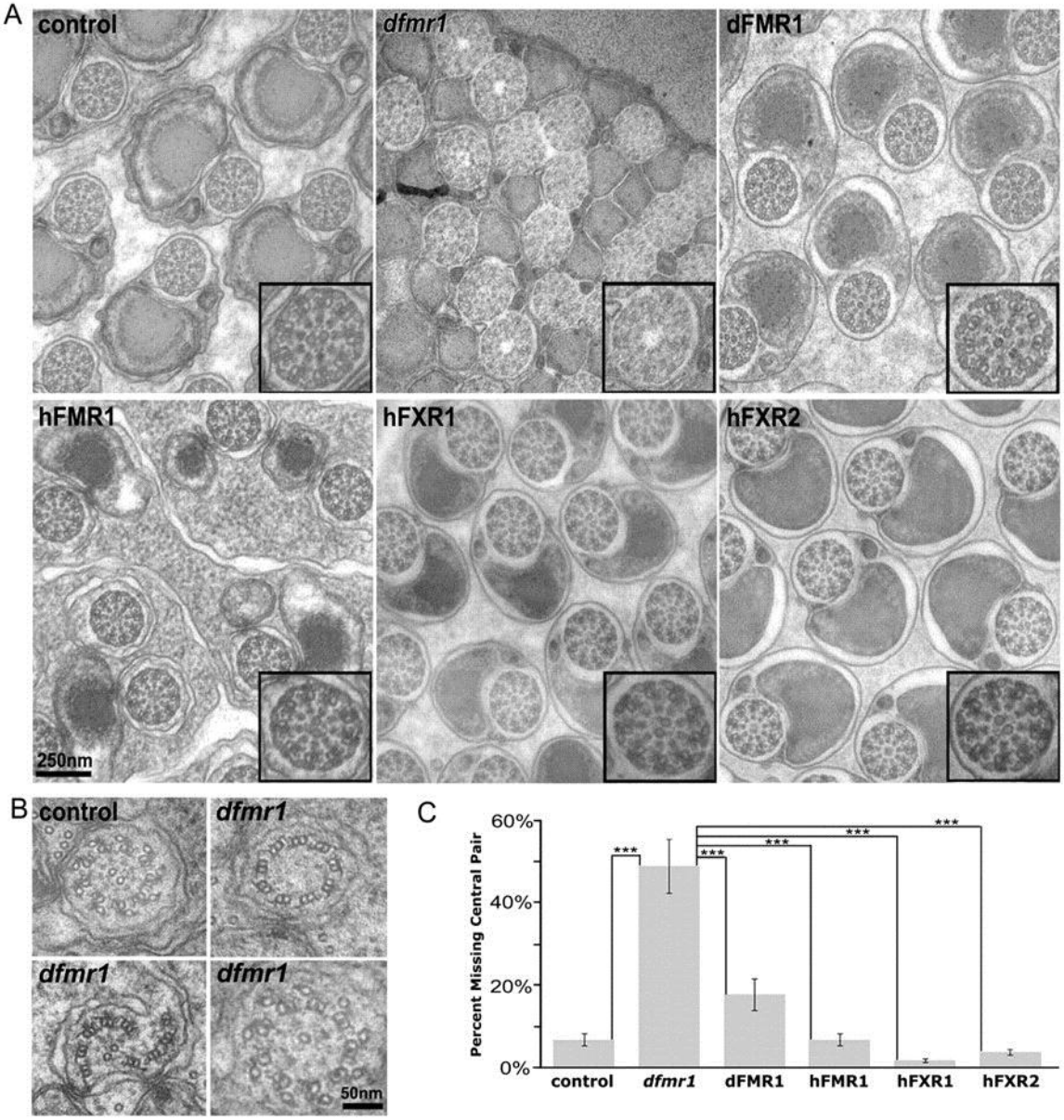

Figure 13. All three human genes rescue *dfmr1* mutant spermatogenesis defects. (A) Representative images of the testes spermatid ultrastructure for all six genotypes. Insets show high-magnification views of a single axoneme. Wild-type sperm tails display the characteristic 9+2 microtubule arrangement of nine outer doublets and the central pair (inset). The *dfmr1* null mutants exhibit disordered microtubules with the central pair missing (inset). Bar, 250 nm. (B) Higher magnification views of the sperm tail axoneme. Control axonemes show a perfectly arranged 9+2 microtubule organization. For *dfmr1* mutants, several examples are shown displaying the range of microtubule disruption phenotypes, including the missing central pair, malformed outer ring. Bar, 50 nm. (C) Quantification of the percentage of spermatids displaying a missing central pair of microtubules from the axoneme for all six genotypes. Significance: ****P*<0.001.

outside of the nervous system. Therefore, this function represents a clearly non-neuronal role for *dFMR1* utilizing an independent molecular mechanism.

To assess the human gene family function, we compared spermatid ultrastructural differentiation in all three UAS human transgenes in the *dfmr1*-null mutant background. Wild-type controls exhibited a consistent 9+2 microtubule array in cross-section of the mature bundled spermatid tails in the testes (Fig. 13B). In contrast, *dfmr1* axoneme abnormalities included variably skewed and malformed outer doublets and the central pair microtubules often completely missing, or occasionally only one microtubule in the central pair was present (Fig. 13B). In wild-type controls, only 7.1±1.2% (*n*=751) of spermatid axonemes lacked a detectable microtubule central pair, whereas *dfmr1* null mutants displayed a 7-fold increase to 49.3±2.5% missing the central pair (*n*=1152, *P*<0.001; Fig. 13C). Expression of the *dFMR1* positive transgenic control was able to strongly restore this axoneme defect (18.4±4.5%) in the null mutant (*n*=588, *P*<0.001; Fig. 13C). To our surprise, all three genes in the human gene family (*hFMR1*, *hFXR1* and *hFXR2*) were also able to fully restore axoneme microtubule architecture to levels comparable with wild-type controls (Fig. 13A). Human *FMR1* expression produced sperm axonemes indistinguishable from wildtype, with only 7.1±1.9% missing the central microtubule pair (*n*=641, *P*<0.001; Fig. 13C). The two paralogs were also fully proficient in this setting, with *hFXR1* rescuing to 2.1±0.7% missing the central pair (*n*=1043, *P*<0.001) and *hFXR2* rescuing to 4.5±1.2% missing the central pair (*n*=1382, *P*<0.001; Fig. 13C). In this non-neuronal assay of function, these results clearly demonstrate complete

redundancy in the function of all three human genes in successfully restoring both male fecundity and the underlying spermatid differentiation defects of *dfmr1*-null mutant animals.

Discussion

Fragile X syndrome (FXS) is caused solely by loss of the *FMR1* gene product. However, humans also have two highly similar gene family paralogs, *FXR1* and *FXR2*, whose function remains comparatively unexplored. The three gene products have been identified as part of the same molecular complex in neurons and other cells, but are clearly not functionally redundant in the FXS disease condition (Bakker et al., 2000; Ceman et al., 1999; Schenck et al., 2001; Zhang et al., 1995). Both homo- and heterodimerization within the gene family may occur, although homodimerization may be more common *in vivo* (Tamanini et al., 1999b). FMRP and FXR2P can be found in complexes lacking FXR1P, indicating possible unique interactive or redundant functional overlap of at least these two proteins (Christie et al., 2009; Tamanini et al., 1999b). The expression of *FXR1* and *FXR2* appear to remain unchanged in FXS patients (Agulhon et al., 1999) and the mouse FXS model, (Bakker et al., 2000) and mutations in *FXR1* or *FXR2* are not associated with FXS or any other disease condition. Nevertheless, *FXR1* is clearly essential, as mouse and zebrafish *FXR1* knockouts are lethal shortly after birth due to cardiac and muscle defects (Mientjes et al., 2004; Van't Padje et al., 2009), showing that *FXR1* has taken on a unique vertebrate muscle function. This is consistent with elevated expression of *FXR1* in muscles (Mientjes et al., 2004). It is not clear what role *FXR1* may play in neurons, where

the protein is present at a lower level. In contrast, mouse *FMR1* and *FXR2* single knockouts display clear neuronal phenotypes (Bontekoe et al., 2002; Comery et al., 1997; Hoogeveen et al., 2002), and the *FMR1/FXR2* double knockout exhibits exaggerated behavioral and neural circuit defects (Spencer et al., 2006; Zhang et al., 2008; Zhang et al., 2009). These findings show that *FXR2*, at least, plays a role in neurons with functional consequences overlapping *FMR1* requirements. However, it is not at all clear whether this link reveals an interaction between *FMR1* and *FXR2* in the same mechanism, or partial compensation permitted because of functional overlap between these two proteins.

Drosophila FMR1 may resemble the common ancestral gene of the vertebrate gene family. *dFMR1* shows high sequence homology, domain conservation and functional properties to *hFMR1* (Zhang et al., 2001; Zhang et al., 2004), but is just as similar to *hFXR1* and *hFXR2*. To validate and further develop the *Drosophila* FXS model, it was critical to determine the evolutionary conservation of *dFMR1* relative to the three human genes. For the last decade, the repeatedly posed question has been whether the *Drosophila* model studies the role of *FMR1*, *FXR1* or *FXR2*, or some combination of all three. Given that FXS is caused solely by loss of *FMR1*, does it play a unique function in the nervous system? If so, is the study of *dFMR1* a good model for this disease-dependent *hFMR1* requirement? To answer these questions, we expressed each of the three human genes independently in the *Drosophila* FXS model and tested for their functional rescue of a carefully selected, diverse range of null mutant

phenotypes. Specifically, we selected the core molecular and cellular phenotypes distributed over the widest range of tissues: the brain, neuromusculature, and testes. Our findings reveal three important conclusions: i) human *FMR1* replaces all *Drosophila FMR1* functions indicating complete functional conservation, ii) *FMR1* has a unique function in *Drosophila* peripheral and central neurons as a translational regulator sculpting synaptic connections, which cannot be compensated for by either *FXR1* or *FXR2*, and iii) the entire human gene family can fully replace the *dFMR1* requirement in the testes, demonstrating a fundamentally different mechanistic requirement in non-neuronal cells.

The hallmark molecular requirement for FMRP is as a negative regulator of translation (Laggerbauer et al., 2001; Schutt et al., 2009; Zalfa et al., 2003; Zhang et al., 2001). FMRP is present in actively translating polyribosomes and inhibits the translation of mRNA targets (Khandjian et al., 2004; Napoli et al., 2008; Reeve et al., 2005; Schutt et al., 2009; Stefani et al., 2004; Yang et al., 2009). In the absence of dFMRP, total protein levels are elevated in the *Drosophila* brain, particularly during the late developmental stages of synaptogenesis and early-use synaptic refinement in newly-eclosed animals (Tessier and Broadie, 2008). This is consistent with the mouse *FMR1* knockout, which also exhibits increased protein synthesis in the brain (Qin et al., 2005). This increase in protein levels is predicted as dFMRP, like mouse FMRP, has been established as a negative regulator of protein translation (Costa et al., 2005; Reeve et al., 2005; Zhang et al., 2001). Using targeted neuronal expression, only *dFMR1* and *hFMR1* can restore elevated brain protein levels

back to the wild-type condition in the *Drosophila* FXS brain. Human FMRP is just as effective as the native fly protein in limiting brain protein expression. Whereas *FMR1* is both necessary and sufficient for this mechanism in neurons, human *FXR1* and *FXR2* are completely unable to rescue this phenotype. Therefore, despite high functional domain conservation, the *FXR* paralogs are unable to compensate for *FMR1* in the mechanism of protein regulation in neurons.

In mammals, *FMR1* and *FXR2* work synergistically (or redundantly) to regulate circadian rhythmicity, with a dramatic impairment only in the double knockout condition (Zhang et al., 2008). While each single mutant animal shows a significant shift of circadian periodicity, the double knockouts are completely arrhythmic and fail to entrain to light. This phenotype is nearly identical to the *dfmr1*-null defect in circadian activity, which has been known for many years (Dockendorff et al., 2002; Inoue et al., 2002). These results suggest that *FMR1* and *FXR2* may cooperate, or be functionally redundant, within the circadian clock neural circuit in a mechanism shared between mammals and flies. In *Drosophila*, the central brain clock circuit is particularly well characterized (Chang, 2006; Helfrich-Forster, 2005; Nitabach and Taghert, 2008). Much attention has focused on the small ventrolateral clock neurons, which secrete the neuropeptide PDF and are sufficient for maintaining circadian rhythms (Grima et al., 2004; Renn et al., 1999; Stoleru et al., 2004). In *dfmr1*-null animals, it has long been known that these neurons produce over-elaborated and over-extended synaptic arbors in the protocerebrum (Gatto and Broadie, 2009a; Morales et al., 2002; Reeve et al., 2005; Sekine et al., 2008). Among the human gene family, only

hFMR1 was able to rescue the synaptic defect in this central circuit. Indeed, *hFMR1* was just as proficient as the native *dFMR1*, indicating full functional conservation of *FMR1* function between flies and humans. In contrast, *hFXR1* and *hFXR2* expression in the clock circuit had absolutely no effect on the null mutant phenotype. Therefore, it is likely that the behavioral augmentation seen in mammals between *FMR1* and *FXR2* is a consequence of effects on complementary pathways that function in the same readout. In any case, it is clear the evolutionarily conserved role in the refinement of central synaptic connections is possessed only by *FMR1* and not its two paralogs, at least in this circuit.

The hallmark cellular defect in FXS patients and genetic disease models is the over-proliferation of synaptic connections, many of which appear to be immature (Grossman et al., 2006; Irwin et al., 2001). Although most research has focused on postsynaptic dendritic spines, apposing presynaptic bouton specializations obviously accumulate in parallel. In the *Drosophila* FXS model, both presynaptic boutons and postsynaptic dendrites are over-grown and over-elaborated in the absence of *dFMR1*, and we have demonstrated that this is a cell-autonomous requirement with neurons (Gatto and Broadie, 2008; Pan et al., 2004). Our previous studies of the well-characterized NMJ synaptic arbor have established a solely presynaptic requirement for *dFMR1* in governing terminal area, synaptic branching and the formation of synaptic boutons (Gatto and Broadie, 2008). Null *dfmr1* synapses display increased terminal area, synaptic branching and supernumerary synaptic boutons. As in the central brain, our work

here demonstrates that only *dFMR1* and *hFMR1* are able to curb growth and restore normal synaptic architecture in the null mutant. In sharp contrast, the *FXR* paralogs do not possess this ability to any detectable degree. Thus, *FMR1* has the unique ability to sculpt synaptic connections also in the context of the *Drosophila* peripheral nervous system.

A defining feature of the overgrown synaptic connections arising in the absence of *dFMR1* is that they appear structurally immature. The NMJ is characterized by the accumulation of so-called “mini” or “satellite” boutons in *dfmr1*-null mutants (Gatto and Broadie, 2008). These immature boutons represent a developmentally arrested state of an otherwise normal stage of bouton maturation (Ashley et al., 2005; Beumer et al., 1999; Dickman et al., 2006; Torroja et al., 1999). In the absence of *dFMR1*, there is a 50% increase in the number of structurally mature boutons, but a striking 10-fold elevation in the abundance of these immature mini-boutons. Only the transgenic introduction of *dFMR1* and *hFMR1* can overcome this developmental arrest, restoring the normal number of mature synaptic boutons and eliminating the accumulation of mini-boutons. *FXR1/2* in contrast, exhibit no restorative activity in synaptic bouton differentiation. Although functional domains appear similar between all members of the human gene family, as well as *dFMR1*, it is not established that FXR1P and FXR2P bind the same target mRNAs as FMRP or, if so, regulate them in the same fashion. Indeed, differential binding and regulative activities have been proposed (Cavallaro et al., 2008; Tamanini et al., 1999a). In the *Drosophila* context, we have shown here that only *FMR1* has any detectable role

in regulating neuronal protein expression. Clearly neuronal expression of either *FXR1* or *FXR2* is not sufficient to remodel synaptic structure, at two very different classes of synapse, or to maintain the normal program of synaptic differentiation. We therefore conclude that *FMR1* has a unique function in mRNA regulation required for the proper development and differentiation of synaptic connections.

The critical breadth of this study came from investigating a key non-neuronal FXS phenotype: the role of *FMR1* in testes development and the maintenance of male fecundity. Male FXS patients have enlarged testes and reduced fecundity accompanied by spermatogenesis defects (Lachiewicz and Dawson, 1994; Nistal et al., 1992; Turner et al., 1980). The *Drosophila* FXS model similarly exhibits enlarged testes and decreased fecundity caused by defects in spermatid maturation resulting in immotile sperm (Zhang et al., 2004). Normal mature sperm tails present the “9+2” microtubule configuration of nine outer doublets and a single, specialized central pair. In *dfmr1*-mutant spermatids, the central pair microtubules are often completely lost, while the outer ring microtubule doublets are more occasionally disordered. To our initial amazement, all three human family genes (*FMR1*, *FXR1* and *FXR2*) are equally capable of fully providing this requirement. Each gene driven by a germline promoter completely restores the null male mutant fecundity and rescues all aspects of the testes development defects. Ultrastructural analyses show normal “9+2” microtubule architecture in all cases. Thus, in contrast to the *FMR1*-specific role in neurons, *FMR1* and its two *FXR* paralogs show complete functional overlap and competency in this non-neuronal context. These results suggest the

startling conclusion that *FMR1* functions in a fundamentally different way in the nervous system compared to the testes.

It is important to note that these experiments were performed using the longest cDNA constructs of each gene, and thus may not take into account the function of unique splice isoforms. At least *FMR1* and *FXR1* are expressed as differential isoforms, with some transcripts expressed more strongly in some tissues than others (Davidovic et al., 2008; Denman and Sung, 2002; Huang et al., 1996; Khandjian et al., 1998; Kirkpatrick et al., 1999; Sittler et al., 1996). The fact that the full-length *FMR1* construct rescues all phenotypes indicates that the *FMR1* transcript heterogeneity is dispensable, at least at the level of phenotypes assayed here. However, the same may not be true for *FXR1*. Note that we have not expressed transgenes postsynaptically in muscle, and therefore cannot rule out some trans-synaptic mechanism by which muscle *FXR1* could potentially alter *dfmr1* NMJ phenotypes. This seems unlikely, however, given that all NMJ structural phenotypes are fully rescued with presynaptic *dFMR1* (Gatto and Broadie, 2008). In regards to *FXR2*, our findings are surprising because previous studies suggest that *FXR2* may have some redundancy with *FMR1* within neurons. Nevertheless, in our dispersed array of neural assays, there was no *FXR2* function detected, suggesting that neuronal roles for *FXR2* appear mammal specific. The primary conclusion is that the much greater complexity of the mammalian nervous system appears to require unique functions mediated at least by *FXR2*. These mechanisms are sufficiently similar that they can somehow impinge on *FMR1* function.

Methods

Drosophila stocks and genetics

All *Drosophila* stocks were maintained at 25°C on standard cornmeal agar. The control genotype was w^{1118} with a single copy of one of two GAL4 driver lines: w^{1118}*; elav*-GAL4/+ (neuronal assays) and w^{1118}*; nos*-GAL4/+ (germline assays). The null mutant genotype was homozygous $dfmr1^{50M}$ (Zhang et al., 2001) with a single copy of the two GAL4 driver lines: $dfmr1^{50M}$; *elav*-GAL4/+ and $dfmr1^{50M}$*; nos*-GAL4/+. For brain staining, the genotypes UAS-GFP/+; OK107/+ and UAS-GFP/+; $dfmr1^{50M}$; OK107/+ were used to identify the mushroom body with GFP antibodies (Fig. 8). As described below, the four transgenic UAS constructs were UAS-MYC-HA-*dFMR1* (positive control) and the three human transgenes UAS-MYC-*hFMR1*, UAS-MYC-*hFXR1* and UAS-MYC-*hFXR2*. Third chromosome transformants were recombined with the $dfmr1^{50M}$ allele by conventional genetic techniques. The GAL4 driver lines e*lav*-GAL4 (P[GawB]*elav*C^{155}); (P{w[+mC]=GAL4-elav.L}2/CyO) and *nos*-GAL4 (P{w[+mC]=GAL4-nos.NGT40}); (P{w[+mC]=GAL4::VP16-nos.UTR}MVD2) were obtained from the Bloomington *Drosophila* Stock Center (Bloomington, IN).

Molecular techniques

Generation of UAS-*dFMR1* control line

The control UAS construct of the wild-type *Drosophila FMR1* transgene was generated through three cloning reactions. First, the *dfmr1* coding sequence was amplified from w^{1118} total cDNA by PCR using the Expand Long Template

PCR System (Roche, Indianapolis, IN) according to manufacturer protocol with primers 5′-GCTCGACGAA TGGAAGATCTCCTCGTGGAAGTTCGGCTC-3′ and 5′-GTCTAGATATGTGGCGG CTACATTCAAGGACATC-3′. This sequence spans from the first base of the *dfmr1* start codon through 155 bases into the 3′UTR. Next, the product was double digested with *Xho*I and *Xba*I and ligated into a similarly digested pUAS-T vector to create pUAS-*dfmr1*. A MYC-HA tag was created using oligo 5′-GGAATTCATGGAACAAAAA CTTATTAGCGAAGAAGATCTTGCATATCCGTATGATGTTCCGGATTATGCAG CGGCCGCAA-3′ and the reverse complement. The product was double digested with *EcoR*I and *Not*I and ligated into similarly digested pUAS-*dfmr1*. Last, the *dfmr1* DNA from 155bp from the start of the 3′UTR to 76bp after the end of the 3′UTR was amplified from genomic DNA by PCR using primers 5′-GTCTAGACACAACAACCAACAACAACCACAC-3′ and 5′-GTCTA GACCCGCACTAATTCATGAAGAAATTAACAAC-3′. The product was digested with *Xba*I and ligated into the similarly digested pUAS-*dfmr1* containing the MYC-HA insert. The final plasmid pUAS-MYC-HA-*dFMR1* was purified and confirmed by sequencing. The plasmid was microinjected into w^{1118} embryos by Genetic Services, Inc. (Cambridge, MA). Transformants with stably integrated genomic inserts were identified and mapped to chromosome locations using standard genetic techniques.

Generation of UAS-*hFMR1/hFXR1/hFXR2* lines

All three human gene family cDNAs in the pTL1 vector were kindly provided by Edouard W. Khandjian, URGHM, Centre de Recherche Hôpital St-François

d'Assise, Québec, Canada. The *hFMR1* cDNA was double digested from the pTL1 vector with *EcoR*I and *Pst*I and subcloned into pBluescript II to provide the necessary *Bgl*II site. The *hFXR1* and *hFXR2* cDNAs were double digested with *EcoR*I and *Bgl*II. All three double digested cDNAs were then ligated singly into digested pUAS-T vectors to generate pUAS-*hFMR1*, pUAS-*hFXR1*, and pUAS-*hFXR2*. A MYC tag was generated using the following oligos: *hFMR1* (5′-AAGAATTCATGGAACAGAAACTGATTAGCGAAGAAGATCTGGAATTCAA-3′ and the reverse complement); *hFXR1* (5′-AAGAATTCAT GGAACAGAAACTGATTAGCGAAGAGGATCTGAGATCTAAA-3′ and the reverse complement); *hFXR2* (5′-AAGAATTCATGGAACAGAAACTGATTAGCGAAGAAG ATCTGAGAATTCAA-3′ and the reverse complement). Oligos were boiled for five mins and allowed to cool to 25°C for 1 hr. The product was digested with *EcoR*I and ligated into the similarly digested pUAST vectors already containing human cDNAs. The final plasmids were purified, sequenced and microinjected into w^{1118} embryos by Genetic Services, Inc. Transformants with stably integrated genomic inserts were identified and mapped to chromosome locations using standard genetic techniques. Multiple transgenic lines were isolated for pUAS-MYC-hFMR1, pUAS-MYC-hFXR1 and pUAS-MYC-hFXR2. In all assays, two independent inserts were assayed for each of the three human transgenic lines.

Western blot analyses

Western blots were performed as described previously (Tessier and Broadie, 2008). In brief, a pool of 4-6 heads was homogenized in 1X NuPage sample buffer (Invitrogen, Carlsbad, CA) supplemented with 40 mM DTT. Debris was pelleted by centrifugation at 12,000 rpm at 25°C and samples boiled for 5 mins. Extracts were loaded onto a 4-12% Bis-Tris gel, electrophoresed and transferred to nitrocellulose. Membranes were rinsed once with NanoPure water, blocked for 1 hr in Odyssey Blocking Buffer (Li-Cor, Lincoln, NE) and probed for 12-16 hrs at 4°C with primary antibodies. Antibodies used include: anti-dFMRP (1:3000; 6A15, Sigma, St. Louis, MO), anti-α-Tubulin (1:400,000; B512, Sigma), anti-MYC (1:15; 9E10, *Drosophila* Studies Hybridoma Bank (DSHB), Iowa City, IA) and anti-MYC (1:1000; 71D10, Cell Signaling Technology, Danvers, MA, USA). Blots were washed with 0.1% Triton-X 100 in PBS (PBST) and then probed for 1 hr at 25°C with secondary antibodies. Antibodies used include: Alexa Fluor 680-conjugated goat anti-mouse (1:10,000) and Alexa Fluor 680-conjugated goat anti-rabbit (1:10,000), both from Invitrogen-Molecular Probes (Carlsbad, CA). Blots were imaged using the Odyssey Infrared Imaging System (Li-Cor, Lincoln, NE). Raw integrated intensities were calculated, with levels were normalized to α-Tubulin.

Protein extraction and assay

Brain protein concentrations were determined as described previously (Tessier and Broadie, 2008). In brief, adult *Drosophila* heads (0-7 hours old)

were rapidly frozen in liquid nitrogen and then stored at -80°C. Protein was extracted from 10-20 pooled heads by homogenizing in 8M Urea, 1% SDS supplemented with 1X Complete Protease Inhibitor Cocktail (Roche). The homogenate was incubated at 60°C for 1 hr. Protein concentrations were determined using a MicroBCA Assay (Pierce, Rockford, IL). All concentrations are reported as mean μg protein per head.

Immunohistochemistry

Adult brains, testes, and third instar larvae were dissected and fixed for immunolabeling as described previously (Gatto and Broadie, 2008; Tessier and Broadie, 2008). In brief, all tissues were fixed for 40 mins with 4% paraformaldehyde in PBS (pH 7.4). Preparations were then rinsed with PBS, blocked and permeabilized with 0.1% Triton X-100 in PBS (PBST) containing 1% bovine serum albumin (BSA) for 1 hr at 25°C. Primary and secondary antibodies were diluted in PBST/BSA and incubated 12-16 hrs at 4°C and 2 hrs at 25°C, respectively. Primary antibodies used: anti-dFMRP (1:500; 6A15, mouse, Sigma), anti-pigment dispersing factor (PDF) (1:5; C7 mouse, DSHB), anti-Discs Large (DLG) (1:200; 4F3, mouse, DSHB), anti-horseradish peroxidase (HRP) (1:250; rabbit, Sigma), anti-GFP (1:50,000; clone 290, rabbit, Abcam, Cambridge, MA), and anti-MYC (1:15; 9E10, mouse, DSHB) (1:500; 71D10, mouse, Cell Signaling Technology). Secondary antibodies used were Alexa Fluor 488-conjugated goat anti-mouse IgG and Alexa Fluor 594-conjugated goat anti-rabbit IgG, both from Invitrogen-Molecular Probes. Preparations were mounted in

FluoroMount G (EMS, Hatfield, PA, USA). All fluorescent images were collected using an upright Zeiss LSM 510 META laser-scanning confocal microscope. Images presented as maximum *z*-projections.

Clock neuron analyses

Brains from staged adult animals were dissected in standard saline and then fixed for 40 minutes with 4% paraformaldehyde/ in PBS, pH 7.4. Dissected brains were blocked and permeablized with 0.2% triton X-100 in PBS (PBST) supplemented with 1% bovine serum albumin (BSA) for 1 hr at RT. The small ventrolateral (sLN_v) clock neurons were labeled with anti-PDF antibody staining with Alexa-Fluor secondary (1:250; Invitrogen-Molecular Probes). Primary and secondary antibodies were diluted in PBST with 0.2% BSA and incubated overnight at 4°C and 2 hrs at RT, respectively. All fluorescent images were collected using a Zeiss confocal microscope. The total number of PDF-positive synaptic punctae (>1 μm diameter) were counted for each sLN_v terminal projection on the right and left hemispheres of the brain, for each *n*=1.

Neuromuscular junction structural analyses

The neuromuscular junction (NMJ) of wandering third instar larvae was quantified for structural features as described previously (Gatto and Broadie, 2008). In brief, the muscle 4 NMJ of abdominal segment 3 (A3) was used for all quantification. Values were determined for both left and right A3 hemi-segments, and then averaged for each animal (*n*=1). Synapse area was measured as the

maximal cross-sectional area in a maximum projection of each collected *z*-stack. A synaptic branch was defined as an axonal projection with at least two synaptic boutons. Synaptic bouton classes defined included i) type Ib (>2 μm diameter) and ii) mini/satellite (≤2 μm diameter and directly attached to a type Ib bouton). Each class is reported as number per terminal. ImageJ (http://rsbweb.nih.gov/ij/) was used for automated regional outline and area calculation.

Fecundity measurements

Transgene expression was driven in the male germline with a *nanos*-GAL4 driver line (*nos*-GAL4; (Schulz et al., 2004)). Assays of male fecundity were done as previously described (Zhang et al., 2004). In brief, for brooding tests, individual males ($n \geq 8$) of each genotype were mated to virgin w^{1118} females ($n=3$) at 25°C, and mated animals were removed from vials after 9 days. Adult progeny from individual vials were then counted for a subsequent 9 days.

Electron microscopy

Ultrastructural analyses of *Drosophila* testes were done as previously described (Zhang et al., 2004). In brief, testes from young adults (<24 hrs post-eclosion) were dissected in PBS and fixed in 2% glutaraldehyde in PBS (pH 7.4) for 1 hr. For light imaging, testes were processed for anti-MYC labeling, as above. For EM, preparations were washed in PBS for 10 mins (2X) and then incubated in tannic acid for 30 mins to increase membrane contrast. Preparations were then transferred to 1% OsO_4 in PBS for 2 hrs, and washed in dH_2O for 10

mins (3X). Following secondary fixation, preparations were stained en bloc with aqueous 1% uranyl acetate for 1 hr, washed in dH_2O (3X) and then dehydrated through an ethanol series (50 – 100%). Finally, samples were passed through propylene oxide as a transition solvent using a 1:1 araldite:propylene oxide mixture. The solution was replaced with pure araldite and put under vacuum at 25hg for 1 hr. Samples were put into fresh resin and placed into a 60°C oven overnight. Ultrathin sections (55 – 65 nm) were obtained on a Leica (Wetzlar, Germany) UCT Ultracut microtome and transferred to Formvar–coated grids. Grids were examined on a Phillips CM10 TEM at 80V and images captured with an AMT 2 mega pixel camera. For quantification, sections were taken at a magnification of 19,000X or 25,000X and scored for axoneme microtubule morphology.

Statistics

All statistical analyses were performed using GraphPad InStat 3 (GraphPad Software, San Diego, CA). Unpaired, nonparametric Tukey-Kramer multiple comparisons tests were used to compare means and were applied in parallel to all control, *dfmr1* null and transgenic construct lines. Significance levels in figures are represented as $P<0.05$ (*), $P<0.01$ (**) and $P<0.001$ (***). All error bars represent standard error of the mean (s.e.m.) for independent trials.

Acknowledgments: We are particularly grateful to members of the Broadie Lab for insightful discussion, especially Drs. Cheryl Gatto and Sarah Repicky for

feedback on this manuscript, and Ms. Emma Rushton for technical advice. We thank the Bloomington *Drosophila* Stock Center and the University of Iowa Developmental Studies Hybridoma Bank for *Drosophila* strains and antibodies, respectively. This work was supported by NIH grant MH084989 to K.B.

CHAPTER III

IN VIVO NEURONAL FUNCTION OF THE FRAGILE X MENTAL RETARDATION PROTEIN IS REGULATED BY PHOSPHORYLATION

This paper has been published under the same title in *Human Molecular Genetics*, 2011

R. Lane Coffee, Jr., Ashley J. Williamson, Christopher M. Adkins, Marisa C. Gray, Terry L. Page, and Kendal Broadie

Department of Biological Sciences, Kennedy Center for Research on Human Development, Vanderbilt University, Nashville, TN

Abstract

Fragile X syndrome (FXS), caused by loss of the *Fragile X Mental Retardation 1* (*FMR1*) gene product (FMRP), is the most common heritable cause of intellectual disability and autism spectrum disorders. It has been long hypothesized that the phosphorylation of serine 500 (S500) in human FMRP controls its function as an RNA-binding translational repressor. To test this hypothesis *in vivo*, we employed neuronally targeted expression of three human *FMR1* transgenes, including wildtype (*hFMR1*), dephosphomimetic (*S500A-hFMR1*) and phosphomimetic (*S500D-hFMR1*), in the *Drosophila* FXS disease model to investigate phosphorylation requirements. At the molecular level, *dfmr1* null mutants exhibit elevated brain protein levels due to loss of translational

repressor activity. This defect is rescued for an individual target protein and across the population of brain proteins by the phosphomimetic, whereas the dephosphomimetic phenocopies the null condition. At the cellular level, *dfmr1* null synapse architecture exhibits increased area, branching and bouton number. The phosphomimetic fully rescues these synaptogenesis defects, whereas the dephosphomimetic provides no rescue. The presence of Futsch-positive (microtubule-associated MAP1B protein) supernumerary microtubule loops is elevated in *dfmr1* null synapses. The human phosphomimetic restores normal Futsch loops, whereas the dephosphomimetic provides no activity. At the behavioral level, *dfmr1* null mutants exhibit strongly impaired olfactory associative learning. The human phosphomimetic targeted only to the brain learning center restores normal learning ability, whereas the dephosphomimetic provides absolutely no rescue. We conclude that human FMRP S500 phosphorylation is necessary for its *in vivo* function as a neuronal translational repressor and regulator of synaptic architecture, and for the manifestation of FMRP-dependent learning behavior.

Introduction

Fragile X syndrome (FXS) is the most common monogenic cause of intellectual disability and autism (Clifford et al., 2007; Cohen et al., 2005; Fisch et al., 2002; Hagerman et al., 2005; Rogers et al., 2001), with an estimated prevalence of ~1:4000 males and ~1:6000 females (Koukoui and Chaudhuri, 2007; Penagarikano et al., 2007). The X-linked neurodevelopmental disorder is

caused by loss of *fragile X mental retardation 1* (*FMR1*) gene function, most frequently via expansion of a CGG trinucleotide repeat (>200 repeats) in the 5′ UTR leading to subsequent hypermethylation, transcriptional silencing, and loss of the FMRP gene product (Heitz et al., 1992; Oberle et al., 1991; Pieretti et al., 1991). FMRP has three well-defined RNA-binding domains, including KH1/2 domains (heterogeneous nuclear ribonucleoprotein K homology) (Siomi et al., 1993) and RGG box (containing repeats of an Arg-Gly-Gly motif) (Darnell et al., 2001). Consistent with its ability to bind mRNA, FMRP regulates transcript trafficking and functions as a negative regulator of translation (Dictenberg et al., 2008; Estes et al., 2008; Laggerbauer et al., 2001; Mazroui et al., 2002). In *Fmr1* null mice, rates of cerebral protein synthesis are increased (Qin et al., 2005), showing that FMRP acts as a negative regulator of translation *in vivo*. FMRP is phosphorylated on a specific serine (human S500; murine S499; *Drosophila* S406) that is N-terminal to the RGG box (Ceman et al., 2003). Following phosphorylation of this residue, hierarchical phosphorylation occurs on two neighboring serines. In a phosphomimetic, the negative charge from the aspartic acid substitution at mouse S499 has been shown to be necessary and sufficient for FMRP function *in vitro* (Ceman et al., 2003). This phosphorylation switch is widely hypothesized to control the activity of FMRP as a translational repressor modulating neuronal function and behavioral output.

Post-mortem analyses of FXS patient brains reveal abnormal synaptic architecture (Irwin et al., 2000; Irwin et al., 2001a). The hallmark of the disease state is an increase in postsynaptic dendritic spines with immature morphology,

and a decrease in spines with mature morphology. In particular, neocortical pyramidal cells in FXS patients exhibit significant elevation of long dendritic spines and fewer mature dendritic spines compared to control subjects (Irwin et al., 2000; Irwin et al., 2001a). These changes in synaptic architecture are thought to underlie the major behavioral symptoms of the FXS disease state, including cognitive dysfunction and learning disabilities (Gallagher and Hallahan, 2011; Mercaldo et al., 2009; Rousseau et al., 1994). FXS has been extensively investigated in both vertebrate and invertebrate genetic model systems (Bassell and Warren, 2008; Bhogal and Jongens, 2010; Gatto and Broadie, 2009a). Both *Drosophila* and mouse disease models exhibit loss of translational control with elevated brain protein levels, synaptic architecture defects and deficits in learning abilities (Bolduc et al., 2008; Dictenberg et al., 2008; Muddashetty et al., 2011; Nakamoto et al., 2007; Narayanan et al., 2008; Pan et al., 2008; Pan et al., 2004; Tessier and Broadie, 2008). Recent studies have shown that phosphorylation of FMRP modulates miR-125a regulation of PSD-95 mRNA translation (Muddashetty et al., 2011). Using the murine phosphomimetic S499D, this work shows significantly reduced PSD-95 protein levels, while expression of the dephosphomimetic S499A had no effect on levels. This work indicates the critical role of S499 in mediating the inhibition and mGluR-mediated activation of PSD-95 mRNA translation involving miR-125a (Muddashetty et al., 2011). Data suggests that dephosphorylation of FMRP is an essential step for subsequent dissociation of RISC from FMRP-bound PSD-95 mRNA and activates mRNA translation. We have shown previously that introduction of human FMRP into the

Drosophila FXS model rescues all defects (Coffee et al., 2010), demonstrating functional conservation. This enables us to now pursue systematic structure-function analyses of human FMRP within the genetically malleable *Drosophila* system. Here, we investigate for the first time the *in vivo* requirements of S500 phosphorylation in human FMRP.

In this study, we generate dephosphomimetic and phosphomimetic transgenes (*S500A-hFMR1* and *S500D-hFMR1*, respectively) transformed into the *Drosophila* FXS disease model (Zhang et al., 2001). Both mutant transgenic conditions are compared with the *dfmr1* null mutant alone (negative control) or containing the wildtype human *FMR1* transgene (positive control), with expression targeted by GAL4 drivers specific to neurons and specific brain regions. Each human transgene is investigated in two independent transgenic lines in the *dfmr1* null mutant background. A wide-ranging series of phenotypic tests at the molecular (Tessier and Broadie, 2008), cellular (Gatto and Broadie, 2008; Pan et al., 2008) and behavioral (Bolduc et al., 2008) levels were selected to survey functional requirements in the nervous system. The results show that the transgene mimicking constitutive phosphorylation of the serine 500 residue, *S500D-hFMR1*, has the ability to completely rescue a full range of FXS neuronal defects. Only *S500D-hFMR1* is able to restore normal brain protein levels and synaptic architecture in *dfmr1* null neurons. *S500A-hFMR1* completely lacks this ability to compensate, mimicking the *dfmr1* null condition. Moreover, *S500D-hFMR1* successfully rescues learning performance back to wildtype levels in a Pavlovian olfactory learning assay. In contrast, *S500A-hFMR1* is unable to

rescue learning deficits and is just as impaired as the complete loss of FMRP condition. These results clearly indicate that phosphorylation of a unique, site-specific serine (S500) within human FMRP is necessary for FMRP function *in vivo*.

Results

Transgenic constructs with targeted pan-neuronal expression

Human, murine and *Drosophila* FMRP are all similarly phosphorylated on a specific, conserved serine residue N-terminal to the RGG box; human S500, murine S499 and *Drosophila* S406 (Ceman et al., 2003; Siomi et al., 1993). Phosphorylation of this key serine is proposed to switch FMRP from a resting state to an active state as a negative translational regulator (Bassell and Warren, 2008; Pfeiffer and Huber, 2007; Siomi et al., 1993). To test the hypothesis that human FMRP function is regulated via S500 phosphorylation, we engineered transgenic human cDNA constructs for wildtype *hFMR1* (positive control), dephosphomimetic (*S500A-hFMR1*) and phosphomimetic (*S500D-hFMR1*). We then expressed each transgene with a neural-specific driver (*elav*-GAL4) in the *Drosophila* FXS model (*dfmr1* null mutant). Several independent lines were made for each transgenic condition. The generation and testing of these transgenic animals is illustrated in Figure 14.

All three cDNA constructs were sub-cloned downstream of the UAS promoter sequence (5X UAS; Fig. 14A). A MYC epitope tag was added at the amino terminus of each transgene to track transgenic protein expression. Each

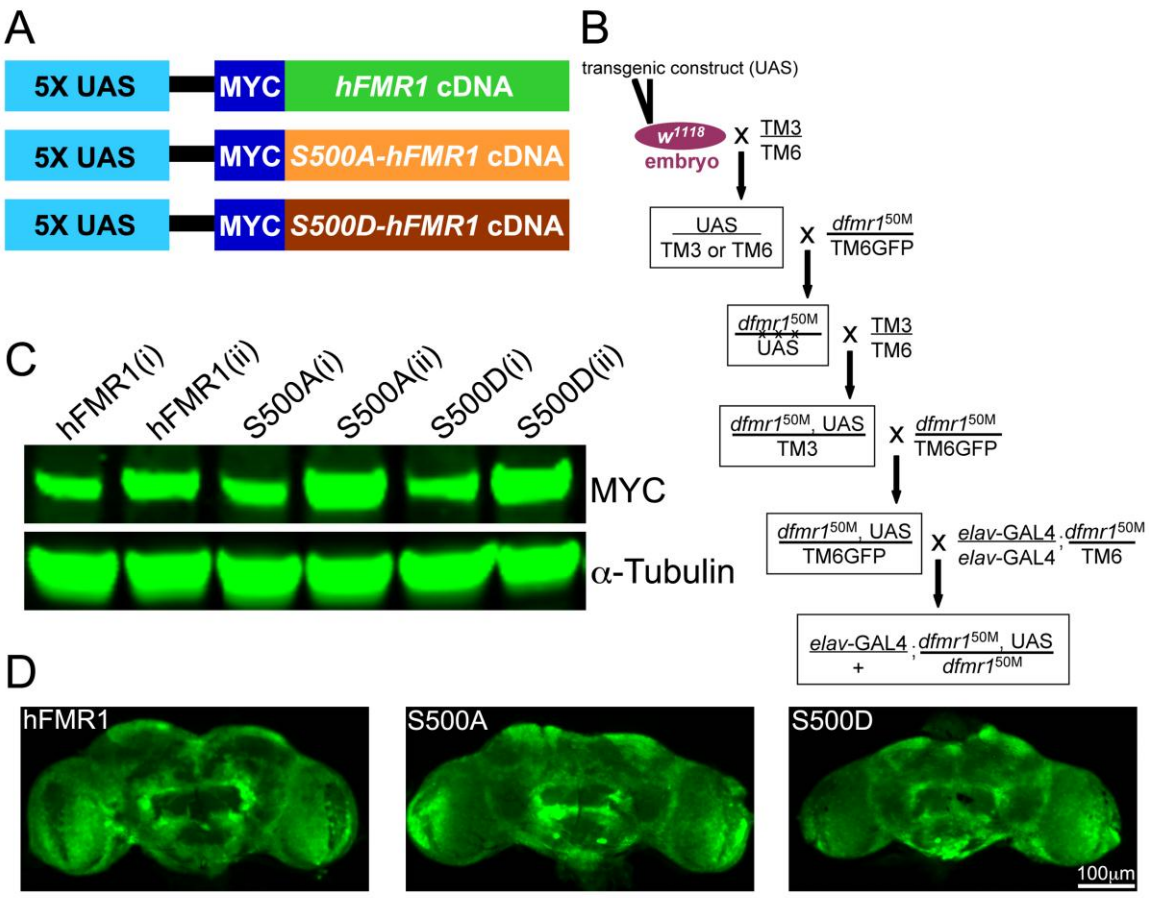

Figure 14. Generation of transgenic constructs with targeted neuronal expression. (A) The three UAS transgenic constructs generated and tested in this study. The positive control is wildtype human *FMR1* (*hFMR1*). The two mimetics are *S500A-hFMR1* and *S500D-hFMR1*. All cDNA transgenic constructs are tagged with a MYC epitope in a pUAST (5X UAS) expression vector to follow protein expression. In all assays, two independent transgenic lines for each human transgenic construct have been analyzed. (B) The embryonic transformation and genetic crossing scheme to introduce each stably integrated UAS transgene into the *dfmr1* null mutant background and then drive expression with the pan-neuronal GAL4 driver *elav*-GAL4. (C) Western blot analyses of transgenic protein expression for the *hFMR1* line (control) and two independent lines of *S500A-hFMR1* and *S500D-hFMR1* (denoted as i/ii). Expression from brain extracts (1-2 day old adult) was tested with anti-MYC against the epitope tag common to all four transgenes (see A). Lines were selected for comparable low/high transgene expression. The loading control is lpha-tubulin. (D) Brain immunocytochemistry for transgene expression of the *hFMR1* line (control) and the two mimetics (*S500A-hFMR1* and *S500D-hFMR1*). *Drosophila* adult brains (1-2 days old) probed with anti-MYC to detect the transgene epitope tag. Comparable transgene expression occurs in all conditions.

construct was microinjected into genetic background control w^{1118} embryos (Fig. 14B). Multiple stably integrated genomic lines for each transgene were isolated and self-perpetuating stocks generated. Third chromosome transformants were recombined onto the *dfmr1* null ($dfmr1^{50M}$) background, and a stock was produced with TM6GFP serving to balance the recombinant chromosome (Fig. 14B). In order to assay neuronal phenotypes, all transgenic lines were crossed with a stock line homozygous for the pan-neuronal driver *elav*-GAL4 and heterozygous for the $dfmr1^{50M}$ allele. The resulting experimental animals were homozygous null for *dfmr1* harboring a single copy of the UAS transgene and a single copy of the *elav*-GAL4 driver (Fig. 14B). Two independent insertion lines for each human transgene were selected for full phenotype analyses, compared to w^{1118} with *elav*-GAL4 driver alone (wildtype control), the *dfmr1* null with *elav*-GAL4 driver alone (negative control) or driving UAS-*hFMR1* (positive control). Thus, eight genetic lines were compared in all subsequent experimental assays.

The expression of all transgenes was compared with a combination of brain Western blots and brain immunocytochemistry imaging for the common MYC epitope tag (Fig. 14C,D). Endogenous *Drosophila* FMRP expression is ubiquitous in neurons and relatively uniform between neurons throughout the wildtype brain (Coffee et al., 2010). We therefore selected *elav*-GAL4 as the best described pan-neuronal driver mimicking this expression (Gatto and Broadie, 2009a). Transgenic lines with low and high *elav*-GAL4 driven expression comparable to matched UAS-*hFMR1* positive controls were selected (Fig. 14C), and two independent insertion lines with comparable expression for each

transgene used for detailed analyses. Western blot analyses of brain protein extracts show comparable MYC epitope tag low/high expression levels across all selected transgenic genotypes (Fig. 14C). Anti-MYC labeling of brains from all three transgenic conditions showed comparable transgene expression levels and protein distribution across genotypes (Fig. 14D). Importantly, the UAS-*hFMR1* positive control was indistinguishable from the two mimetic human transgenes in brain expression profile (Fig. 14D). Matched lines were thus selected to systematically test their ability to rescue a wide range of *dfmr1* null mutant phenotypes.

Only *S500D-hFMR1* restores brain protein translation levels

In both rodents and *Drosophila*, FMRP acts as a negative regulator of protein synthesis in neurons (Lu et al., 2004; Reeve et al., 2005; Schutt et al., 2009; Zhang et al., 2001). Loss of FMRP-dependent translational regulation is believed to be the root cause of all FXS impairments. In the *dfmr1* null mutant condition, the specific target Chickadee (homolog of actin-binding Profilin) and total brain protein levels are significantly elevated during key stages of synaptic development and refinement, particularly in the immature brain shortly following eclosion (Coffee et al., 2010; Tessier and Broadie, 2008). We therefore first examined if these fundamental molecular defects could be differentially rescued by the *hFMR1* phosphomimetic vs. dephosphomimetic proteins. The *dfmr1* null mutant brain is unaltered in size and gross architecture compared to wildtype and genetic controls (Coffee et al., 2010). Lysates from single *Drosophila* heads were

analyzed at the developmental time window of 0-3 hours post-eclosion (25°C) to compare Chickadee expression levels among genotypes. Total protein was extracted from developmentally-staged heads at 0-7 hours post-eclosion (25°C) to compare gross protein levels among genotypes. Eight independent genetic lines were analyzed in parallel; the wildtype control, *dfmr1* null mutant (negative control), wildtype UAS-*hFMR1* in the *dfmr1* null background (positive control) and two independent lines for the phosphomimetic and dephosphomimetic transgenes.

In order to confirm that hFMRP is indeed phosphorylated in our transgenic animals, we first analyzed Western blots for phospho-hFMRP expression in brain extracts (Fig. 15A). The phospho-specific antibody specifically detects phosphorylation of the targeted amino acid residue S500. Two independent wildtype UAS-*hFMR1* lines showed robust phosphorylation at S500, revealing that human FMRP is phosphorylated normally in the *Drosophila* brain (Fig. 15A). Next we examined two lines of both the phosphomimetic and dephosphomimetic transgenes. As expected, neither S500A nor S500D have detectable bands, denoting phosphorylation does not occur at these residues due to the introduced point mutations (Fig. 15A). A MYC antibody was used to compare protein-loading levels among the genotypes, confirming an equal comparison. We then turned our attention to a well-known FMRP target, Chickadee/Profilin, to assess the function of the mimetics at the level of a single protein. Chickadee protein levels are elevated in the *dfmr1* null animals compared to w^{1118} control (Fig. 15B). Both *hFMR1* and *S500D-hFMR1* were able to restore Chickadee protein levels to

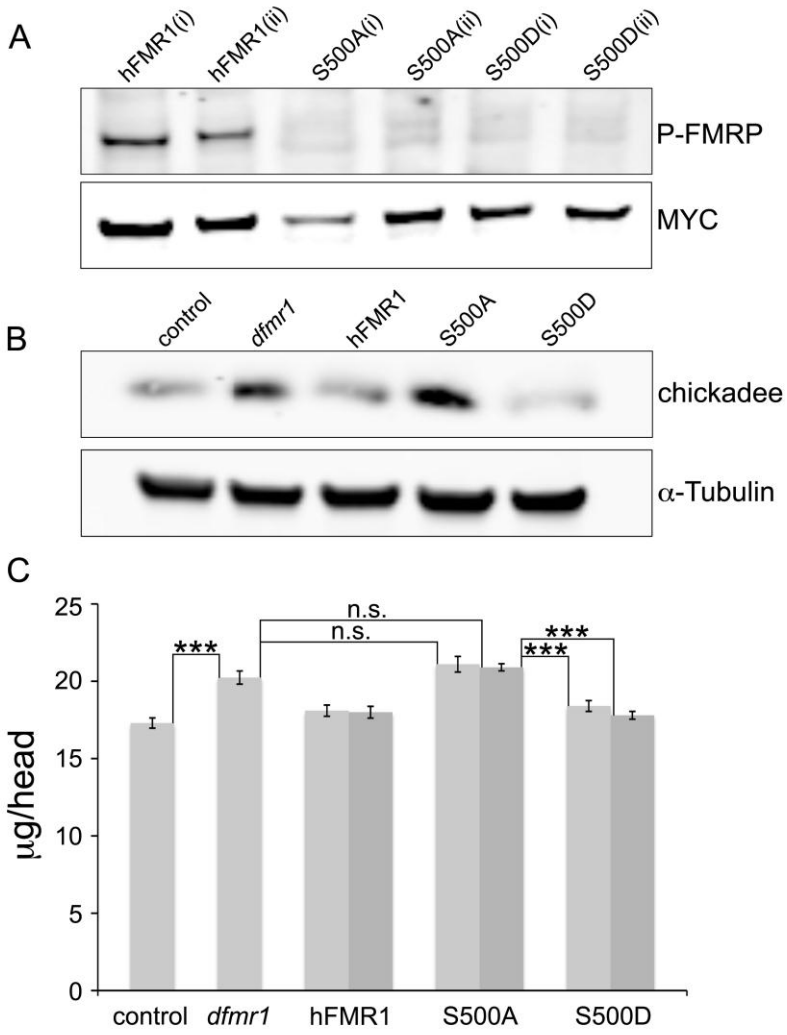

Figure 15. *S500D-hFMR1* rescues elevated brain protein levels in *dfmr1* null. (A) Representative Western blot of S500 phosphorylation state of wildtype *hFMR1* and the two mimetic transgenes in the *dfmr1* null (*dfmr1*^{50M}) *Drosophila* brain. Brain extracts (2 days old) were probed with anti-phospho-FMRP and anti-MYC to control for levels of protein. The two independent lines for each genotype are denoted as i/ii. (B) Representative Western blot of Chickadee expression levels in wildtype control, *dfmr1* null and the three human transgenic lines. Brain extracts (0-3 hour post eclosion) were probed with anti-Chickadee, with anti-α-tubulin used for protein loading control (C) Total brain protein was extracted from young adult (0-7 hour post-eclosion) animals and quantified with a MicroBCA assay. The five genotypes compared are *w*^{1118} control, *dfmr1* null (*dfmr1*^{50M}) and *elav*-GAL4 driving UAS-*hFMR1* (positive control) and two independent lines each of UAS-*S500A-hFMR1* and UAS-*S500D-hFMR1* (light and dark gray bars) in the *dfmr1* null background. Each bar shows the average protein (μg per head). Sample size: 10-20 pooled heads per sample, *n*=8. Significance: ****P*<0.001.

control brain levels. The dephosphomimetic, *S500A-hFMR1*, was unable to restore the level of protein expression and mimics the *dfmr1* null condition (Fig. 15B). A tubulin antibody was used to compare protein-loading levels among the genotypes, confirming an equal comparison (Fig. 15B).

We next measured gross brain protein levels in all five genotypes. Null *dfmr1* mutants with the *elav*-GAL4 driver alone (*elav*/+; $dfmr1^{50M}/dfmr1^{50M}$) have ~20% higher brain protein levels compared to genetic controls (*elav*-GAL4/+) (Fig. 15C). Protein levels per head were 17.3±0.33 μg in control compared to 20.2±0.43 μg in the null mutant ($P<0.001$, $n=8$). The positive transgenic control, *elav*-GAL4 driven UAS-*hFMR1* in the null mutant background, displayed protein levels of 18.0±0.36 μg per head, showing rescue to control levels (not significantly different from wildtype, $n=8$; Fig. 15C). Both independent UAS-*hFMR1* lines (light and dark bars) restored brain protein levels indistinguishable from wildtype control (18.1±0.36 μg, 18.0±0.38 μg; not significantly different from wildtype, $n=8$). Both dephosphomimetic lines, UAS-*S500A-hFMR1*, exhibited elevated brain protein levels comparable to *dfmr1* nulls, with no indication of rescue. The two independent lines showed levels of 21.1±0.51 μg and 20.9±0.23 μg per head, significantly increased from positive controls ($P<0.001$, $n=8$; Fig. 15C). In sharp contrast, both phosphomimetic lines, UAS-*S500D-hFMR1*, rescued brain protein expression back to control levels. The two independent lines showed levels of 18.4±0.35 μg and 17.8±0.25 μg, significantly different from *dfmr1* null ($P<0.001$, $n=8$; Fig. 15C).

These results demonstrate that only the phosphomimetic S500D can rescue the hallmark elevation of brain protein levels in the *dfmr1* null back to the control condition. The dephosphomimetic S500A is unable to restore normal brain protein levels, which remain elevated comparable to the *dfmr1* null. By mimicking the negative charge of a phosphate group with an aspartic acid residue on S500, the phosphomimetic thus appears functionally active. In contrast, by preventing S500 phosphorylation, the dephosphomimetic appears to provide no activity and thus resembles the null protein state. This is the first demonstration that S500 phosphorylation is necessary and sufficient in controlling the functional state of FMRP as a negative translational regulator in the *in vivo* brain.

Only *S500D-hFMR1* restores neuromuscular junction synaptic architecture

In the *Drosophila* FXS model, phenotypes at the glutamatergic neuromuscular junction (NMJ) synapse are extremely well characterized (Coffee et al., 2010; Gatto and Broadie, 2008; Pan et al., 2008; Zhang et al., 2001). The size and accessibility of this synaptic arbor, combined with the wealth of synaptic markers and structural information, make this terminal particularly suited to a systematic investigation. Null *dfmr1* mutants display synaptogenesis defects on several levels of synaptic architecture, including elevated synaptic area, increased synaptic branching and the formation of supernumerary synaptic boutons. Most strikingly, developmentally arrested satellite boutons accumulate in the absence of FMRP function (Coffee et al., 2010; Gatto and Broadie, 2008),

which represent an early stage of normal bouton maturation (Beumer et al., 1999; Gorczyca et al., 2007; Ruiz-Canada et al., 2004). To compare synaptic structure in transgenic animals, we co-labeled wandering third instar larval NMJs with presynaptic (HRP membrane marker) and postsynaptic (DLG scaffold marker) antibody probes. We then quantified synaptic morphology in the wildtype control, *dfmr1* null, *elav*-GAL4 (presynaptic) driven UAS-*hFMR1* positive control, and the phosphomimetic and dephosphomimetic transgenes in the *dfmr1* null mutant background.

Labeling for anti-HRP delineates the innervating presynaptic neuron (red), and co-labeling with anti-DLG reveals the postsynaptic domain (green) of the target muscle (Fig. 16A). The positive transgenic control of *elav*-GAL4 driven UAS-*hFMR1* fully rescued both the enlarged junctional area and increased synaptic branching that characterizes the *dfmr1* null condition (Fig. 16B, C). To quantify synaptic area, the junction delimited by DLG expression was measured. The *dfmr1* null mutation resulted in a significant increase in synaptic area (control, 228.4±5.4 μm^2; *dfmr1* null, 357.6±15.1 μm^2; $n \geq 10$, $P<0.001$; Fig. 16B), while presynaptic wildtype human *FMR1* expression in the null mutant background completely restored junctional area to control levels (236.3±6.9 μm^2; $n \geq 10$, not significantly different from wildtype; Fig. 16B). To quantify branching, HRP-labeled synaptic arbor projections with more than two boutons were counted. There was a significant increase in branching in the *dfmr1* mutants (control, 2.0±0.17; *dfmr1* null 3.1±0.16; $n \geq 10$, $P<0.001$; Fig. 16C). Presynaptic *hFMR1* expression completely restored synaptic branching from the elevated

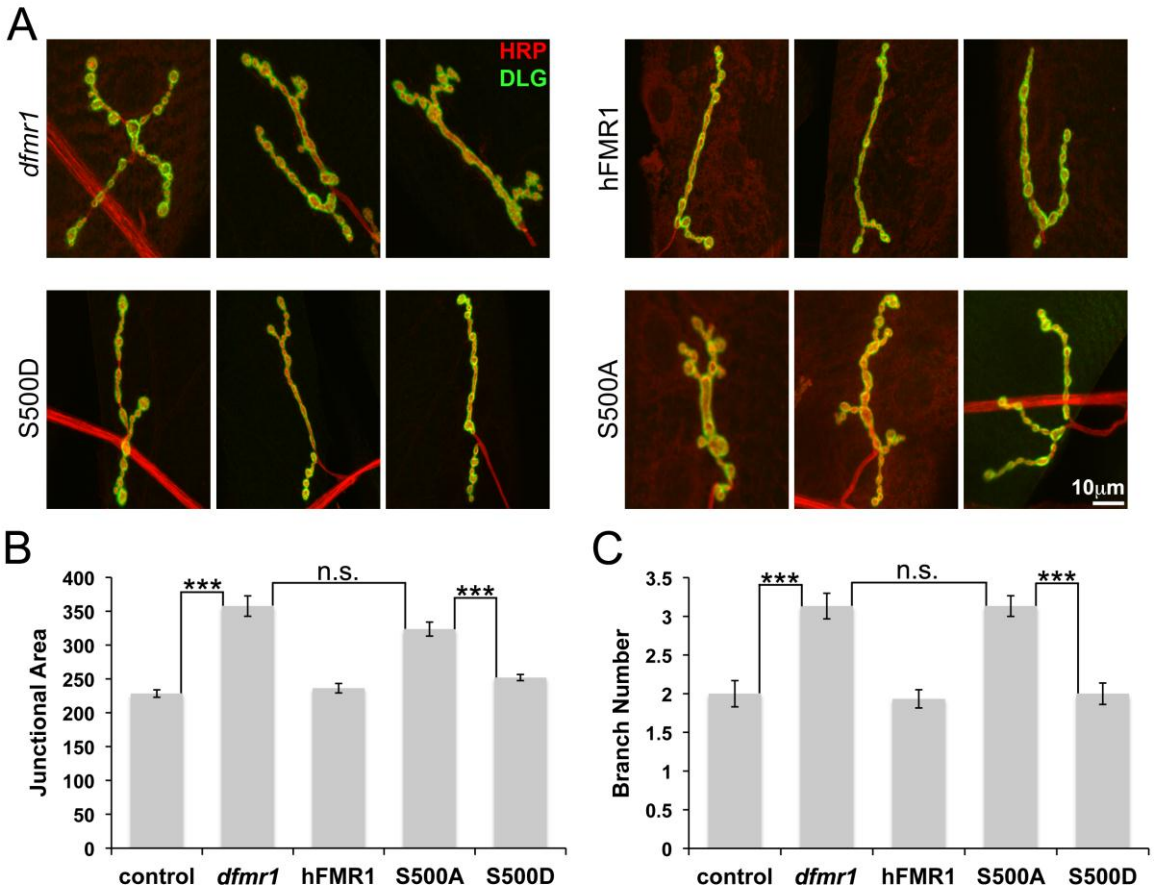

Figure 16. *S500D-hFMR1* rescues NMJ synapse architecture in *dfmr1* null mutant. The wandering third instar NMJ synapse was co-labeled with presynaptic and postsynaptic markers and compared among the five genotypes: wild-type control, *dfmr1* null and *elav*-GAL4 driven expression in the *dfmr1* null background of *hFMR1* (positive control) and two independent lines each of *S500A-hFMR1* and *S500D-hFMR1.* (A) Representative images of the muscle 4 NMJ labeled for presynaptic HRP (red) and postsynaptic DLG (green). Three example synaptic arbors are shown for each of the five genotypes. Scale bar: 10 μm. Quantification of synapse junction area measured based on DLG domain expression (B) and the number of synaptic branches measured based on HRP labeling (C). The two independent lines for each human transgene were not significantly different in any case, and were therefore pooled for these comparisons. Sample size: $n \geq 10$ animals. Significance: ***$P<0.001$.

mutant levels (1.9±0.11 branches; $n \geq 10$, $P<0.001$). Strikingly, *S500D-hFMR1* was equally able to restore synaptic junctional area and arbor branching to wildtype levels (252±4.5 μm^2 area, 2.0±0.14 branches; $n \geq 10$, not significantly different from wildtype; Fig. 16B,C). In sharp contrast, the *S500A-hFMR1* dephosphomimetic was unable to restore synaptic area in the null mutant (323.7±10.3 μm^2; $n \geq 10$; Fig. 16B). Similarly, *S500A-hFMR1* failed to restore normal synaptic branch number in the mutant (3.1±0.13 branches; $n \geq 10$; Fig. 16C). Thus, only the *S500D-hFMR1* phosphomimetic has the ability to maintain gross synaptic architecture, and *S500A-hFMR1* dephosphomimetic completely lacks this ability.

FMRP plays a key role in limiting synaptic bouton number and regulating the normal rate of bouton differentiation (Coffee et al., 2010; Gatto and Broadie, 2008; Siller and Broadie, 2011). To quantify mature type Ib bouton number, HRP/DLG co-labeled varicosities >2μm in minimum diameter were counted within individual synaptic arbors (Fig. 17A). Null *dfmr1* mutants exhibit a significantly increased number of synaptic boutons compared to controls (*dfmr1*, 29.7±0.4; control, 18.7±0.44; $n \geq 10$, $P<0.001$; Fig. 17B). Presynaptic *elav*-GAL4 driven expression of the UAS-*hFMR1* positive control rescued bouton number back to control levels (19.7±0.35; $n \geq 10$, not significantly different from wildtype; Fig. 17B). Strikingly, *S500D-hFMR1* was also able to completely rescue the supernumerary synaptic bouton number to the wildtype array (20.0±0.37 boutons; $n \geq 10$, not significantly different from wildtype; Fig. 17B). Conversely, the *S500A-hFMR1* had little or no impact on synaptic bouton number in the null

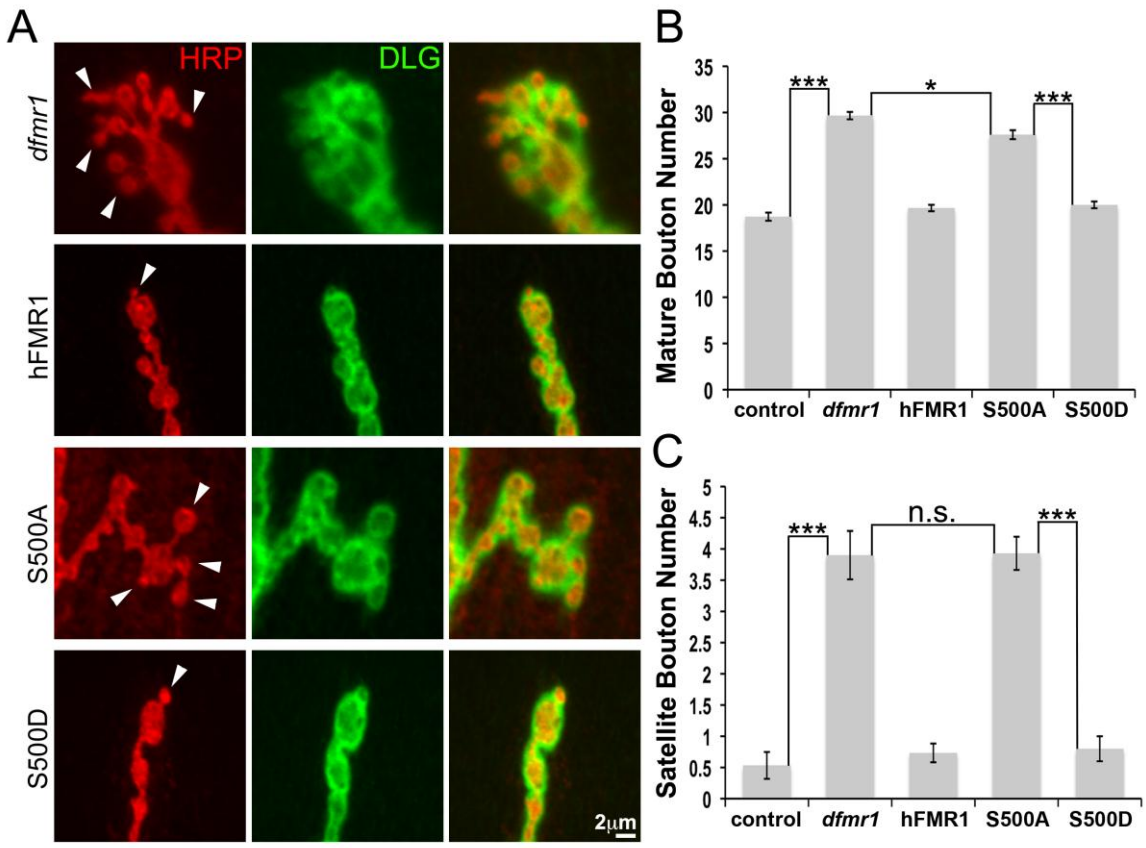

Figure 17. *S500D-hFMR1* rescues synapse bouton differentiation in *dfmr1* null. (A) Representative high magnification images of synaptic boutons. Mature type 1b boutons defined as >2 μm in minimal diameter. Satellite boutons, representing an early stage in bouton differentiation, are <2 μm diameter and directly attached to a mature type 1b bouton (arrows). Developmentally arrested satellite boutons accumulate in the *dfmr1* null mutant. Quantification of the number of mature boutons (B) and satellite boutons (C) per synaptic arbor in the five genotypes is shown. The two independent lines for each human transgene were not significantly different, and were therefore pooled for these comparisons. Sample size: $n \geq 10$ animals for each genotype. Significance: ***$P<0.001$ for all comparisons.

mutant (27.6±0.49; $n \geq 10$, $P<0.001$; Fig. 17B). A key feature of the null mutant phenotype is the accumulation of satellite (immature) boutons (Fig. 17A; arrows). These boutons were elevated 8-fold in the *dfmr1* null compared to genetic controls (*dfmr1*, 3.9±0.4; control, 0.53±0.22; $n \geq 10$, $P<0.001$; Fig. 17C). The positive control *hFMR1* was able to rescue satellite bouton number back to wildtype levels (0.73±0.15; $n \geq 10$, not significantly different from wildtype; Fig. 17C). Similarly, *S500D-hFMR1* was equally able to completely rescue satellite bouton number to the wildtype condition (0.8±0.2 boutons; $n \geq 10$, not significantly different from wildtype; Fig. 17C). Conversely, *S500A-hFMR1* failed to restore satellite bouton number in the null mutant (3.9±0.27; $n \geq 10$, $P<0.001$; Fig. 17C). Thus, only the *S500D-hFMR1* phosphomimetic has the ability to regulate synaptogenesis and thus maintain fine synaptic architecture, whereas the *S500A-hFMR1* dephosphomimetic completely lacks this ability and provides no activity beyond the null mutant condition.

Only *S500D-hFMR1* restores Futsch/MAP1B synaptic cytoskeletal loops

Synaptic architecture is highly dependent on the microtubule cytoskeleton, which is tightly regulated by the FMRP-target Futsch (MAP1B homolog) (Hummel et al., 2000). Futsch/MAP1B is associated with the axonal nerve-terminal microtubule cytoskeleton and is necessary for the regulation of normal synaptic growth and bouton differentiation (Roos et al., 2000; Ruiz-Canada et al., 2004). Futsch/MAP1B translation is negatively regulated by FMRP via a direct mRNA-binding interaction (Zhang et al., 2001), and excess Futsch-positive microtubule

loops accumulate in the synaptic arbor in the *dfmr1* null mutant condition (Gatto and Broadie, 2008). In order to quantify the number of Futsch loops per synaptic junction, wandering third instar larval synaptic arbors were co-labeled with anti-HRP, to outline the terminal boutons, and with anti-Futsch antibody to reveal protein levels and outline microtubule loops (Fig. 18A).

Futsch/MAP1B cytoskeletal loops were compared and quantified in all five genotypes in parallel (Fig. 18B,C). Only Futsch loops that made a completely enclosed circuit (arrowheads) were quantified, with partial-forming loops (asterisks) not included in the counts (Fig. 18A). Null *dfmr1* mutants exhibit significantly increased Futsch synaptic loops compared to controls (*dfmr1*, 4.3±0.41 loops; control, 2.4±0.21 loops; $n \geq 10$, $P<0.01$; Fig. 18B,C). Presynaptic *elav*-GAL4 driven expression of the UAS-*hFMR1* positive control completely rescued Futsch loop number back to control levels (2.2±0.3; $n \geq 10$, not significantly different from wildtype; Fig. 18B,C). *S500D-hFMR1* was equally able to completely rescue synaptic loop number to wildtype levels (2.3±0.26 loops; $n \geq 10$, not significantly different from wildtype; Fig. 18B,C). Conversely, *S500A-hFMR1* was totally unable to restore synaptic Futsch loop number in the null mutant (5.35±0.54; $n \geq 10$, $P<0.001$; Fig. 18B, C). Thus, only the *S500D-hFMR1* phosphomimetic has the ability to correctly regulate synaptic Futsch/MAP1B and maintain the synaptic Futsch loop refinement, whereas the *S500A-hFMR1* dephosphomimetic completely lacks this ability and functionally resembles the complete absence of FMRP protein.

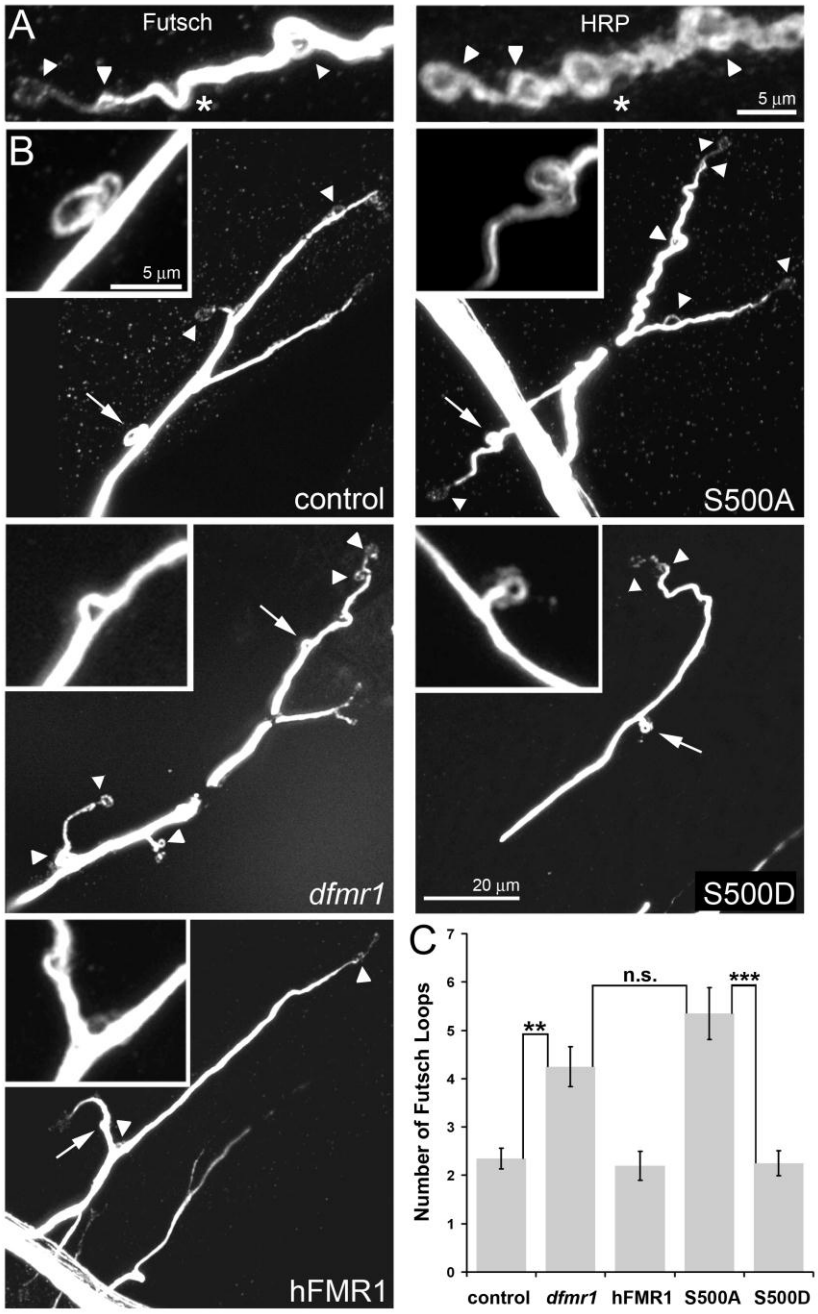

Figure 18. *S500D-hFMR1* rescues Futsch/MAP1B loops in *dfmr1* null synapse. (A) Representative high magnification images of Futsch loops located within NMJ synaptic boutons labeled with anti-HRP. Complete loops were quantified (arrows), but incomplete loops (asterisks) were not counted. (B) Representative images from the five genotypes are shown (loops denoted with an arrowhead) with a high magnification inset of the Futsch loops (loop in inset denoted with an arrow). (C) Quantification of the number of Futsch-positive loops per NMJ terminal. The two independent lines for each human transgene were not significantly different, and were therefore pooled for these comparisons. Sample size: $n \geq 10$ animals for each genotype. Significance: ***$P<0.001$ or **$P<0.01$.

Only *S500D-hFMR1* restores brain circuit synaptic architecture

The hallmark defect in FXS patients and disease models is inappropriate synaptic connectivity in the central brain (Braun and Segal, 2000; Bureau et al., 2008; Comery et al., 1997; Hanson and Madison, 2007). In both mouse and *Drosophila* models, brain synapse architecture also appears immature or developmentally arrested. We therefore next examined synapse architecture in the central brain, based on well-established *dfmr1* phenotypes. In *Drosophila*, a particularly well-defined system is the circadian clock circuitry, in which the small ventrolateral (sLN_v) neurons drive pacemaker activity (Grima et al., 2004; Renn et al., 1999; Stoleru et al., 2004). Null *dfmr1* mutants exhibit strikingly abnormal sLN_v synaptic architecture with expanded terminals containing supernumerary synaptic boutons (Dockendorff et al., 2002; Gatto and Broadie, 2009a; Morales et al., 2002; Sofola et al., 2008). These neurons express the neuropeptide Pigment Dispersing Factor (PDF) and exhibit a characteristic branching pattern with axonal processes projecting dorsally to a defasiculation point in the protocerebrum and then synaptic processes extending medially (Helfrich-Forster, 1995; Helfrich-Forster, 2005). We used anti-PDF labeling on isolated brains to examine impacts on these phenotypes in the *elav*-GAL4 driven UAS-*hFMR1* positive control and the phosphomimetic and dephosphomimetic transgenes in the *dfmr1* null background.

Brains labeled with anti-PDF clearly display the dorsal sLN_v projections into the protocerebrum (Fig. 19A). At the point of axonal defasiculation, the processes split into a localized array comprised of a small synaptic projection at

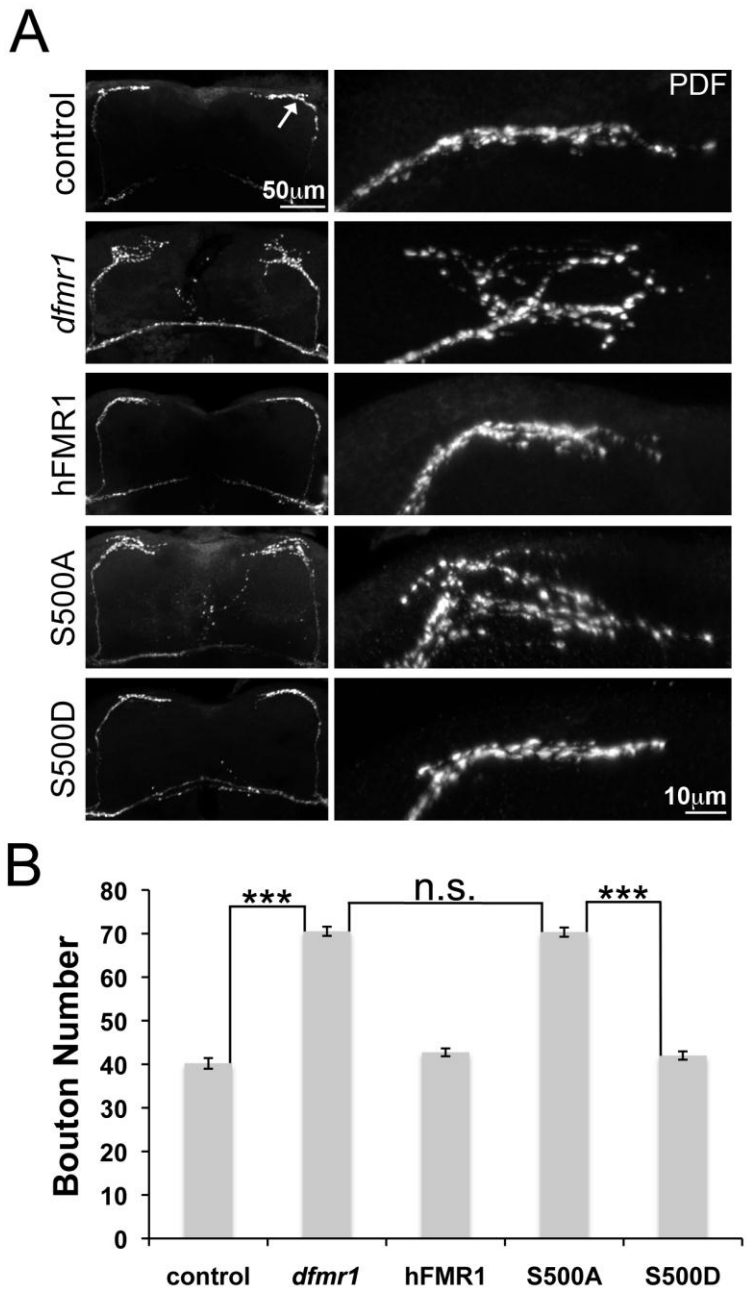

Figure 19. *S500D-hFMR1* rescues central brain synapse arbors in *dfmr1* null. (A) Representative images of adult brain small ventrolateral (sLN_v) neurons labeled with anti-PDF. The low magnification image on the left shows the bilaterally symmetrical sLN_v projections, terminating in synaptic arbor projections (arrow) in the dorsal protocerebrum. The higher magnification images show the left side (right panel) synaptic arbors. Representative images shown from the five genotypes assayed: w^{1118} (control), $dfmr1^{50M}$ null (*dfmr1*) and the null background with *elav*-GAL4 driven *hFMR1*, *S500A-hFMR1*, and *S500D-hFMR1*. (B) Quantification of the number of PDF-positive boutons per synaptic arbor in the five genotypes shown. Sample size: $n \geq 10$ animals for each genotype.

the dorsal horn and into the protocerebrum. These projections are bilaterally symmetrical on the two sides of the brain (Fig. 19A). Null *dfmr1* animals exhibited a highly significant ($n \geq 10$; $P < 0.001$) increase in the individually identifiable number of PDF-labeled boutons compared to controls (Fig. 19A,B). Wildtype terminals contained a mean of 40.2±1.2 boutons compared to 70.5±1.1 in the *dfmr1* null. Thus, the mutant condition shows a ~75% increase in PDF-positive synaptic boutons (Fig. 19B). Expression of wildtype *hFMR1* completely rescued the synaptic overgrowth and excessive defasiculation characterizing the null mutant, and the terminals become clearly more restricted in extent and refined in number of synaptic boutons (Fig. 19B). In the positive control, there was 42.7±1.0 boutons, a number indistinguishable from control and significantly ($n \geq 10$; $P < 0.001$) rescued compared to the *dfmr1* null condition (Fig. 19B). Each mimetic transgene was next expressed to evaluate rescue of the sLN_v synaptic arbor defect in *dfmr1* nulls. *S500D-hFMR1* was able to completely rescue the synaptic bouton number to the wildtype level (42.0±1 boutons; $n \geq 10$, not significantly different from wildtype; Fig. 19B). Conversely, the *S500A-hFMR1* transgenic condition failed to restore synaptic bouton number in the null mutant (70.3±1.1 boutons; $n \geq 10$, $P < 0.001$; Fig. 19B). Thus, only the *S500D-hFMR1* phosphomimetic has the ability to regulate synaptic architecture, whereas the *S500A-hFMR1* dephosphomimetic completely lacks this ability and provides no discernable activity beyond the null mutant condition.

Only *S500D-hFMR1* restores associative learning

To conclude our tests of FMRP requirements, we assayed a key behavioral output. The hallmark of FXS is cognitive dysfunction, including learning disabilities (Gallagher and Hallahan, 2011; Mercaldo et al., 2009; Rousseau et al., 1994). Likewise, both mouse and *Drosophila* FXS genetic models manifest clear learning impairments (Bolduc et al., 2008; Chang et al., 2008; Dockendorff et al., 2002; Krueger et al.; Larson et al., 2008; MacLeod et al.; McBride et al., 2005). In this study, we employed the best-characterized assay for associative learning in *Drosophila*, olfactory learning dependent on the mushroom body (MB) learning center in the central brain. Classical conditioning experiments for olfactory learning were employed (Tully et al., 1994; Tully and Quinn, 1985). Animals were acclimated in a cylindrical shock tube and then exposed to one of two odors (3-octanol or 4-methylcyclohexanol). Following training trials pairing one odor with the aversive shock, the animals were then lowered into a T-maze choice point between the two odors. Wildtype controls have a high learning index with movement toward the un-paired odor, whereas *dfmr1* null mutants display a highly significant decrease in olfactory learning (Bolduc et al., 2008). Here, we assay whether this learning defect can be rescued by introduction of human FMRP, and then test the rescue abilities of the phosphomimetic and dephosphomimetic transgenes in this behavioral paradigm (Fig. 20).

Each human transgenic line was targeted specifically to the MB learning center with the *OK107*-GAL4 driver (Fig. 20A). The arrows indicate transgenic

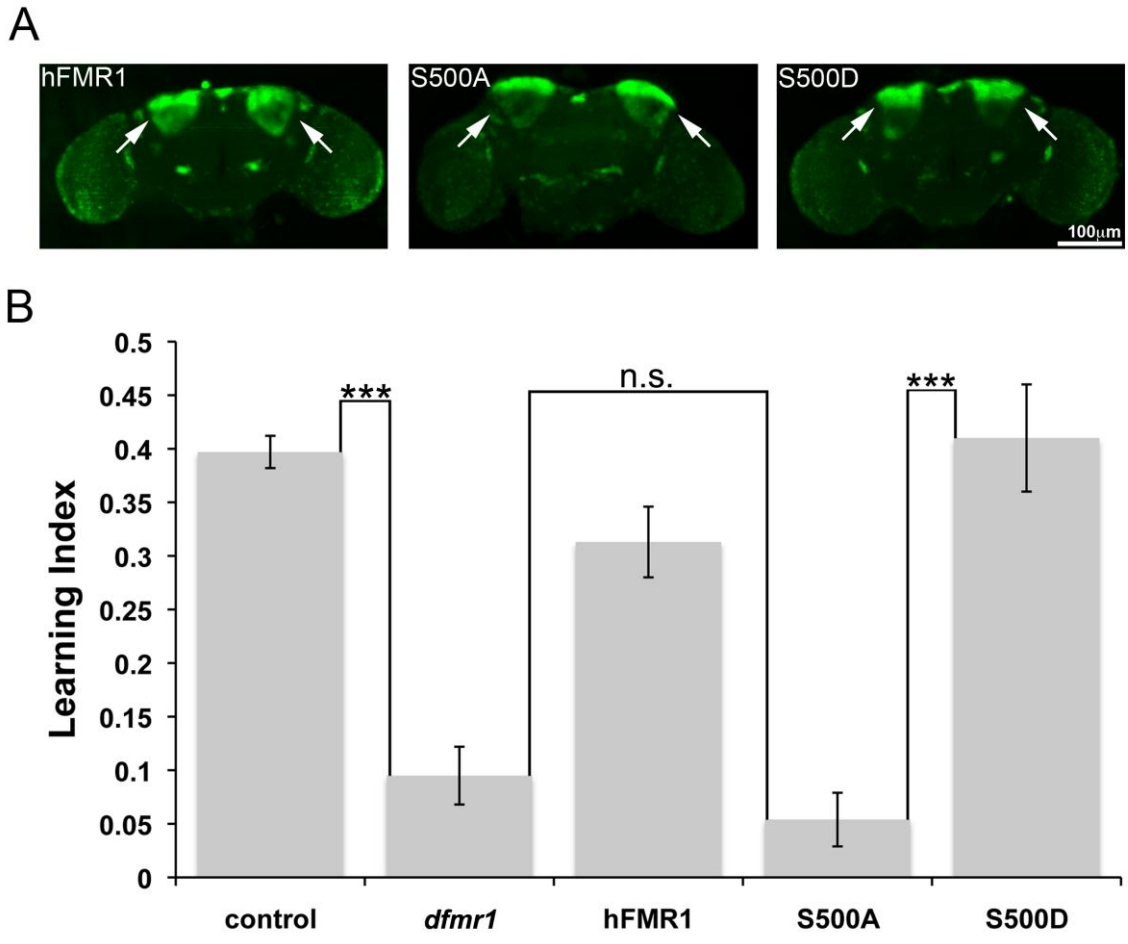

Figure 20. Only *S500D-hFMR1* restores olfactory learning in *dfmr1* null. (A) Representative images of anti-hFMRP brain expression profiles with the mushroom body (MB) specific driver *OK107*-GAL4. Expression specifically targeted to the MB Kenyon cells (arrows). (B) Quantification of learning indices for each of the five genotypes is shown. Only *S500D-hFMR1* restores learning to wildtype levels. Sample size: 75-100 animals per *n*; *n*=10 for each genotype. Significance: ****P*<0.001.

expression restricted to MB Kenyon cell bodies with high specificity. The intensity and distribution of hFMRP was indistinguishable between wildtype and the two mimetic conditions (Fig. 20A). In order to evaluate learning performance indices, 3-octanol and 4-methylcyclohexanol were employed as matched aversive odors. Null *dfmr1* mutants exhibit a significantly decreased learning index compared to controls (*dfmr1*, 0.10±0.03; control, 0.40±0.02; $n \geq 10$, $P < 0.001$; Fig. 20B). There was a 4-fold decrease in learning performance in the absence of FMRP protein. MB *OK107*-GAL4 driven expression of the wildtype *hFMR1* positive control strongly rescued the null mutant learning index back towards control levels (0.31±0.03; $n \geq 10$, not significantly different from wildtype; Fig. 20B). Strikingly, *S500D-hFMR1* was able to completely rescue learning to the wildtype level (0.41±0.05; $n \geq 10$, not significantly different from wildtype; Fig. 20B). Conversely, *S500A-hFMR1* was totally unable to restore learning index in the null mutant (0.05±0.03; $n \geq 10$, $P < 0.001$; Fig. 20B). Learning performance was reduced 8-fold when the FMRP protein was present but could not be phosphorylated at S500. Thus, only the *S500D-hFMR1* phosphomimetic has the ability to rescue the severe learning deficit characterizing the *dfmr1* null mutants. The *S500A-hFMR1* dephosphomimetic exhibits little learning ability and is functionally equivalent to the complete absence of the FMRP protein.

Discussion

Fragile X syndrome (FXS) is caused solely by loss of human FMRP. It has been widely hypothesized that the phosphorylation state of S500 acts as a

“switch” to transition human FMRP from an inactive to active state (Ceman et al., 2003; Cheever and Ceman, 2009; Pfeiffer and Huber, 2007). This hypothesis predicts that human FMRP that cannot be phosphorylated will remain functionally inactive, equivalent to full protein loss, whereas a constitutively phosphorylated protein will be constantly active, but this has never been tested *in vivo*. To test this hypothesis, we expressed both a phosphomimetic (*S500D-hFMR1*) and a dephosphomimetic (*S500A-hFMR1*) in the well-characterized *Drosophila* FXS model (*dfmr1* null mutant; (Gatto and Broadie, 2009b; Tessier and Broadie, 2009)). We then tested for functional *in vivo* rescue of a diverse range of null mutant phenotypes. Specifically, we assayed core molecular and cellular phenotypes in diverse circuits in the neuromusculature and brain, as well as the core behavioral defect of learning impairment. Our findings show that the phosphorylation of the S500 residue of human FMRP is necessary for protein function as a regulator of translation and modulator of synaptic connectivity, which, in turn, lays the foundation for normal behavioral output. The phosphomimetic, *S500D-hFMR1*, provides activity that restores normal function at all levels, to closely mimic the wildtype state. Since the phosphomimetic rescues the morphological defects seen in the *dfmr1* null mutants, our data suggest that the excess growth may be due to elevated protein synthesis. In contrast, the dephosphomimetic, *S500A-hFMR1*, is incapable of providing any functional rescue and closely mimics *dfmr1* null phenotypes at molecular, cellular and behavioral levels.

FMRP is an mRNA-binding protein best characterized as a negative regulator of translation (Laggerbauer et al., 2001; Schutt et al., 2009; Zalfa et al., 2003; Zhang et al., 2001). FMRP is present in stalled polyribosomes and inhibits the translation of mRNA targets (Ceman et al., 2003; Khandjian et al., 2004; Napoli et al., 2008; Reeve et al., 2005; Schutt et al., 2009; Stefani et al., 2004; Yang et al., 2009). In the absence of FMRP, total protein levels are elevated in the *Drosophila* brain, particularly acutely during the late developmental stages of synaptogenesis and early-use synaptic refinement (Tessier and Broadie, 2008). The mouse *FMR1* knockout similarly exhibits increased protein synthesis in the brain (Qin et al., 2005). Phosphorylation mechanisms regulate activity-dependent protein synthesis (Routtenberg and Rekart, 2005). Phosphorylated FMRP preferentially associates with stalled polyribosomes, whereas non-phosphorylated FMRP associates with actively translating polyribosomes (Ceman et al., 2003). Phosphorylation likely confers a protein-binding site conformational change that modulates ribosomal association. Although the molecular mechanism by which FMRP stalls ribosomes has not been elucidated, it is likely to be dynamic, as it can be acutely reversed by RNA decoys in run-off assays (Darnell et al., 2011). This reversibility would most likely be modulated by FMRP phosphorylation (Ceman et al., 2003), but could also involve FMRP degradation (Hou et al., 2006). We have shown previously that human FMRP is just as effective as the native fly protein in restraining brain protein expression, although neither of the human paralogs (*FXR1*, *FXR2*) provides any activity (Coffee et al., 2010). Using targeted neuronal expression, we show here that only

the phosphomimetic (*S500D-hFMR1*) can restore the elevated brain protein levels back to the wildtype condition in the *Drosophila* FXS model. Whereas *S500D-hFMR1* is both necessary and sufficient for this inhibitory mechanism in neurons, *S500A-hFMR1* is unable to provide any function. This provides the first proof that S500 phosphorylation is an essential prerequisite for FMRP's function as a negative translational regulator in the *in vivo* brain.

The hallmark cellular defect in FXS patients, as well as both murine and *Drosophila* disease models, is the over-proliferation of synaptic connections, many of which appear to be immature (Grossman et al., 2006; Irwin et al., 2000; Irwin et al., 2001b). Although most research has focused on the elevated number of postsynaptic dendritic spines, apposing presynaptic bouton specializations accumulate in parallel. In the *Drosophila* FXS model, both presynaptic boutons and postsynaptic dendrites are over-grown and over-elaborated in the absence of FMRP, and we have demonstrated that this is a FMRP cell-autonomous requirement within neurons (Gatto and Broadie, 2008; Pan et al., 2004). Our previous studies of the well-characterized NMJ synaptic arbor have established a solely presynaptic requirement for FMRP in restraining terminal area, synaptic branching and synaptic bouton differentiation (Gatto and Broadie, 2008). Null *dfmr1* synapses display increased terminal area, synaptic branching and supernumerary synaptic boutons (Coffee et al., 2010; Gatto and Broadie, 2008). Our work here demonstrates that only the phosphomimetic (*S500D-hFMR1*) is able to curb growth and restore normal synaptic architecture in the *dfmr1* null mutant. In sharp contrast, the dephosphomimetic (*S500A-hFMR1*) does not

possess this ability to any detectable degree. Thus, phosphorylation is required for FMRP function in regulating synapse architecture.

A defining feature of the overgrown synaptic connections arising in the absence of FMRP is that they appear structurally immature. For example, the *dfmr1* null NMJ is characterized by the accumulation of mini/satellite boutons (Coffee et al., 2010; Gatto and Broadie, 2008). These immature boutons represent a developmentally arrested state of an otherwise normal stage of bouton maturation (Ashley et al., 2005; Beumer et al., 1999; Dickman et al., 2006; Torroja et al., 1999). In the absence of FMRP, there is a ~50% increase in the number of structurally mature boutons, but a striking 8 to 10-fold elevation in the abundance of these immature satellite boutons. Only the transgenic introduction of *hFMR1* and *S500D-hFMR1* can overcome this developmental arrest, restoring the normal number of mature synaptic boutons and eliminating the accumulation of developmentally arrested satellite-boutons. Dephosphorylated *S500A-hFMR1*, in contrast, exhibits no restorative activity in synaptic bouton differentiation or in alleviating the synaptogenic arrest. Thus, phosphorylation of human FMRP is absolutely required for the protein to regulate synaptogenesis.

We first showed that FMRP acts to translationally repress Futsch/MAP1B, and that *dfmr1* null synaptic structure defects are rescued by restoring normal Futsch expression levels (Zhang et al., 2001). At the *Drosophila* NMJ, Futsch binds microtubule loops in a subset of developing synaptic boutons (Roos et al., 2000). These Futsch-positive microtubule structures are proposed to regulate

synaptic growth and bouton differentiation (Dent and Kalil, 2001; Tanaka and Kirschner, 1991). In *dfmr1* null mutants, there is an increased number of Futsch-positive loops throughout the overgrown synaptic arbor, and these supernumerary structures are removed by presynaptic FMRP expression (Gatto and Broadie, 2008). This current study shows a doubling in the number of Futsch loops in the absence of FMRP, compared to wildtype control. Only the transgenic introduction of *hFMR1* and *S500D-hFMR1* can overcome this Futsch elevation, restoring the normal number of Futsch-positive loops in mutant synapses. Dephosphorylated *S500A-hFMR1*, in contrast, exhibits no restorative activity. Thus, phosphorylation of human FMRP is absolutely required for the regulation of Futsch/MAP1B during synaptogenesis.

In the *Drosophila* central brain, the clock circuit is particularly well characterized (Chang, 2006; Helfrich-Forster, 2005; Nitabach and Taghert, 2008). Much attention has focused on the small ventrolateral clock neurons, which secrete the neuropeptide PDF and regulate circadian rhythms (Grima et al., 2004; Renn et al., 1999; Stoleru et al., 2004). In *dfmr1* null mutants, it has long been known that these neurons exhibit over-elaborated and over-extended synaptic arbors in the protocerebrum (Gatto and Broadie, 2009a; Morales et al., 2002; Reeve et al., 2005; Sekine et al., 2008), a phenotype strikingly similar to the NMJ defect. Introduction of human FMRP can fully rescue this synaptic architecture defect. Moreover, only the phosphomimetic (*S500D-hFMR1*) is able to rescue the synaptic defect in the central brain. In contrast, the dephosphomimetic (*S500A-hFMR1*) has absolutely no effect on the null mutant

phenotype. Thus, there is the same requirement for human FMRP phosphorylation in very distinctive neural circuits: in a peripheral motor circuit and in a central brain circuit. These results demonstrate for the first time the absolute requirement for FMRP phosphorylation to regulate synaptic connectivity *in vivo*.

The hallmark of FXS is cognitive dysfunction learning disabilities (Gallagher and Hallahan, 2011; Mercaldo et al., 2009; Rousseau et al., 1994). Consistently, both mouse and *Drosophila* FXS genetic models manifest clear learning impairments (Bolduc et al., 2008; Chang et al., 2008; Dockendorff et al., 2002; Krueger et al.; Larson et al., 2008; MacLeod et al.; McBride et al., 2005). A key brain center of learning in *Drosophila* is the Mushroom Body (MB) and *dfmr1* null mutants have defects in MB organization (β lobe midline crossing) and synaptic connectivity (Bolduc et al., 2008; Michel et al., 2004). Consistently, our previous work has shown that *dfmr1* null mutants have significant defects in MB-dependent learning (Bolduc et al., 2008). Wildtype controls learn to move toward an odor not paired to electrical shock at a T-maze choice point, whereas *dfmr1* nulls have strong deficits in this associative learning task (Bolduc et al., 2008). We show here that MB-targeted expression of human FMRP rescues this defect, and that only the phosphomimetic (*S500D-hFMR1*) maintains this function. In contrast, the dephosphomimetic (*S500A-hFMR1*) has absolutely no effect on the null mutant phenotype. These results show that the FMRP functional requirement in learning is conserved from man to fly, that this requirement occurs within the learning circuit in the central brain, and that phosphorylation of human FMRP at S500 is an absolute prerequisite for function in behavioral learning output. The

current model is that the FMRP-mRNA complex at the synapse exists in a phosphorylated translationally-repressed state until a signal, e.g. mGluR activation, triggers FMRP dephosphorylation that leads to a burst of local translation. Our data show that mRNAs are over-translated in the presence of an unphosphorylated form of FMRP (S500A-hFMRP), but that the phosphomimetic constitutively inhibits translation.

Mouse FMRP is dynamically phosphorylated by ribosomal protein S6 kinase (S6K1) downstream of the mammalian target of rapamycin (mTOR) pathway, and dephosphorylated by the phosphatase PP2A (Narayanan et al., 2007; Narayanan et al., 2008). In murine hippocampal cultures, the non-phosphorylatable murine *S499A-mFMR1* fails to associate with S6K1. In *Drosophila*, FMRP is phosphorylated *in vitro* by casein kinase II (Siomi et al., 2002), although S6K1 might similarly be involved. FMRP was first suggested to be a translational repressor in *in vitro* studies using recombinant FMRP (Laggerbauer et al., 2001). Early work on mouse FMRP phosphomimetic and dephosphomimetic constructs (S499D and S499A, respectively) has strongly suggested that the phosphorylation state regulates translation repressor function (Ceman et al., 2003). More recently, loss of hippocampal S6K1 or introduction of S499A-FMRP has been shown to similarly elevate expression of SAPAP3, a synaptic FMRP target (Narayanan et al., 2008). The current study supports and expands on this work, showing a similar phosphorylation requirement for human FMRP in the broad context of the *Drosophila* FXS model. Surprisingly, however, the constitutive phosphorylation mimicry achieved by human FMRP S500D is

quite adequate to recapitulate wildtype FMRP function in all molecular, cellular and behavioral assays pursued here. *In vivo* FMRP is dynamically phosphorylated and dephosphorylated – shuttling between a functional and non-functional form – in an activity-dependent mechanism (Ceman et al., 2003; Cheever and Ceman, 2009; Pfeiffer and Huber, 2007). Why then does the S500D transgene not produce gain-of-function phenotypes, or simply fail to function? Perhaps animals expressing the FMRP phosphomimetic develop an adaptive mechanism in to manage constitutive activation induced by the phosphorylation state of the transgenic protein. FMRP is acutely degraded upon synaptic stimulation (Gabel et al., 2004), and so one possibility is increased FMRP degradation after synaptic stimulation releases the critical subset of mRNAs from translation repression. Another possibility is that even though there is constitutively mimicked upregulation of the FMRP phosphorylated state, the phosphomimetic may not yield activation comparable to native phosphorylation, but rather more partial phosphorylation mimicry. Experimentally, while this is the best available mimic condition, it is not phosphorylation *per se*, but rather substitution of a phosphate group with a negatively charged aspartic acid residue. Thus, the phosphomimetic may enable partial function resembling an averaged state between the normal dynamic conformations of phosphorylation and dephosphorylation, thereby rescuing near the wildtype level. Of course, this explanation does not adequately address the need for a dynamic “switch,” which seems dispensable based on all the molecular, cellular and behavioral studies presented here.

Materials and Methods

Drosophila stocks and genetics

All *Drosophila* stocks were maintained on standard cornmeal/agar/molasses medium at 25°C in incubators with a 12 hr light:dark cycle. The GAL4 driver lines e*lav*-GAL4 i) (P[GawB]*elav*C^{155}); ii) (P{w[+mC]=GAL4-elav.L}2/CyO) and *OK107*-GAL4 (P{GawB}ey [OK107]) were obtained from the Bloomington *Drosophila* Stock Center (Bloomington, IN). The control genotype was w^{1118} with a single copy of one of two GAL4 driver lines: *elav*-GAL4/+ (all neuronal assays) and *OK107*-GAL4/+ (behavioral learning assays). The null mutant genotype was homozygous *dfmr1*^{50M} (Zhang et al., 2001) with a single copy of the two GAL4 driver lines: *elav*-GAL4/+; *dfmr1*^{50M} and *dfmr1*^{50M}*; OK107*-GAL4/+. As described below, the three transgenic UAS constructs generated were UAS-MYC-*hFMR1* (positive control), UAS-MYC-*S500A-hFMR1* (dephosphomimetic) and UAS-MYC-*S500D-hFMR1* (phosphomimetic). Third chromosome transformants were recombined with the *dfmr1*^{50M} allele by conventional genetic techniques.

Generation of UAS-*hFMR1/S500A-hFMR1/S500D-hFMR1*

An *hFMR1* cDNA was subcloned into pBluescript II and used for the generation of both amino acid substitution constructs using the QuikChange site-directed mutagenesis kit (Stratagene, Cedar Creek, TX). Primers used for *S500A-hFMR1* (alanine at 500) substitution construct: 5′-GAAGCATCAAATGCTGCTGAAACAGAATCTGACCACAGAG AC-3′ and the

reverse complement. Primers used for *S500D-hFMR1* (aspartic acid at 500) substitution construct: 5′-GAAGCATCAAATGCTGATGAAACAGAATCTGACCAC AGAGAC-3′ and the reverse complement. Substituted cDNA fragments were double digested out of pBluescript II with *Eco*RI and *Not*1. Each double digested mutation fragment was then ligated singly into similarly digested pUAS-T vectors to generate pUAS-*S500A-hFMR1* and pUAS-*S500D-hFMR1*. A MYC tag was generated using the following oligo: 5′-AAGAATTCATGGAACAGAAACTGATTAGCGAAGAAGATCTGGAAT TCAA-3′ and the reverse complement. Oligos were boiled for five mins and allowed to cool to 25°C for 1 h. The product was digested with *Eco*RI and ligated into the similarly digested pUAS-T vectors already containing the substituted human cDNAs. The final plasmids were purified, sequenced and microinjected into w^{1118} embryos by Genetic Services, Inc. (Cambridge, MA). Transformants with stably integrated cDNA inserts were identified and mapped to chromosome locations using standard genetic techniques. Multiple transgenic lines were isolated for pUAS-MYC-hFMR1, pUAS-MYC-S500A-hFMR1 and pUAS-MYC-S500D-hFMR1. In all assays, two independent inserts were assayed for each of the three human transgenic lines.

Western blot analyses

Western blots were performed as described previously (Coffee et al., 2010; Tessier and Broadie, 2008). In brief, a pool of 4-6 heads was homogenized

in 1X NuPage sample buffer (Invitrogen, Carlsbad, CA) supplemented with 40 mM DTT. Debris was pelleted by centrifugation at 12,000 rpm at 25°C and samples boiled for 5 mins. Extracts were loaded onto a 4-12% Bis-Tris gel, electrophoresed (1 h. @ 200V) and transferred (1 h. @ 100V) to nitrocellulose. Membranes were rinsed once with NanoPure water, blocked for 1 hr in Odyssey Blocking Buffer (Li-Cor, Lincoln, NE) and probed for 12-16 hrs at 4°C with primary antibodies. Antibodies used include: anti-phospho-hFMRP (1 μg/ml; ab48127, AbCam, Cambridge, MA), anti-α-Tubulin (1:400,000; B512, Sigma, St. Louis, MO), anti-MYC (1:15; 9E10, *Drosophila* Studies Hybridoma Bank (DSHB), Iowa City, IA), anti-Chickadee (1:10; Chi1J, DSHB, Iowa City, IA), and anti-MYC (1:1000; 71D10, Cell Signaling Technology, Danvers, MA). Blots were washed with THAM/NaCl/NP-40 buffer and then probed for 1 h. at 25°C with secondary antibodies. Antibodies used include: Alexa Fluor 680-conjugated goat anti-mouse (1:10,000) and Alexa Fluor 680-conjugated goat anti-rabbit (1:10,000) (Invitrogen-Molecular Probes, Carlsbad, CA). Blots were imaged using the Odyssey Infrared Imaging System (Li-Cor). Raw integrated intensities were calculated, with levels normalized to □lpha-tubulin.

Protein extraction and assay

Brain protein concentrations were determined as described previously (Coffee et al., 2010; Tessier and Broadie, 2008). In brief, adult *Drosophila* heads (0-7 hours old) were rapidly frozen in liquid nitrogen and then stored at -80°C. Protein was extracted from 10-20 pooled heads by homogenizing in 8M Urea,

1% SDS supplemented with 1X Complete Protease Inhibitor Cocktail (Roche, Indianapolis, IN). The homogenate was incubated at 60°C for 1 hr. Protein concentrations were determined using a MicroBCA Assay (Pierce, Rockford, IL). All concentrations are reported as μg protein per head.

Immunocytochemistry

Adult brains and third instar larvae were dissected and fixed for immunolabeling as described previously (Coffee et al., 2010; Tessier and Broadie, 2008). In brief, all tissues were fixed for 40 mins with 4% paraformaldehyde in PBS (pH 7.4). Preparations were then rinsed with PBS, blocked and permeabilized with 0.2% Triton X-100 in PBS (PBST) containing 1% bovine serum albumin (BSA) for 1 h at 25°C. Primary and secondary antibodies were diluted in PBST/BSA and incubated 12-16 h at 4°C and 2 hrs at 25°C, respectively. Primary antibodies used: anti-dFMRP (1:500; 6A15, mouse, Sigma), anti-pigment dispersing factor (PDF) (1:5; C7 mouse, DSHB), anti-hFMRP (1:200; mouse, Chemicon, Temecula, CA), anti-Discs Large (DLG) (1:200; 4F3, mouse, DSHB), anti-horseradish peroxidase (HRP) (1:250; rabbit, Sigma), anti-Futsch (1:200; 22C10, mouse, DSHB), and anti-MYC (1:15; 9E10, mouse, DSHB) (1:500; 71D10, rabbit, Cell Signaling Technology). Secondary antibodies used were Alexa Fluor 488-conjugated goat anti-mouse IgG and Alexa Fluor 594-conjugated goat anti-rabbit IgG, (1:250; Invitrogen-Molecular Probes). Preparations were mounted in FluoroMount G (EMS, Hatfield, PA).

Fluorescent images were collected using an upright Zeiss LSM 510 META laser-scanning confocal microscope. Images are presented as maximum *z*-projections.

Neuromuscular junction analyses

The wandering third instar larval NMJ was quantified for structural features as described previously (Coffee et al., 2010; Gatto and Broadie, 2008). In brief, the muscle 4 NMJ of abdominal segment 3 (A3) was used for all quantification. All fluorescent images were collected using a Zeiss confocal microscope. Intensity values were determined for both left and right A3 hemi-segments, and then averaged for each animal (n=1). Synapse area was measured as the maximal cross-sectional area in a maximum projection of each collected *z*-stack. A synaptic branch was defined as an axonal projection with at least two synaptic boutons. Synaptic bouton classes defined included i) type Ib (>2 μm diameter) and ii) mini/satellite (≤2 μm diameter and directly attached to a type Ib bouton). Each class is reported as number per terminal. ImageJ (http://rsbweb.nih.gov/ij/) was used for automated regional outline and area calculation.

Brain circuit analyses

Brains from staged adult animals (*zeitgeber* time 2-4 h; ZT 2-4) were dissected in standard saline and then fixed for 40 minutes with 4% paraformaldehyde in PBS, pH 7.4 (Coffee et al., 2010; Gatto and Broadie, 2009a). Dissected brains were blocked and permeablized with 0.2% triton X-100 in PBS (PBST) supplemented with 1% bovine serum albumin (BSA) for 1 h at

25°C. The small ventrolateral (sLN_v) clock neurons were labeled with anti-PDF antibody staining with Alexa-Fluor secondary (1:250; Invitrogen-Molecular Probes). Primary and secondary antibodies were diluted in PBST with 0.2% BSA and incubated overnight at 4°C and 2 h at 25°C, respectively. All fluorescent images were collected using a Zeiss confocal microscope. The total number of PDF-positive synaptic boutons (>1 μm diameter) were counted for each sLN_v terminal projection on the right and left hemispheres of the brain, and then averaged for each animal (*n*=1).

Pavlovian olfactory learning

For classical conditioning, *Drosophila* were raised at 25°C in a 12:12 light/dark cycle with lights on at 3:00 AM and lights off at 3:00 PM. To avoid variation due to circadian modulation (Lyons and Roman, 2009) all flies were tested at ZT 14-16. Flies two to four days post-eclosion were used in all assays. Training and testing were carried out in a dark box kept between 22-23°C and humidified to 85-95% humidity. The experiments were performed in dim red light provided by a darkroom safelight equipped with a filter that limited wavelengths to greater than 600 nm (Kodak 1A or GBX-2, Rochester, NY). Light intensity was adjusted with a rheostat to a final intensity of 0.5 $\mu E\ m^{-2}\ sec^{-1}$. Classical conditioning procedures were similar to those used in previous studies (e.g. (Bolduc et al., 2008; Tully et al., 1994; Tully and Quinn, 1985)). Seventy-five to 100 flies were loaded into a cylindrical “shock tube” and acclimated for 2 minutes. The flies were then exposed for 1 min to one of two odors diluted in mineral oil:

10^{-3} 3-octanol (OCT) or $1.5x10^{-3}$ 4-methylcyclohexanol (MCH) - carried by an air current of 500 ml/min. The concentrations used were experimentally determined to be equally aversive to the flies in a T-maze. During exposure to the odor serving as the conditioned stimulus (CS+) flies were subjected to a series of 10 shocks (2.5 seconds, 80V DC) given every 5 seconds via a copper grid that covered the inner surface of the tube. Air was then administered for 50 sec to flush the tube of residual odor, and the second odor (the control stimulus or CS-) was presented without shock. The chamber was again flushed with air for 1 min and the flies were gently tapped into a central compartment where they were acclimated for 2 min. The central compartment was lowered to the T-maze where the flies were exposed to two converging currents of odorant, one from each arm of the maze, and given 2 min to choose between the CS+ and the CS- odors. Flies were then trapped in the arms of the maze, anesthetized with CO_2, and counted. In each experiment two groups of flies of identical age and genotype were trained and tested, one in which the OCT was used as the CS+ and one in which the MCH was the CS+. A learning index (LI) was calculated by taking the number of flies who had chosen the arm with the un-shocked odor and subtracting by the number of flies who had preferred the arm with the shocked odor, and then dividing by the total number of flies within the two arms. To control for any residual odor bias, the LI for each experiment was the average of the two consecutive trials, one in which MCH was paired with a shock and the second in which OCT was paired with the shock.

Statistics

All statistical analyses were performed using GraphPad InStat 3 (GraphPad Software, San Diego, CA). Unpaired, nonparametric Tukey-Kramer multiple comparisons tests were used to compare means and were applied in parallel to all control, *dfmr1* null and transgenic construct lines in the *dfmr1* null background. Significance levels in figures are represented as $P<0.05$ (*), $P<0.01$ (**) and $P<0.001$ (***). All error bars represent standard error of the mean (s.e.m.) for independent trials.

Acknowledgments: We thank Dr. Cheryl Gatto for many discussions and her critical input on this manuscript. We are grateful for the Bloomington *Drosophila* Stock Center and the University of Iowa Developmental Studies Hybridoma Bank for *Drosophila* strains and antibodies, respectively. This work was fully supported by the National Institutes of Health (NIH) grant MH084989 to K.B.

CHAPTER IV

CONCLUSIONS AND FUTURE DIRECTIONS

Martin and Bell first described Fragile X syndrome (FXS) in 1943, initially as Martin-Bell Syndrome, and reported the first pedigree of any sex-linked form of mental retardation (Martin and Bell, 1943). The *FMR1* gene was subsequently mapped to a 'fragile site' – a gap in the metaphase chromosome at position Xq27.3 on the X chromosome (Krawczun et al., 1985) – and finally identified 20 years ago by yeast artificial chromosome (YAC) cloning and shown to be adjacent to the massive expansion of the fragile X-related CpG island in the FXS patient genome (Verkerk et al., 1991). *FMR1* is a highly conserved gene from *Drosophila* to zebrafish to mouse and human, but is not present in the *C. elegans* or yeast genomes. *FMR1* is composed of 17 exons, spans ~40 kb of DNA, and encodes an mRNA of 3.9 kb. The gene can be highly alternatively spliced, which is not typically tissue-specific (Ashley et al., 1993). FMRP expression is fairly ubiquitous, but with the most abundant expression in the brain and testes (Abitbol et al., 1993; Devys et al., 1993). In addition to the common CGG trinucleotide repeat expansion, FXS can also be caused by deletions or single point mutations in the *FMR1* coding sequence (Gedeon et al., 1992; Hirst et al., 1995). FXS segregates as an X-linked dominant disorder with reduced penetrance, since either sex, when carrying the mutation, may exhibit intellectual

disability (Sherman et al., 1985). Fully penetrant males rarely reproduce, and so it has been suggested that the frequency of new fragile X mutations may be as high as 1 in 3000 germ cells, to maintain the known population frequency (Brown, 1990).

The FMRP RNA-binding protein is associated with polyribosomes and also the RISC complex with a known function in translational repression (Ceman et al., 2003; Cheever and Ceman, 2009; Darnell et al., 2009; Wang et al., 2008). The human genome also encodes two *FMR*-related proteins, FXR1P and FXR2P. All three proteins show ultrastructurally overlapping expression, can be co-immunoprecipitated, and can associate with many of the same protein partners (Bakker et al., 2000; Ceman et al., 1999; Christie et al., 2009; Zhang et al., 1995). Both hetero- and homo-dimerization of the three-protein family has been proposed to occur (Christie et al., 2009; Tamanini et al., 1999). For example, *FXR2* has not only been shown to be present in a FMRP complex, but has also been shown to be present alone. The *Drosophila* genome encodes only a single homologous gene, *dFMR1*, and the *Drosophila* genetic system has been used extensively to probe FMRP functions. The extraordinarily well-established *Drosophila* FXS disease model has been incredibly useful in dissecting causative mechanisms that may be responsible for disease state symptoms (Banerjee et al., 2010; Dockendorff et al., 2002; Estes et al., 2008; Gatto and Broadie, 2008; Siller and Broadie, 2011; Tessier and Broadie, 2011).

In my first aim, I investigated the evolutionary conservation of the human FXS gene family using the *Drosophila* disease model. Null *dfmr1* mutants

recapitulate FXS-associated molecular, cellular and behavioral phenotypes, suggesting *FMR1* function has been conserved, albeit with specific functions probably sub-served by the expanded human gene family. For example, mouse *Fxr1* knockout animals die shortly after birth, owing to defects in cardiac and skeletal muscle development (Mientjes et al., 2004). Conversely, both *Fmr1* and *Fxr2* knockouts as well as *Fmr1/Fxr2* double knockouts are completely viable. Both *Fmr1* and *Fxr2* knockout mice exhibit some FXS-like phenotypes, albeit fairly weakly, including learning defects, hyperactivity and macroorchidism (Chen and Toth, 2001; McNaughton et al., 2008). Interestingly, the *Fmr1/Fxr2* double knockout results in some augmented defects, including exaggerated behavioral phenotypes of open-field activity and circadian arrhythmicity (Spencer et al., 2006; Zhang et al., 2008). To test evolutionary conservation, I used tissue-targeted transgenic expression of all three human genes (*FMR1*, *FXR1*, *FXR2*) in the *Drosophila* disease model to investigate function at molecular, neuronal and non-neuronal levels. In neurons, *dfmr1* null mutants exhibit elevated protein levels altering central brain and NMJ synaptic architecture, including increased synapse area, branching and bouton numbers. *hFMR1* can fully rescue both the molecular and cellular defects in neurons, comparably to the native *dFMR1*, whereas *hFXR1* and *hFXR2* provide no rescue. For non-neuronal requirements, I assayed male fecundity and testes function. Null *dfmr1* mutants are effectively sterile due to disruption of the 9+2 microtubule organization in the sperm tail. Amazingly, all three human genes fully rescue mutant fecundity and spermatogenesis defects. These results indicate that *FMR1* gene function is

evolutionarily conserved in neural mechanisms and cannot be compensated by either *FXR1* or *FXR2*, but that all three proteins can substitute for each other in non-neuronal requirements (Coffee et al., 2010).

Next, I investigated the hypothesis that the phosphorylation of the serine at 500 (S500) in human FMRP controls its function as an RNA-binding translational repressor. It has been hypothesized that the phosphorylation state of S500 acts as a "switch" to transition FMRP from an inactive to active state (Ceman et al., 2003; Pfeiffer and Huber, 2007). This hypothesis predicts that FMRP that cannot be phosphorylated will remain functionally inactive, equivalent to full protein loss, whereas a constitutively phosphorylated protein will be constantly active, but this has never been tested *in vivo*. Using the *Drosophila* FXS model, I used targeted expression of human *FMR1* transgenes, including wildtype (*hFMR1*), dephosphomimetic (*S500A-hFMR1*), and phosphomimetic (*S500D-hFMR1*) to investigate phosphorylation requirements. Null *dfmr1* mutants exhibit elevated brain protein levels, overgrowth of synaptic architecture and defects in olfactory-based associative learning due to loss of translational repressor activity. The human phosphomimetic rescues these defects, while the dephosphomimetic phenocopies the disease state.

Synaptic architecture is highly dependent on the microtubule cytoskeleton, which is tightly regulated by the FMRP-target Futsch (MAP1B homolog) (Hummel et al., 2000). Futsch is associated with the axonal nerve-terminal microtubule cytoskeleton and is necessary for the regulation of normal synaptic growth and bouton differentiation (Roos et al., 2000; Ruiz-Canada et al., 2004). It is

proposed that Futsch-positive loops are enriched in developing, immature synaptic boutons. Futsch translation is negatively regulated by FMRP via a direct mRNA-binding interaction, and excess Futsch-positive microtubule loops accumulate in the synaptic arbor in the *dfmr1* null mutant condition (Gatto and Broadie, 2008). At the *Drosophila* NMJ, Futsch binds microtubule loops in a subset of developing synaptic boutons (Roos et al., 2000). These Futsch-positive microtubule structures are proposed to regulate synaptic growth and bouton differentiation (Dent and Kalil, 2001; Tanaka and Kirschner, 1991). In *dfmr1* null mutants, there is an increased number of Futsch-positive loops throughout the overgrown synaptic arbor, and these supernumerary structures are removed by presynaptic FMRP expression. I show a doubling in the number of Futsch loops in the absence of FMRP, compared to wildtype control. Only the transgenic introduction of *hFMR1* and *S500D-hFMR1* can overcome this Futsch elevation, restoring the normal number of Futsch-positive loops in mutant synapses. Dephosphorylated *S500A-hFMR1*, in contrast, exhibits no restorative activity. I conclude that human FMRP S500 phosphorylation is necessary for its *in vivo* function as a neuronal translational repressor and regulator of synaptic architecture, and for the manifestation of FMRP-dependent learning behavior (Coffee et al., 2011).

Taken together, my work has demonstrated that *FMR1* is conserved from *Drosophila* to human because *hFMR1* rescues all *dfmr1* neuronal and non-neuronal defects assayed in this body of work, whereas *hFXR1* and *hFXR2* can only compensate non-neuronally. One possible mechanism for the divergent

roles of the paralogs could be due to the fact that each has varying levels of expression in different tissues. While there is overall overlap of expression among the family members, *FXR1*, for example, has elevated expression in muscle (Mientjes et al., 2004). Findings from the *Fmr1/Fxr2* double knockout mouse model suggest *FXR2* has at least some overlap in function with *FMR1*, but it is not clear whether this only occurs in a combinatorial fashion with *FMR1* because *FXR2* expression levels are unchanged in FXS and do not compensate to rescue disease phenotypes (Spencer et al., 2006). Though there is extremely high sequence homology among the three family members, the paralogs diverge in sequence similarity in their C-terminal ends (Kirkpatrick et al., 2001). This could possibly explain the tissue expression differences and divergent function of the paralogs as examined in this body of work. Furthermore, I have shown that phosphorylation of residue S500 in hFMRP is critically important for the function of the protein as a translational repressor. The *S500D-hFMR1* phosphomimetic rescues neuronal FXS defects, while the dephosphomimetic (S500A-hFMRP) phenocopies the FXS disease condition. These studies provide great insight into the *in vivo* function of the *FMR1* gene family, and this insight should help to elucidate mechanisms for major FXS phenotypes. Further *in vivo* dissection of the functional importance of various hFMRP domains should be performed to garner insights into FMRP mechanistic roles in neurons and other cell types.

It has previously been shown that one human FXS patient, lacking the cytogenetic expression of FRAXA as revealed by folate deprivation cell culture experiments and harboring a normal CGG repeat length and unmethylated CpG

island, harbors a *de novo* missense mutation (I304N) within the KH2 RNA-binding domain (De Boulle et al., 1993). This patient presents with an unusually severe FXS phenotype, including severe mental retardation (IQ<20), 'impressive' macroorchidism and peripheral neuropathy of lower extremities (De Boulle et al., 1993). A general feature of KH domain-containing proteins is their incorporation into RNP (ribonucleoprotein particle) complexes via a RNA-interaction surface (Leffers et al., 1995). The 1304N mutation has been reported to unfold the *FMR1* KH2 domain, leading to disturbance of the normal interactions within the corresponding RNP complexes and an abrogation of RNA binding, at least at high salt concentrations (Siomi et al., 1994). However, at physiological salt conditions, RNA-binding activity of this missense mutation is not abolished to cytoplasmic mRNAs or to RNA homopolymers (Siomi et al., 1994). Instead of causing impaired RNA binding, the I304N mutation abolishes the association of FMRP with polyribosomes, suggesting the KH domain is important in FMRP-polyribosome association *in vivo* (Feng et al., 1997). Therefore, conclusions from this study suggest that the mutation phenotype arises in the sequestration of mRNAs from their translational regulation by forming nontranslatable mRNP particles.

More recently, it has been suggested that the I304N mutation might have a dominant negative effect by affecting the structure of the mRNP complexes containing FMRP (Darnell et al., 2005). Darnell and colleagues identified the RNA target for the KH2 domain as a sequence-specific element within a complex tertiary structured termed the FMRP "kissing complex", and demonstrated that

FMRP association with brain polyribosomes is abrogated by competition with kissing complex RNA (Darnell et al., 2005). I have previously sub-cloned the *I304N-hFMR1* cDNA into the pUAST expression vector and had this construct transformed into *Drosophila* embryos. It would be interesting to analyze this transgenic construct in our *Drosophila* FXS disease model (Coffee et al., 2010; Zhang et al., 2001). What array of neuronal vs. non-neuronal phenotypes would this transgenic animal be able to rescue when present in the *dfmr1* null background? Would we observe an exacerbated disease phenotype as was seen in the human patient with this mutation? In addition to prior established neuronal assays of brain protein levels and synaptic architecture, quantitative RT-PCR and Western blots of several known mRNA targets could be conducted in order to assess the ability or lack thereof of the mutated KH2 domain in properly associating with mRNP complexes and negatively regulating translation. Perhaps I would predict that this transgenic animal would phenocopy the disease animal, but with an even more severe FXS phenotype. Although to date this mutation has only been found in one FXS patient, this case has definitely indicated the value of screening for further structure-function mutations within the *FMR1* gene that could be responsible for modifying the disease state.

Another FMRP domain, which, while studied *in vitro*, should be investigated *in vivo*, is the RGG box domain (Siomi et al., 1993). The RGG box associates with G-quartets with nanomolar affinity and is considered to be the primary mRNA-binding domain present in FMRP due to the vast majority of FMRP targets possessing the G-quartets bound by the RGG box (Darnell et al.,

2001; Menon and Mihailescu, 2007; Schaeffer et al., 2001). The RGG box has been shown to be post-translationally methylated on arginines, which is significant because this hints at this domain being able to differentially bind potential partners (Stetler et al., 2006). FMRP lacking the RGG box does not distribute normally on polyribosome fractions, demonstrating the intact domain is critically important for FMRP function and without it, FMRP may not be able to function normally as a translational regulator (Mazroui et al., 2003). Since this domain is the primary FMRP mRNA-binding domain, it could be expected that FMRP would have reduced affinity for mRNA in the absence of the RGG box.

Recently, the Ceman laboratory has investigated the RGG box arginines important for FMRP function and their role in polyribosome and mRNA association (Blackwell et al., 2010), and found that arginines 533 and 538 (in mouse FMRP) are required for normal FMRP polyribosome association, whereas all four arginines (533, 538, 543, 545) play a role in mRNA binding. The model G-quartet RNA sc1 (Darnell et al., 2001) required arginines 533 and 538 for canonical association with FMRP. The second most abundant co-immunoprecipitating brain mRNA containing a G-quartet is AATYK (Brown et al., 2001), which does not require the 533/538 arginines for binding (Blackwell et al., 2010). This suggests that different arginines of the RGG box are involved in binding different target mRNAs. Methylation of arginine residues 533 and 538, or 543 and 545, leads to loss of sc1 RNA binding (Blackwell et al., 2010). However, it is still not known whether methylation inhibits mRNA binding or occurs on selective arginines to control the selection and specificity of bound RNAs.

Proteins can be partially methylated and released from the methyl transferase to re-associate later and become fully methylated (Kolbel et al., 2009), in order to modulate protein-protein interactions. It would be interesting to determine whether FMRP exists in two populations, methylated and unmethylated, or some combination of both (Blackwell et al., 2010). If it exists as a collection of proteins with distinct methylated arginines, this would allow the cell to express FMRPs with varying RNA binding abilities.

I have generated an RGG box deletion (ΔRGG) within *hFMR1* cDNA and sub-cloned this into the pUAST expression vector. In addition to established neuronal assays of brain protein levels and synaptic architecture, quantitative RT-PCR of known mRNA targets and Western blots of known protein changes could be conducted to assess the ability of the RGG box deletion in properly associating with mRNP complexes. What array of neuronal vs. non-neuronal phenotypes might this transgenic animal be able to rescue in the *dfmr1* null background? I would predict that due to the RGG box being the major RNA-binding domain that the *ΔRGG-hFMR1* construct would fail to rescue *dfmr1* null defects in many, if not all, of established neuronal assays. Interestingly, would the *I304N-hFMR1* construct mimic the *ΔRGG-hFMR1* construct? Perhaps many of our morphological assays would show similar phenotypes within each of these human transgenic lines. However, on the molecular level, I would predict differences as these mutations are within two distinct RNA-binding domains. Different RNA targets should show differential regulation in each of these transgenic models. The comparisons between these two transgenic animals,

each predicted to disrupt/delete an mRNA-binding domain, would be extremely informative. To date, there are very few *in vivo* mutational studies that have been conducted to assess *FMR1* structure-function relationships that may underlie defects causative for FXS. Future genetic screens should help reveal additional mutations within the *FMR1* gene that can cause FXS, including informative point mutations within the RGG box.

In addition to the neuronal and non-neuronal assays employed in the work, as described in Chapters II and III, I have investigated several additional phenotypes throughout my thesis work that could be used in the future to provide insights into the mechanisms of FXS dysfunction. One assay I have pursued at great length involves monitoring circadian activity rhythms using *Drosophila* Activity Monitoring (DAM) Systems (TriKinetics, Waltham, MA). FXS patients display disrupted circadian sleep patterns (Gould et al., 2000; Kronk et al., 2010; Weiskop et al., 2005), and *dfmr1* null mutants similarly display a loss of normal circadian rhythms (Inoue et al., 2002). A normal fly is active for 12-14 hours during the daylight and virtually inactive for 10-12 hours at night. The sleep pattern is strikingly similar to that of humans. If entrained to a light:dark cycle of 12 hours of light followed by 12 hours of dark (LD12:12) for several days, a wild-type fly will maintain this normal pattern of activity in total darkness for at least several weeks. However, *dfmr1* null mutants lack this capacity and display an erratic pattern of non-rhythmic activity, punctuated by periodic bouts of hyperactivity (Dockendorff et al., 2002). My preliminary actogram data show that wild-type flies can be entrained to light and have bimodal activity (in both LD and

DD), peak of activity as lights are turned on in the morning, followed by a period of rest, and peak of activity as lights are about to be turned off at night (Fig. 21). Once entrained to light, wild-type flies are able to predict the onset of darkness as evidenced by the activity increase. Wild-type flies exhibit a normal period of ~23.8 h. and are able to maintain this period for days/weeks in the DD free-running challenge. In contrast, *dfmr1* null mutants, while able to be weakly entrained to light, are unable to maintain bimodality and rhythm with the DD challenge (Fig. 21). Null flies also exhibit hyperactivity compared to controls as measured by the number of infrared beam crosses per day. There is a wealth of information that can be attained studying the circadian rhythmicity in the *Drosophila* FXS model. With all of my human transgenic lines, it would be extremely interesting to dissect the functions of the human paralogs in comparison with *hFMR1* in regulating circadian defects and hyperactivity.

A second avenue that I have begun to investigate is polyribosome association assays (Ceman et al., 2003). FMRP associates with heavy-sedimenting polyribosome complexes (translating polyribosomes) that contain mRNAs bound by multiple ribosomes (Ceman et al., 2003; Khandjian et al., 1996; Tamanini et al., 1996). Polyribosome association has been shown to be critical to FMRP function in the I304N missense mutation condition, with disruption in the KH2 domain causing FMRP to no longer associate (Feng et al., 1997). mRNAs found to be associated with FMRP by immunoprecipitation also display altered association with polyribosomes in the absence of FMRP, suggesting that FMRP

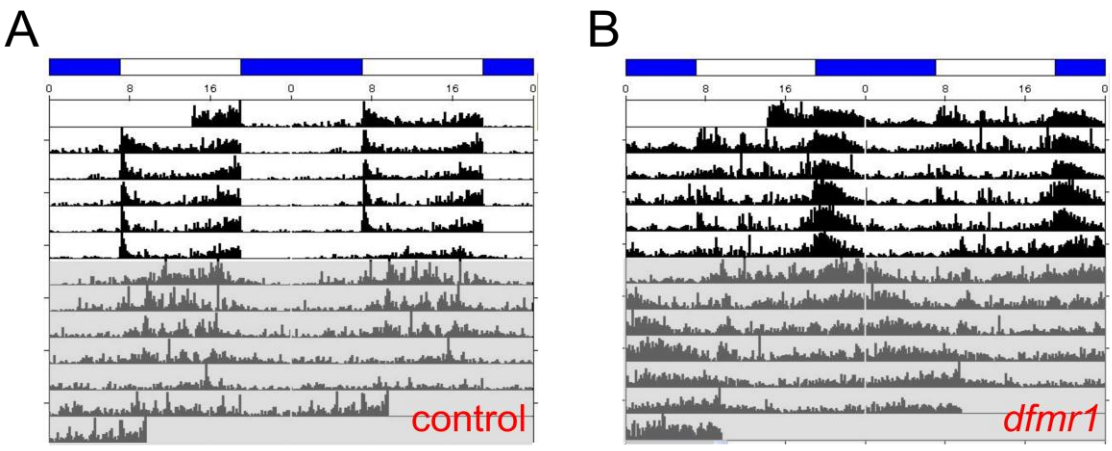

Figure 21. Circadian actograms of control (w^{1118}) and *dfmr1* null animals. (A) Representative actograms from control flies and (B) mutant flies. Flies that had been entrained to a light:dark cycle were placed in the activity monitors for 5 days in LD, then shifted to constant darkness (DD; shaded area) and their activity was recorded for an additional 5 days. Flies expressing *dFMR1* have rhythmic patterns of rest and activity and maintain these throughout DD, while flies lacking wild-type *dFMR1* have relatively high activity and are arrhythmic.

interacts with the translational machinery to modulate protein expression of associated mRNAs (Brown et al., 2001). *In vitro* work by Ceman and colleagues has demonstrated that unphosphorylated FMRP associates with actively translating polyribosomes, while phosphorylated FMRP is associated with stalled polyribosomes (Ceman et al., 2003). This suggests that phosphorylation regulates FMRP polyribosome association and that the release of FMRP-induced translational suppression may involve a dephosphorylation signal. A breadth of knowledge could be gained by assessing polyribosome association *in vivo* using our established FXS *Drosophila* model.

I have conducted preliminary work on polyribosome assays with wild-type animals. Briefly, fly head lysates were generated from approximately 1-1.5 mL of total heads (as measured in an Eppendorf tube) and overlayed onto a 15-45% sucrose gradient. Gradients are then centrifuged for 2 hrs at 188,000*g* at 4ºC. Each gradient was then fractionated into 1 mL fractions by bottom displacement using a gradient fractionator with the ribosomal profile monitored at OD_{254}. Western blot analysis could also be conducted on the fractions and probed with an FMRP antibody in order to determine whether FMRP is located within the mRNP complex, associating with polyribosomes, or if it is present in both sedimenting fractions. Preliminary data from w^{1118} control animals show that FMRP is primarily associated with the mRNP complex and light polyribosomal fractions (Fig. 22). It would be extremely interesting to assay the dephospho- and phosphomimetic human transgenic lines in this polyribosome assay. Using a translational inhibitor, such as puromycin, polyribosome run-off assays could be

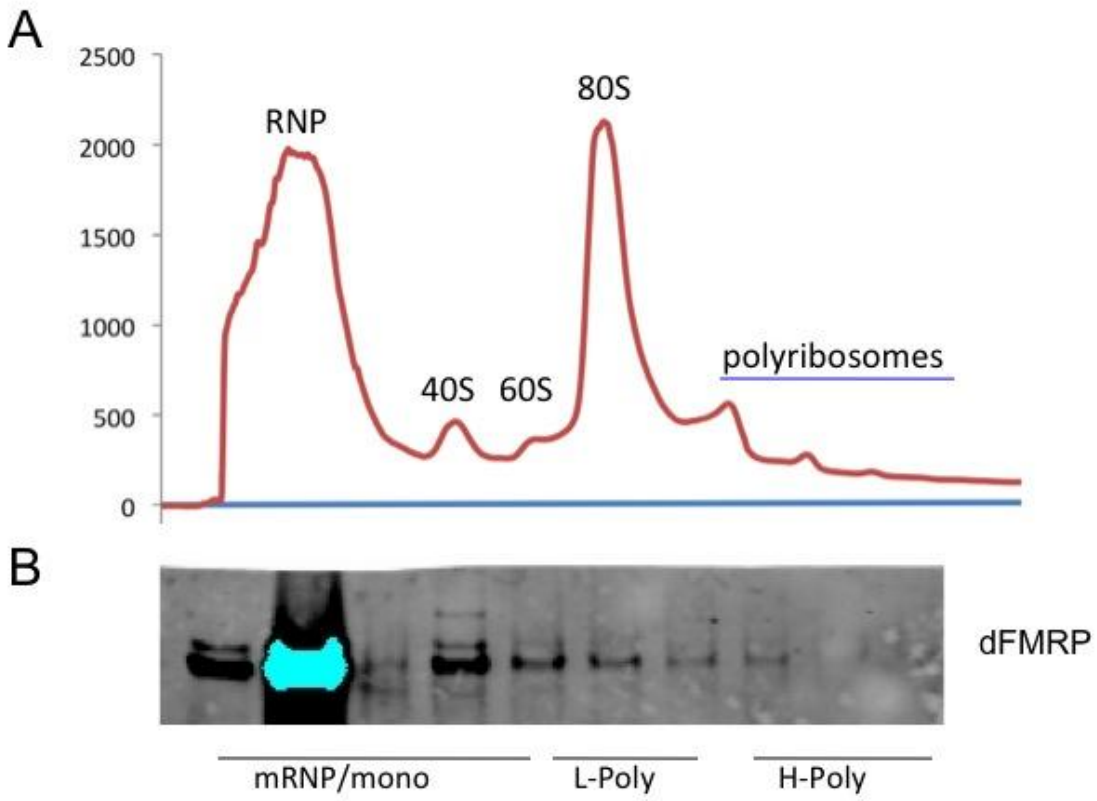

Figure 22. Polyribosomal association profile of *w*^{1118} control animals. Head lysates were prepared and then fractionated on a linear 15-45% sucrose gradient. The profile (A) is shown as absorbance at 254 nm. The positions of the 40S, 60S, and 80S monosomes are denoted. Wild type FMRP is associated with actively-translating light-polyribosomes as well as the mRNP complex as seen in the Western blot probed with dFMRP (B).

conducted in order to assess the location of each of FMRP in these mimetics. I would predict the dephosphomimetic would resemble the *dfmr1* null condition and show ribosome run-off (denoting presence on actively translating polyribosomes). Conversely, the phosphomimetic would be predicted to resemble the wild-type condition and not show ribosome run-off, suggesting FMRP is associating with stalled polyribosomes and inhibiting the translational machinery. Utilizing these assays would provide the first *in vivo* evidence of the molecular mechanisms involved in FMRP negative translational regulation.

Work presented in this dissertation on the conservation and phosphorylation-dependent functions of the human Fragile X syndrome gene family has helped to elucidate important control and regulatory mechanisms of *FMR1* and its associated paralogs. The *Drosophila* FXS disease model has made it possible to conduct these insightful experiments. Combining the established neuronal and non-neuronal assays discussed in Chapters II and III, with more preliminary assays described in this chapter, a large amount of informative future work could be done on the existing human transgenic lines that I have made, in order to better understand FMRP function as it relates to this pervasive, wide-spectrum neurological disorder.

REFERENCES

Abitbol, M., Menini, C., Delezoide, A. L., Rhyner, T., Vekemans, M. and Mallet, J. (1993). Nucleus basalis magnocellularis and hippocampus are the major sites of FMR-1 expression in the human fetal brain. *Nat Genet* **4**, 147-53.

Adinolfi, S., Ramos, A., Martin, S. R., Dal Piaz, F., Pucci, P., Bardoni, B., Mandel, J. L. and Pastore, A. (2003). The N-terminus of the fragile X mental retardation protein contains a novel domain involved in dimerization and RNA binding. *Biochemistry* **42**, 10437-44.

Agulhon, C., Blanchet, P., Kobetz, A., Marchant, D., Faucon, N., Sarda, P., Moraine, C., Sittler, A., Biancalana, V., Malafosse, A. et al. (1999). Expression of FMR1, FXR1, and FXR2 genes in human prenatal tissues. *J Neuropathol Exp Neurol* **58**, 867-80.

Amir, R. E., Van den Veyver, I. B., Wan, M., Tran, C. Q., Francke, U. and Zoghbi, H. Y. (1999). Rett syndrome is caused by mutations in X-linked MECP2, encoding methyl-CpG-binding protein 2. *Nat Genet* **23**, 185-8.

Anderson, D. K., Lord, C., Risi, S., DiLavore, P. S., Shulman, C., Thurm, A., Welch, K. and Pickles, A. (2007). Patterns of growth in verbal abilities among children with autism spectrum disorder. *J Consult Clin Psychol* **75**, 594-604.

Andreassi, C. and Riccio, A. (2009). To localize or not to localize: mRNA fate is in 3'UTR ends. *Trends Cell Biol* **19**, 465-74.

Aschrafi, A., Cunningham, B. A., Edelman, G. M. and Vanderklish, P. W. (2005). The fragile X mental retardation protein and group I metabotropic glutamate receptors regulate levels of mRNA granules in brain. *Proc Natl Acad Sci U S A* **102**, 2180-5.

Ashley, C. T., Sutcliffe, J. S., Kunst, C. B., Leiner, H. A., Eichler, E. E., Nelson, D. L. and Warren, S. T. (1993). Human and murine FMR-1: alternative splicing and translational initiation downstream of the CGG-repeat. *Nat Genet* **4**, 244-51.

Ashley, J., Packard, M., Ataman, B. and Budnik, V. (2005). Fasciclin II signals new synapse formation through amyloid precursor protein and the scaffolding protein dX11/Mint. *J Neurosci* **25**, 5943-55.

Ashraf, S. I., McLoon, A. L., Sclarsic, S. M. and Kunes, S. (2006). Synaptic protein synthesis associated with memory is regulated by the RISC pathway in Drosophila. *Cell* **124**, 191-205.

Asperger, H. (1944). Die autistischen psychopathen in kindersalter. *Cambridge: Cambridge University Press*.

Bagni, C. and Greenough, W. T. (2005). From mRNP trafficking to spine dysmorphogenesis: the roots of fragile X syndrome. *Nat Rev Neurosci* **6**, 376-87.

Bailey, C. H., Bartsch, D. and Kandel, E. R. (1996). Toward a molecular definition of long-term memory storage. *Proc Natl Acad Sci U S A* **93**, 13445-52.

Bailey, D. B., Jr., Raspa, M., Olmsted, M. and Holiday, D. B. (2008). Co-occurring conditions associated with FMR1 gene variations: findings from a national parent survey. *Am J Med Genet A* **146A**, 2060-9.

Bakker, C., Verheij, C., Willemsen, R. and van der Helm, R. (1994). Fmr1 knockout mice: a model to study fragile X mental retardation. The Dutch-Belgian Fragile X Consortium. *Cell* **78**, 23-33.

Bakker, C. E., de Diego Otero, Y., Bontekoe, C., Raghoe, P., Luteijn, T., Hoogeveen, A. T., Oostra, B. A. and Willemsen, R. (2000). Immunocytochemical and biochemical characterization of FMRP, FXR1P, and FXR2P in the mouse. *Exp Cell Res* **258**, 162-70.

Banerjee, P., Nayar, S., Hebbar, S., Fox, C. F., Jacobs, M. C., Park, J. H., Fernandes, J. J. and Dockendorff, T. C. (2007). Substitution of critical isoleucines in the KH domains of Drosophila fragile X protein results in partial loss-of-function phenotypes. *Genetics* **175**, 1241-50.

Banerjee, P., Schoenfeld, B. P., Bell, A. J., Choi, C. H., Bradley, M. P., Hinchey, P., Kollaros, M., Park, J. H., McBride, S. M. and Dockendorff, T. C. (2010). Short- and long-term memory are modulated by multiple isoforms of the fragile X mental retardation protein. *J Neurosci* **30**, 6782-92.

Banko, J. L., Poulin, F., Hou, L., DeMaria, C. T., Sonenberg, N. and Klann, E. (2005). The translation repressor 4E-BP2 is critical for eIF4F complex formation, synaptic plasticity, and memory in the hippocampus. *J Neurosci* **25**, 9581-90.

Bardoni, B., Castets, M., Huot, M. E., Schenck, A., Adinolfi, S., Corbin, F., Pastore, A., Khandjian, E. W. and Mandel, J. L. (2003). 82-FIP, a novel FMRP (fragile X mental retardation protein) interacting protein, shows a cell cycle-dependent intracellular localization. *Hum Mol Genet* **12**, 1689-98.

Bardoni, B., Mandel, J. L. and Fisch, G. S. (2000). FMR1 gene and fragile X syndrome. *Am J Med Genet* **97**, 153-63.

Bardoni, B., Schenck, A. and Mandel, J. L. (1999). A novel RNA-binding nuclear protein that interacts with the fragile X mental retardation (FMR1) protein. *Hum Mol Genet* **8**, 2557-66.

Bassell, G. J. and Warren, S. T. (2008). Fragile X syndrome: loss of local mRNA regulation alters synaptic development and function. *Neuron* **60**, 201-14.

Bear, M. F., Huber, K. M. and Warren, S. T. (2004). The mGluR theory of fragile X mental retardation. *Trends Neurosci* **27**, 370-7.

Bechara, E. G., Didiot, M. C., Melko, M., Davidovic, L., Bensaid, M., Martin, P., Castets, M., Pognonec, P., Khandjian, E. W., Moine, H. et al. (2009). A novel function for fragile X mental retardation protein in translational activation. *PLoS Biol* **7**, e16.

Belmonte, M. K. and Bourgeron, T. (2006). Fragile X syndrome and autism at the intersection of genetic and neural networks. *Nat Neurosci* **9**, 1221-5.

Beumer, K. J., Rohrbough, J., Prokop, A. and Broadie, K. (1999). A role for PS integrins in morphological growth and synaptic function at the postembryonic neuromuscular junction of Drosophila. *Development* **126**, 5833-46.

Bhogal, B. and Jongens, T. A. (2010). Fragile X syndrome and model organisms: identifying potential routes of therapeutic intervention. *Dis Model Mech* **3**, 693-700.

Blackwell, E., Zhang, X. and Ceman, S. (2010). Arginines of the RGG box regulate FMRP association with polyribosomes and mRNA. *Hum Mol Genet* **19**, 1314-23.

Blonden, L., van 't Padje, S., Severijnen, L. A., Destree, O., Oostra, B. A. and Willemsen, R. (2005). Two members of the Fxr gene family, Fmr1 and Fxr1, are differentially expressed in Xenopus tropicalis. *Int J Dev Biol* **49**, 437-41.

Boccia, M. L. and Roberts, J. E. (2000). Behavior and autonomic nervous system function assessed via heart period measures: the case of hyperarousal in boys with fragile X syndrome. *Behav Res Methods Instrum Comput* **32**, 5-10.

Bolduc, F. V., Bell, K., Cox, H., Broadie, K. S. and Tully, T. (2008). Excess protein synthesis in Drosophila fragile X mutants impairs long-term memory. *Nat Neurosci* **11**, 1143-5.

Bontekoe, C. J., Bakker, C. E., Nieuwenhuizen, I. M., van der Linde, H., Lans, H., de Lange, D., Hirst, M. C. and Oostra, B. A. (2001). Instability of a (CGG)98 repeat in the Fmr1 promoter. *Hum Mol Genet* **10**, 1693-9.

Bontekoe, C. J., McIlwain, K. L., Nieuwenhuizen, I. M., Yuva-Paylor, L. A., Nellis, A., Willemsen, R., Fang, Z., Kirkpatrick, L., Bakker, C. E., McAninch, R. et al. (2002). Knockout mouse model for Fxr2: a model for mental retardation. *Hum Mol Genet* **11**, 487-98.

Bradshaw, K. D., Emptage, N. J. and Bliss, T. V. (2003). A role for dendritic protein synthesis in hippocampal late LTP. *Eur J Neurosci* **18**, 3150-2.

Braun, K. and Segal, M. (2000). FMRP involvement in formation of synapses among cultured hippocampal neurons. *Cereb Cortex* **10**, 1045-52.

Bredt, D. S. and Nicoll, R. A. (2003). AMPA receptor trafficking at excitatory synapses. *Neuron* **40**, 361-79.

Brendel, C., Rehbein, M., Kreienkamp, H. J., Buck, F., Richter, D. and Kindler, S. (2004). Characterization of Staufen 1 ribonucleoprotein complexes. *Biochem J* **384**, 239-46.

Broadie, K. and Pan, L. (2005). Translational complexity of the fragile x mental retardation protein: insights from the fly. *Mol Cell* **17**, 757-9.

Brouwer, J. R., Huizer, K., Severijnen, L. A., Hukema, R. K., Berman, R. F., Oostra, B. A. and Willemsen, R. (2008). CGG-repeat length and neuropathological and molecular correlates in a mouse model for fragile X-associated tremor/ataxia syndrome. *J Neurochem* **107**, 1671-82.

Brouwer, J. R., Mientjes, E. J., Bakker, C. E., Nieuwenhuizen, I. M., Severijnen, L. A., Van der Linde, H. C., Nelson, D. L., Oostra, B. A. and Willemsen, R. (2007). Elevated Fmr1 mRNA levels and reduced protein expression in a mouse model with an unmethylated Fragile X full mutation. *Exp Cell Res* **313**, 244-53.

Brown, V., Jin, P., Ceman, S., Darnell, J. C., O'Donnell, W. T., Tenenbaum, S. A., Jin, X., Feng, Y., Wilkinson, K. D., Keene, J. D. et al. (2001). Microarray identification of FMRP-associated brain mRNAs and altered mRNA translational profiles in fragile X syndrome. *Cell* **107**, 477-87.

Brown, V., Small, K., Lakkis, L., Feng, Y., Gunter, C., Wilkinson, K. D. and Warren, S. T. (1998). Purified recombinant Fmrp exhibits selective RNA binding as an intrinsic property of the fragile X mental retardation protein. *J Biol Chem* **273**, 15521-7.

Brown, W. T. (1990). The fragile X: progress toward solving the puzzle. *Am J Hum Genet* **47**, 175-80.

Bureau, I., Shepherd, G. M. and Svoboda, K. (2008). Circuit and plasticity defects in the developing somatosensory cortex of FMR1 knock-out mice. *J Neurosci* **28**, 5178-88.

Bushey, D., Tononi, G. and Cirelli, C. (2009). The Drosophila fragile X mental retardation gene regulates sleep need. *J Neurosci* **29**, 1948-61.

Cajigas, I. J., Will, T. and Schuman, E. M. (2010). Protein homeostasis and synaptic plasticity. *Embo J* **29**, 2746-52.

Castets, M., Schaeffer, C., Bechara, E., Schenck, A., Khandjian, E. W., Luche, S., Moine, H., Rabilloud, T., Mandel, J. L. and Bardoni, B. (2005). FMRP interferes with the Rac1 pathway and controls actin cytoskeleton dynamics in murine fibroblasts. *Hum Mol Genet* **14**, 835-44.

Caudy, A. A., Myers, M., Hannon, G. J. and Hammond, S. M. (2002). Fragile X-related protein and VIG associate with the RNA interference machinery. *Genes Dev* **16**, 2491-6.

Cavallaro, S., Paratore, S., Fradale, F., de Vrij, F. M., Willemsen, R. and Oostra, B. A. (2008). Genes and pathways differentially expressed in the brains of Fxr2 knockout mice. *Neurobiol Dis* **32**, 510-20.

Ceman, S., Brown, V. and Warren, S. T. (1999). Isolation of an FMRP-associated messenger ribonucleoprotein particle and identification of nucleolin and the fragile X-related proteins as components of the complex. *Mol Cell Biol* **19**, 7925-32.

Ceman, S., O'Donnell, W. T., Reed, M., Patton, S., Pohl, J. and Warren, S. T. (2003). Phosphorylation influences the translation state of FMRP-associated polyribosomes. *Hum Mol Genet* **12**, 3295-305.

Centonze, D., Rossi, S., Napoli, I., Mercaldo, V., Lacoux, C., Ferrari, F., Ciotti, M. T., De Chiara, V., Prosperetti, C., Maccarrone, M. et al. (2007). The brain cytoplasmic RNA BC1 regulates dopamine D2 receptor-mediated transmission in the striatum. *J Neurosci* **27**, 8885-92.

Chang, D. C. (2006). Neural circuits underlying circadian behavior in Drosophila melanogaster. *Behav Processes* **71**, 211-25.

Chang, S., Bray, S. M., Li, Z., Zarnescu, D. C., He, C., Jin, P. and Warren, S. T. (2008). Identification of small molecules rescuing fragile X syndrome phenotypes in Drosophila. *Nat Chem Biol* **4**, 256-63.

Chao, H. T., Zoghbi, H. Y. and Rosenmund, C. (2007). MeCP2 controls excitatory synaptic strength by regulating glutamatergic synapse number. *Neuron* **56**, 58-65.

Cheever, A. and Ceman, S. (2009a). Phosphorylation of FMRP inhibits association with Dicer. *RNA* **15**, 362-6.

Cheever, A. and Ceman, S. (2009b). Translation regulation of mRNAs by the fragile X family of proteins through the microRNA pathway. *RNA Biol* **6**.

Chelly, J., Khelfaoui, M., Francis, F., Cherif, B. and Bienvenu, T. (2006). Genetics and pathophysiology of mental retardation. *Eur J Hum Genet* **14**, 701-13.

Chelly, J. and Mandel, J. L. (2001). Monogenic causes of X-linked mental retardation. *Nat Rev Genet* **2**, 669-80.

Chen, L. and Toth, M. (2001). Fragile X mice develop sensory hyperreactivity to auditory stimuli. *Neuroscience* **103**, 1043-50.

Chen, L., Yun, S. W., Seto, J., Liu, W. and Toth, M. (2003a). The fragile X mental retardation protein binds and regulates a novel class of mRNAs containing U rich target sequences. *Neuroscience* **120**, 1005-17.

Chen, L. S., Tassone, F., Sahota, P. and Hagerman, P. J. (2003b). The (CGG)n repeat element within the 5' untranslated region of the FMR1 message provides both positive and negative cis effects on in vivo translation of a downstream reporter. *Hum Mol Genet* **12**, 3067-74.

Chonchaiya, W., Schneider, A. and Hagerman, R. J. (2009). Fragile X: a family of disorders. *Adv Pediatr* **56**, 165-86.

Chowdhury, S., Shepherd, J. D., Okuno, H., Lyford, G., Petralia, R. S., Plath, N., Kuhl, D., Huganir, R. L. and Worley, P. F. (2006). Arc/Arg3.1 interacts with the endocytic machinery to regulate AMPA receptor trafficking. *Neuron* **52**, 445-59.

Christie, S. B., Akins, M. R., Schwob, J. E. and Fallon, J. R. (2009). The FXG: a presynaptic fragile X granule expressed in a subset of developing brain circuits. *J Neurosci* **29**, 1514-24.

Chudley, A. E. and Hagerman, R. J. (1987). Fragile X syndrome. *J Pediatr* **110**, 821-31.

Clifford, S., Dissanayake, C., Bui, Q. M., Huggins, R., Taylor, A. K. and Loesch, D. Z. (2007). Autism spectrum phenotype in males and females with fragile X full mutation and premutation. *J Autism Dev Disord* **37**, 738-47.

Coffee, B., Ikeda, M., Budimirovic, D. B., Hjelm, L. N., Kaufmann, W. E. and Warren, S. T. (2008). Mosaic FMR1 deletion causes fragile X syndrome and can lead to molecular misdiagnosis: a case report and review of the literature. *Am J Med Genet A* **146A**, 1358-67.

Coffee, B., Keith, K., Albizua, I., Malone, T., Mowrey, J., Sherman, S. L. and Warren, S. T. (2009). Incidence of fragile X syndrome by newborn screening for methylated FMR1 DNA. *Am J Hum Genet* **85**, 503-14.

Coffee, R. L., Jr., Tessier, C. R., Woodruff, E. A., 3rd and Broadie, K. (2010). Fragile X mental retardation protein has a unique, evolutionarily conserved neuronal function not shared with FXR1P or FXR2P. *Dis Model Mech* **3**, 471-85.

Coffee, R. L., Jr., Williamson, A. J., Adkins, C. M., Gray, M. C., Page, T. L. and Broadie, K. (2011). In vivo neuronal function of the fragile x mental retardation protein is regulated by phosphorylation. *Hum Mol Genet*, DOI: DDR527.

Cohen, D., Pichard, N., Tordjman, S., Baumann, C., Burglen, L., Excoffier, E., Lazar, G., Mazet, P., Pinquier, C., Verloes, A. et al. (2005). Specific genetic disorders and autism: clinical contribution towards their identification. *J Autism Dev Disord* **35**, 103-16.

Comery, T. A., Harris, J. B., Willems, P. J., Oostra, B. A., Irwin, S. A., Weiler, I. J. and Greenough, W. T. (1997). Abnormal dendritic spines in fragile X knockout mice: maturation and pruning deficits. *Proc Natl Acad Sci U S A* **94**, 5401-4.

Cornish, K., Munir, F. and Wilding, J. (2001). [A neuropsychological and behavioural profile of attention deficits in fragile X syndrome]. *Rev Neurol* **33 Suppl 1**, S24-9.

Costa, A., Wang, Y., Dockendorff, T. C., Erdjument-Bromage, H., Tempst, P., Schedl, P. and Jongens, T. A. (2005). The Drosophila fragile X protein functions as a negative regulator in the orb autoregulatory pathway. *Dev Cell* **8**, 331-42.

Costa-Mattioli, M., Sossin, W. S., Klann, E. and Sonenberg, N. (2009). Translational control of long-lasting synaptic plasticity and memory. *Neuron* **61**, 10-26.

Coy, J. F., Sedlacek, Z., Bachner, D., Hameister, H., Joos, S., Lichter, P., Delius, H. and Poustka, A. (1995). Highly conserved 3' UTR and expression pattern of FXR1 points to a divergent gene regulation of FXR1 and FMR1. *Hum Mol Genet* **4**, 2209-18.

Croen, L. A., Grether, J. K. and Selvin, S. (2001). The epidemiology of mental retardation of unknown cause. *Pediatrics* **107**, E86.

Curry, C. J., Stevenson, R. E., Aughton, D., Byrne, J., Carey, J. C., Cassidy, S., Cunniff, C., Graham, J. M., Jr., Jones, M. C., Kaback, M. M. et al. (1997). Evaluation of mental retardation: recommendations of a Consensus Conference: American College of Medical Genetics. *Am J Med Genet* **72**, 468-77.

Cziko, A. M., McCann, C. T., Howlett, I. C., Barbee, S. A., Duncan, R. P., Luedemann, R., Zarnescu, D., Zinsmaier, K. E., Parker, R. R. and Ramaswami, M. (2009). Genetic modifiers of dFMR1 encode RNA granule components in Drosophila. *Genetics* **182**, 1051-60.

D'Hulst, C., De Geest, N., Reeve, S. P., Van Dam, D., De Deyn, P. P., Hassan, B. A. and Kooy, R. F. (2006). Decreased expression of the GABAA receptor in fragile X syndrome. *Brain Res* **1121**, 238-45.

D'Hulst, C., Heulens, I., Brouwer, J. R., Willemsen, R., De Geest, N., Reeve, S. P., De Deyn, P. P., Hassan, B. A. and Kooy, R. F. (2009). Expression of the GABAergic system in animal models for fragile X syndrome and fragile X associated tremor/ataxia syndrome (FXTAS). *Brain Res* **1253**, 176-83.

Darnell, J. (2011). Defects in translational regulation contributing to human cognitive and behavioral disease. *Curr Opin Genet Dev* **21**, 465-73.

Darnell, J. C., Fraser, C. E., Mostovetsky, O. and Darnell, R. B. (2009). Discrimination of common and unique RNA-binding activities among Fragile X mental retardation protein paralogs. *Hum Mol Genet* **18**, 3164-77.

Darnell, J. C., Fraser, C. E., Mostovetsky, O., Stefani, G., Jones, T. A., Eddy, S. R. and Darnell, R. B. (2005). Kissing complex RNAs mediate interaction between the Fragile-X mental retardation protein KH2 domain and brain polyribosomes. *Genes Dev* **19**, 903-18.

Darnell, J. C., Jensen, K. B., Jin, P., Brown, V., Warren, S. T. and Darnell, R. B. (2001). Fragile X mental retardation protein targets G quartet mRNAs important for neuronal function. *Cell* **107**, 489-99.

Darnell, J. C., Van Driesche, S. J., Zhang, C., Hung, K. Y., Mele, A., Fraser, C. E., Stone, E. F., Chen, C., Fak, J. J., Chi, S. W. et al. (2011). FMRP stalls ribosomal translocation on mRNAs linked to synaptic function and autism. *Cell* **146**, 247-61.

Davidovic, L., Jaglin, X. H., Lepagnol-Bestel, A. M., Tremblay, S., Simonneau, M., Bardoni, B. and Khandjian, E. W. (2007). The fragile X mental retardation protein is a molecular adaptor between the neurospecific KIF3C kinesin and dendritic RNA granules. *Hum Mol Genet* **16**, 3047-58.

Davidovic, L., Sacconi, S., Bechara, E. G., Delplace, S., Allegra, M., Desnuelle, C. and Bardoni, B. (2008). Alteration of expression of muscle specific isoforms of the fragile X related protein 1 (FXR1P) in facioscapulohumeral muscular dystrophy patients. *J Med Genet* **45**, 679-85.

Davis, H. P. and Squire, L. R. (1984). Protein synthesis and memory: a review. *Psychol Bull* **96**, 518-59.

De Boulle, K., Verkerk, A. J., Reyniers, E., Vits, L., Hendrickx, J., Van Roy, B., Van den Bos, F., de Graaff, E., Oostra, B. A. and Willems, P. J. (1993). A point mutation in the FMR-1 gene associated with fragile X mental retardation. *Nat Genet* **3**, 31-5.

de Vries, B. B., Halley, D. J., Oostra, B. A. and Niermeijer, M. F. (1998). The fragile X syndrome. *J Med Genet* **35**, 579-89.

Dejgaard, K. and Leffers, H. (1996). Characterisation of the nucleic-acid-binding activity of KH domains. Different properties of different domains. *Eur J Biochem* **241**, 425-31.

Deng, P. Y., Sojka, D. and Klyachko, V. A. (2011). Abnormal presynaptic short-term plasticity and information processing in a mouse model of fragile X syndrome. *J Neurosci* **31**, 10971-82.

Deng, P. Y., Xiao, Z. and Lei, S. (2010a). Distinct modes of modulation of GABAergic transmission by Group I metabotropic glutamate receptors in rat entorhinal cortex. *Hippocampus* **20**, 980-93.

Deng, W., Aimone, J. B. and Gage, F. H. (2010b). New neurons and new memories: how does adult hippocampal neurogenesis affect learning and memory? *Nat Rev Neurosci* **11**, 339-50.

Denman, R. B. and Sung, Y. J. (2002). Species-specific and isoform-specific RNA binding of human and mouse fragile X mental retardation proteins. *Biochem Biophys Res Commun* **292**, 1063-9.

Dent, E. W. and Kalil, K. (2001). Axon branching requires interactions between dynamic microtubules and actin filaments. *J Neurosci* **21**, 9757-69.

Devys, D., Lutz, Y., Rouyer, N., Bellocq, J. P. and Mandel, J. L. (1993). The FMR-1 protein is cytoplasmic, most abundant in neurons and appears normal in carriers of a fragile X premutation. *Nat Genet* **4**, 335-40.

Dickman, D. K., Lu, Z., Meinertzhagen, I. A. and Schwarz, T. L. (2006). Altered synaptic development and active zone spacing in endocytosis mutants. *Curr Biol* **16**, 591-8.

Dictenberg, J. B., Swanger, S. A., Antar, L. N., Singer, R. H. and Bassell, G. J. (2008). A direct role for FMRP in activity-dependent dendritic mRNA transport links filopodial-spine morphogenesis to fragile X syndrome. *Dev Cell* **14**, 926-39.

Dobkin, C., Rabe, A., Dumas, R., El Idrissi, A., Haubenstock, H. and Brown, W. T. (2000). Fmr1 knockout mouse has a distinctive strain-specific learning impairment. *Neuroscience* **100**, 423-9.

Dockendorff, T. C., Su, H. S., McBride, S. M., Yang, Z., Choi, C. H., Siwicki, K. K., Sehgal, A. and Jongens, T. A. (2002). Drosophila lacking dfmr1 activity show defects in circadian output and fail to maintain courtship interest. *Neuron* **34**, 973-84.

Dolen, G., Osterweil, E., Rao, B. S., Smith, G. B., Auerbach, B. D., Chattarji, S. and Bear, M. F. (2007). Correction of fragile X syndrome in mice. *Neuron* **56**, 955-62.

Drews, C. D., Yeargin-Allsopp, M., Decoufle, P. and Murphy, C. C. (1995). Variation in the influence of selected sociodemographic risk factors for mental retardation. *Am J Public Health* **85**, 329-34.

Duan, R. and Jin, P. (2006). Identification of messenger RNAs and microRNAs associated with fragile X mental retardation protein. *Methods Mol Biol* **342**, 267-76.

Eberhart, D. E., Malter, H. E., Feng, Y. and Warren, S. T. (1996). The fragile X mental retardation protein is a ribonucleoprotein containing both nuclear localization and nuclear export signals. *Hum Mol Genet* **5**, 1083-91.

Edbauer, D., Neilson, J. R., Foster, K. A., Wang, C. F., Seeburg, D. P., Batterton, M. N., Tada, T., Dolan, B. M., Sharp, P. A. and Sheng, M. (2010). Regulation of synaptic structure and function by FMRP-associated microRNAs miR-125b and miR-132. *Neuron* **65**, 373-84.

Ehninger, D., Han, S., Shilyansky, C., Zhou, Y., Li, W., Kwiatkowski, D. J., Ramesh, V. and Silva, A. J. (2008). Reversal of learning deficits in a Tsc2+/- mouse model of tuberous sclerosis. *Nat Med* **14**, 843-8.

Einfeld, S., Hall, W. and Levy, F. (1991). Hyperactivity and the fragile X syndrome. *J Abnorm Child Psychol* **19**, 253-62.

English, J. D. and Sweatt, J. D. (1997). A requirement for the mitogen-activated protein kinase cascade in hippocampal long term potentiation. *J Biol Chem* **272**, 19103-6.

Epstein, A. M., Bauer, C. R., Ho, A., Bosco, G. and Zarnescu, D. C. (2009). Drosophila Fragile X protein controls cellular proliferation by regulating cbl levels in the ovary. *Dev Biol* **330**, 83-92.

Estes, P. S., O'Shea, M., Clasen, S. and Zarnescu, D. C. (2008). Fragile X protein controls the efficacy of mRNA transport in Drosophila neurons. *Mol Cell Neurosci* **39**, 170-9.

Feliciano, P. (2011). Fragile X protein stalls ribosomes. *Nat Genet* **43**, 824-824.

Feng, Y., Absher, D., Eberhart, D. E., Brown, V., Malter, H. E. and Warren, S. T. (1997a). FMRP associates with polyribosomes as an mRNP, and the I304N mutation of severe fragile X syndrome abolishes this association. *Mol Cell* **1**, 109-18.

Feng, Y., Gutekunst, C. A., Eberhart, D. E., Yi, H., Warren, S. T. and Hersch, S. M. (1997b). Fragile X mental retardation protein: nucleocytoplasmic shuttling and association with somatodendritic ribosomes. *J Neurosci* **17**, 1539-47.

Fernandez, B. A., Roberts, W., Chung, B., Weksberg, R., Meyn, S., Szatmari, P., Joseph-George, A. M., Mackay, S., Whitten, K., Noble, B. et al. (2010). Phenotypic spectrum associated with de novo and inherited deletions and duplications at 16p11.2 in individuals ascertained for diagnosis of autism spectrum disorder. *J Med Genet* **47**, 195-203.

Fisch, G. S., Simensen, R. J. and Schroer, R. J. (2002). Longitudinal changes in cognitive and adaptive behavior scores in children and adolescents with the fragile X mutation or autism. *J Autism Dev Disord* **32**, 107-14.

Fishburn, J., Turner, G., Daniel, A. and Brookwell, R. (1983). The diagnosis and frequency of X-linked conditions in a cohort of moderately retarded males with affected brothers. *Am J Med Genet* **14**, 713-24.

Freund, L. S. and Reiss, A. L. (1991). Cognitive profiles associated with the fra(X) syndrome in males and females. *Am J Med Genet* **38**, 542-7.

Fryns, J. P. (1984). The fragile X syndrome. A study of 83 families. *Clin Genet* **26**, 497-528.

Fryns, J. P., Jacobs, J., Kleczkowska, A. and van den Berghe, H. (1984). The psychological profile of the fragile X syndrome. *Clin Genet* **25**, 131-4.

Gabel, L. A., Won, S., Kawai, H., McKinney, M., Tartakoff, A. M. and Fallon, J. R. (2004). Visual experience regulates transient expression and dendritic localization of fragile X mental retardation protein. *J Neurosci* **24**, 10579-83.

Gabus, C., Mazroui, R., Tremblay, S., Khandjian, E. W. and Darlix, J. L. (2004). The fragile X mental retardation protein has nucleic acid chaperone properties. *Nucleic Acids Res* **32**, 2129-37.

Gallagher, A. and Hallahan, B. (2011). Fragile X-associated disorders: a clinical overview. *J Neurol*.

Galvez, R. and Greenough, W. T. (2005). Sequence of abnormal dendritic spine development in primary somatosensory cortex of a mouse model of the fragile X mental retardation syndrome. *Am J Med Genet A* **135**, 155-60.

Gantois, I., Vandesompele, J., Speleman, F., Reyniers, E., D'Hooge, R., Severijnen, L. A., Willemsen, R., Tassone, F. and Kooy, R. F. (2006). Expression profiling suggests underexpression of the GABA(A) receptor subunit delta in the fragile X knockout mouse model. *Neurobiol Dis* **21**, 346-57.

Gatto, C. L. and Broadie, K. (2008). Temporal requirements of the fragile X mental retardation protein in the regulation of synaptic structure. *Development* **135**, 2637-48.

Gatto, C. L. and Broadie, K. (2009a). Temporal requirements of the fragile x mental retardation protein in modulating circadian clock circuit synaptic architecture. *Front Neural Circuits* **3**, 8.

Gatto, C. L. and Broadie, K. (2009b). The fragile X mental retardation protein in circadian rhythmicity and memory consolidation. *Mol Neurobiol* **39**, 107-29.

Gedeon, A. K., Baker, E., Robinson, H., Partington, M. W., Gross, B., Manca, A., Korn, B., Poustka, A., Yu, S., Sutherland, G. R. et al. (1992). Fragile X syndrome without CCG amplification has an FMR1 deletion. *Nat Genet* **1**, 341-4.

Giangreco, C. A., Steele, M. W., Aston, C. E., Cummins, J. H. and Wenger, S. L. (1996). A simplified six-item checklist for screening for fragile X syndrome in the pediatric population. *J Pediatr* **129**, 611-4.

Gibson, J. R., Bartley, A. F., Hays, S. A. and Huber, K. M. (2008). Imbalance of neocortical excitation and inhibition and altered UP states reflect network hyperexcitability in the mouse model of fragile X syndrome. *J Neurophysiol* **100**, 2615-26.

Gladding, C. M., Fitzjohn, S. M. and Molnar, E. (2009). Metabotropic glutamate receptor-mediated long-term depression: molecular mechanisms. *Pharmacol Rev* **61**, 395-412.

Gorczyca, D., Ashley, J., Speese, S., Gherbesi, N., Thomas, U., Gundelfinger, E., Gramates, L. S. and Budnik, V. (2007). Postsynaptic membrane addition depends on the Discs-Large-interacting t-SNARE Gtaxin. *J Neurosci* **27**, 1033-44.

Gould, E. L., Loesch, D. Z., Martin, M. J., Hagerman, R. J., Armstrong, S. M. and Huggins, R. M. (2000). Melatonin profiles and sleep characteristics in boys with fragile X syndrome: a preliminary study. *Am J Med Genet* **95**, 307-15.

Grima, B., Chelot, E., Xia, R. and Rouyer, F. (2004). Morning and evening peaks of activity rely on different clock neurons of the Drosophila brain. *Nature* **431**, 869-73.

Gross, C., Berry-Kravis, E. M. and Bassell, G. J. (2011). Therapeutic Strategies in Fragile X Syndrome: Dysregulated mGluR Signaling and Beyond. *Neuropsychopharmacology*.

Grossman, A. W., Elisseou, N. M., McKinney, B. C. and Greenough, W. T. (2006). Hippocampal pyramidal cells in adult Fmr1 knockout mice exhibit an immature-appearing profile of dendritic spines. *Brain Res* **1084**, 158-64.

Guo, W., Allan, A. M., Zong, R., Zhang, L., Johnson, E. B., Schaller, E. G., Murthy, A. C., Goggin, S. L., Eisch, A. J., Oostra, B. A. et al. (2011). Ablation of Fmrp in adult neural stem cells disrupts hippocampus-dependent learning. *Nat Med* **17**, 559-65.

Haas, K. F. and Broadie, K. (2008). Roles of ubiquitination at the synapse. *Biochim Biophys Acta* **1779**, 495-506.

Hagerman, P. J. (2008). The fragile X prevalence paradox. *J Med Genet* **45**, 498-9.

Hagerman, R. J. and Hagerman, P. J. (2002). The fragile X premutation: into the phenotypic fold. *Curr Opin Genet Dev* **12**, 278-83.

Hagerman, R. J., Jackson, A. W., 3rd, Levitas, A., Rimland, B. and Braden, M. (1986). An analysis of autism in fifty males with the fragile X syndrome. *Am J Med Genet* **23**, 359-74.

Hagerman, R. J., Leehey, M., Heinrichs, W., Tassone, F., Wilson, R., Hills, J., Grigsby, J., Gage, B. and Hagerman, P. J. (2001). Intention tremor, parkinsonism, and generalized brain atrophy in male carriers of fragile X. *Neurology* **57**, 127-30.

Hagerman, R. J., Ono, M. Y. and Hagerman, P. J. (2005). Recent advances in fragile X: a model for autism and neurodegeneration. *Curr Opin Psychiatry* **18**, 490-6.

Hanson, J. E. and Madison, D. V. (2007). Presynaptic FMR1 genotype influences the degree of synaptic connectivity in a mosaic mouse model of fragile X syndrome. *J Neurosci* **27**, 4014-8.

Heitz, D., Devys, D., Imbert, G., Kretz, C. and Mandel, J. L. (1992). Inheritance of the fragile X syndrome: size of the fragile X premutation is a major determinant of the transition to full mutation. *J Med Genet* **29**, 794-801.

Helfrich-Forster, C. (1995). The period clock gene is expressed in central nervous system neurons which also produce a neuropeptide that reveals the projections of circadian pacemaker cells within the brain of Drosophila melanogaster. *Proc Natl Acad Sci U S A* **92**, 612-6.

Helfrich-Forster, C. (2005). Neurobiology of the fruit fly's circadian clock. *Genes Brain Behav* **4**, 65-76.

Hessl, D., Dyer-Friedman, J., Glaser, B., Wisbeck, J., Barajas, R. G., Taylor, A. and Reiss, A. L. (2001). The influence of environmental and genetic factors on behavior problems and autistic symptoms in boys and girls with fragile X syndrome. *Pediatrics* **108**, E88.

Heulens, I. and Kooy, F. (2011). Fragile X syndrome: from gene discovery to therapy. *Front Biosci* **16**, 1211-32.

Hinton, V. J., Brown, W. T., Wisniewski, K. and Rudelli, R. D. (1991). Analysis of neocortex in three males with the fragile X syndrome. *Am J Med Genet* **41**, 289-94.

Hirono, M., Yoshioka, T. and Konishi, S. (2001). GABA(B) receptor activation enhances mGluR-mediated responses at cerebellar excitatory synapses. *Nat Neurosci* **4**, 1207-16.

Hirst, M., Grewal, P., Flannery, A., Slatter, R., Maher, E., Barton, D., Fryns, J. P. and Davies, K. (1995). Two new cases of FMR1 deletion associated with mental impairment. *Am J Hum Genet* **56**, 67-74.

Hoeffer, C. A. and Klann, E. (2010). mTOR signaling: at the crossroads of plasticity, memory and disease. *Trends Neurosci* **33**, 67-75.

Hoogeveen, A. T., Willemsen, R. and Oostra, B. A. (2002). Fragile X syndrome, the Fragile X related proteins, and animal models. *Microsc Res Tech* **57**, 148-55.

Huang, T., Li, L. Y., Shen, Y., Qin, X. B., Pang, Z. L. and Wu, G. Y. (1996). Alternative splicing of the FMR1 gene in human fetal brain neurons. *Am J Med Genet* **64**, 252-5.

Huber, K. M., Gallagher, S. M., Warren, S. T. and Bear, M. F. (2002). Altered synaptic plasticity in a mouse model of fragile X mental retardation. *Proc Natl Acad Sci U S A* **99**, 7746-50.

Hummel, T., Krukkert, K., Roos, J., Davis, G. and Klambt, C. (2000). Drosophila Futsch/22C10 is a MAP1B-like protein required for dendritic and axonal development. *Neuron* **26**, 357-70.

Huot, M. E., Mazroui, R., Leclerc, P. and Khandjian, E. W. (2001). Developmental expression of the fragile X-related 1 proteins in mouse testis: association with microtubule elements. *Hum Mol Genet* **10**, 2803-11.

Iacoangeli, A., Rozhdestvensky, T. S., Dolzhanskaya, N., Tournier, B., Schutt, J., Brosius, J., Denman, R. B., Khandjian, E. W., Kindler, S. and Tiedge, H. (2008). On BC1 RNA and the fragile X mental retardation protein. *Proc Natl Acad Sci U S A* **105**, 734-9.

Inoue, S., Shimoda, M., Nishinokubi, I., Siomi, M. C., Okamura, M., Nakamura, A., Kobayashi, S., Ishida, N. and Siomi, H. (2002). A role for the Drosophila fragile X-related gene in circadian output. *Curr Biol* **12**, 1331-5.

Irwin, S. A., Galvez, R. and Greenough, W. T. (2000). Dendritic spine structural anomalies in fragile-X mental retardation syndrome. *Cereb Cortex* **10**, 1038-44.

Irwin, S. A., Idupulapati, M., Gilbert, M. E., Harris, J. B., Chakravarti, A. B., Rogers, E. J., Crisostomo, R. A., Larsen, B. P., Mehta, A., Alcantara, C. J. et al. (2002). Dendritic spine and dendritic field characteristics of layer V pyramidal neurons in the visual cortex of fragile-X knockout mice. *Am J Med Genet* **111**, 140-6.

Irwin, S. A., Patel, B., Idupulapati, M., Harris, J. B., Crisostomo, R. A., Larsen, B. P., Kooy, F., Willems, P. J., Cras, P., Kozlowski, P. B. et al. (2001). Abnormal dendritic spine characteristics in the temporal and visual cortices of patients with fragile-X syndrome: a quantitative examination. *Am J Med Genet* **98**, 161-7.

Ishizuka, A., Siomi, M. C. and Siomi, H. (2002). A Drosophila fragile X protein interacts with components of RNAi and ribosomal proteins. *Genes Dev* **16**, 2497-508.

Jamain, S., Quach, H., Betancur, C., Rastam, M., Colineaux, C., Gillberg, I. C., Soderstrom, H., Giros, B., Leboyer, M., Gillberg, C. et al. (2003). Mutations of the X-linked genes encoding neuroligins NLGN3 and NLGN4 are associated with autism. *Nat Genet* **34**, 27-9.

Jenuwein, T. (2002). Molecular biology. An RNA-guided pathway for the epigenome. *Science* **297**, 2215-8.

Jin, P., Zarnescu, D. C., Ceman, S., Nakamoto, M., Mowrey, J., Jongens, T. A., Nelson, D. L., Moses, K. and Warren, S. T. (2004). Biochemical and genetic interaction between the fragile X mental retardation protein and the microRNA pathway. *Nat Neurosci* **7**, 113-7.

Johannisson, R., Rehder, H., Wendt, V. and Schwinger, E. (1987). Spermatogenesis in two patients with the fragile X syndrome. I. Histology: light and electron microscopy. *Hum Genet* **76**, 141-7.

Kanai, Y., Dohmae, N. and Hirokawa, N. (2004). Kinesin transports RNA: isolation and characterization of an RNA-transporting granule. *Neuron* **43**, 513-25.

Kandel, E. R. (2001). The molecular biology of memory storage: a dialogue between genes and synapses. *Science* **294**, 1030-8.

Kanner, L. (1971). Follow-up study of eleven autistic children originally reported in 1943. *J Autism Child Schizophr* **1**, 119-45.

Kao, D. I., Aldridge, G. M., Weiler, I. J. and Greenough, W. T. (2010). Altered mRNA transport, docking, and protein translation in neurons lacking fragile X mental retardation protein. *Proc Natl Acad Sci U S A* **107**, 15601-6.

Kelleher, R. J., 3rd and Bear, M. F. (2008). The autistic neuron: troubled translation? *Cell* **135**, 401-6.

Khandjian, E. W., Bardoni, B., Corbin, F., Sittler, A., Giroux, S., Heitz, D., Tremblay, S., Pinset, C., Montarras, D., Rousseau, F. et al. (1998). Novel isoforms of the fragile X related protein FXR1P are expressed during myogenesis. *Hum Mol Genet* **7**, 2121-8.

Khandjian, E. W., Corbin, F., Woerly, S. and Rousseau, F. (1996). The fragile X mental retardation protein is associated with ribosomes. *Nat Genet* **12**, 91-3.

Khandjian, E. W., Huot, M. E., Tremblay, S., Davidovic, L., Mazroui, R. and Bardoni, B. (2004). Biochemical evidence for the association of fragile X mental retardation protein with brain polyribosomal ribonucleoparticles. *Proc Natl Acad Sci U S A* **101**, 13357-62.

Kim, S. H., Dong, W. K., Weiler, I. J. and Greenough, W. T. (2006). Fragile X mental retardation protein shifts between polyribosomes and stress granules after neuronal injury by arsenite stress or in vivo hippocampal electrode insertion. *J Neurosci* **26**, 2413-8.

Kirkpatrick, L. L., McIlwain, K. A. and Nelson, D. L. (1999). Alternative splicing in the murine and human FXR1 genes. *Genomics* **59**, 193-202.

Kirkpatrick, L. L., McIlwain, K. A. and Nelson, D. L. (2001). Comparative genomic sequence analysis of the FXR gene family: FMR1, FXR1, and FXR2. *Genomics* **78**, 169-77.

Kogan, M. D., Blumberg, S. J., Schieve, L. A., Boyle, C. A., Perrin, J. M., Ghandour, R. M., Singh, G. K., Strickland, B. B., Trevathan, E. and van Dyck, P. C. (2009). Prevalence of parent-reported diagnosis of autism spectrum disorder among children in the US, 2007. *Pediatrics* **124**, 1395-403.

Kolbel, K., Ihling, C., Bellmann-Sickert, K., Neundorf, I., Beck-Sickinger, A. G., Sinz, A., Kuhn, U. and Wahle, E. (2009). Type I Arginine Methyltransferases PRMT1 and PRMT-3 Act Distributively. *J Biol Chem* **284**, 8274-82.

Koukoui, S. D. and Chaudhuri, A. (2007). Neuroanatomical, molecular genetic, and behavioral correlates of fragile X syndrome. *Brain Res Rev* **53**, 27-38.

Krawczun, M. S., Jenkins, E. C. and Brown, W. T. (1985). Analysis of the fragile-X chromosome: localization and detection of the fragile site in high resolution preparations. *Hum Genet* **69**, 209-11.

Kronk, R., Bishop, E. E., Raspa, M., Bickel, J. O., Mandel, D. A. and Bailey, D. B., Jr. (2010). Prevalence, nature, and correlates of sleep problems among children with fragile X syndrome based on a large scale parent survey. *Sleep* **33**, 679-87.

Krueger, D. D., Osterweil, E. K., Chen, S. P., Tye, L. D. and Bear, M. F. (2011). Cognitive dysfunction and prefrontal synaptic abnormalities in a mouse model of fragile X syndrome. *Proc Natl Acad Sci U S A* **108**, 2587-92.

Lachiewicz, A. M. and Dawson, D. V. (1994). Do young boys with fragile X syndrome have macroorchidism? *Pediatrics* **93**, 992-5.

Laggerbauer, B., Ostareck, D., Keidel, E. M., Ostareck-Lederer, A. and Fischer, U. (2001). Evidence that fragile X mental retardation protein is a negative regulator of translation. *Hum Mol Genet* **10**, 329-38.

Larson, J., Jessen, R. E., Kim, D., Fine, A. K. and du Hoffmann, J. (2005). Age-dependent and selective impairment of long-term potentiation in the anterior piriform cortex of mice lacking the fragile X mental retardation protein. *J Neurosci* **25**, 9460-9.

Larson, J., Kim, D., Patel, R. C. and Floreani, C. (2008). Olfactory discrimination learning in mice lacking the fragile X mental retardation protein. *Neurobiol Learn Mem* **90**, 90-102.

Lee, A., Li, W., Xu, K., Bogert, B. A., Su, K. and Gao, F. B. (2003). Control of dendritic development by the Drosophila fragile X-related gene involves the small GTPase Rac1. *Development* **130**, 5543-52.

Leffers, H., Dejgaard, K. and Celis, J. E. (1995). Characterisation of two major cellular poly(rC)-binding human proteins, each containing three K-homologous (KH) domains. *Eur J Biochem* **230**, 447-53.

Lehrke, R. (1972). A theory of X-linkage of major intellectual traits. Response to Dr. Anastasi and to the Drs. Nance and Engel. *Am J Ment Defic* **76**, 626-31.

Leonard, H. and Wen, X. (2002). The epidemiology of mental retardation: challenges and opportunities in the new millennium. *Ment Retard Dev Disabil Res Rev* **8**, 117-34.

Levenga, J., Buijsen, R. A., Rife, M., Moine, H., Nelson, D. L., Oostra, B. A., Willemsen, R. and de Vrij, F. M. (2009). Ultrastructural analysis of the functional domains in FMRP using primary hippocampal mouse neurons. *Neurobiol Dis* **35**, 241-50.

Limprasert, P., Jaruratanasirikul, S. and Vasiknanonte, P. (2000). Unilateral macroorchidism in fragile X syndrome. *Am J Med Genet* **95**, 516-7.

Lin, C. H., Yeh, S. H., Lu, K. T., Leu, T. H., Chang, W. C. and Gean, P. W. (2001). A role for the PI-3 kinase signaling pathway in fear conditioning and synaptic plasticity in the amygdala. *Neuron* **31**, 841-51.

Lord, C., Shulman, C. and DiLavore, P. (2004). Regression and word loss in autistic spectrum disorders. *J Child Psychol Psychiatry* **45**, 936-55.

Lu, R., Wang, H., Liang, Z., Ku, L., O'Donnell W, T., Li, W., Warren, S. T. and Feng, Y. (2004). The fragile X protein controls microtubule-associated protein 1B translation and microtubule stability in brain neuron development. *Proc Natl Acad Sci U S A* **101**, 15201-6.

Lubs, H. A. (1969). A marker X chromosome. *Am J Hum Genet* **21**, 231-44.

Lyons, L. C. and Roman, G. (2009). Circadian modulation of short-term memory in Drosophila. *Learn Mem* **16**, 19-27.

MacLeod, L. S., Kogan, C. S., Collin, C. A., Berry-Kravis, E., Messier, C. and Gandhi, R. (2010). A comparative study of the performance of individuals with fragile X syndrome and Fmr1 knockout mice on Hebb-Williams mazes. *Genes Brain Behav* **9**, 53-64.

Martin, J. P. and Bell, J. (1943). A Pedigree of Mental Defect Showing Sex-Linkage. *J Neurol Psychiatry* **6**, 154-7.

Martin, K. C. and Ephrussi, A. (2009). mRNA localization: gene expression in the spatial dimension. *Cell* **136**, 719-30.

Matzke, M. A. and Birchler, J. A. (2005). RNAi-mediated pathways in the nucleus. *Nat Rev Genet* **6**, 24-35.

Mazroui, R., Huot, M. E., Tremblay, S., Boilard, N., Labelle, Y. and Khandjian, E. W. (2003). Fragile X Mental Retardation protein determinants required for its association with polyribosomal mRNPs. *Hum Mol Genet* **12**, 3087-96.

Mazroui, R., Huot, M. E., Tremblay, S., Filion, C., Labelle, Y. and Khandjian, E. W. (2002). Trapping of messenger RNA by Fragile X Mental Retardation protein into cytoplasmic granules induces translation repression. *Hum Mol Genet* **11**, 3007-17.

McBride, S. M., Choi, C. H., Wang, Y., Liebelt, D., Braunstein, E., Ferreiro, D., Sehgal, A., Siwicki, K. K., Dockendorff, T. C., Nguyen, H. T. et al. (2005). Pharmacological rescue of synaptic plasticity, courtship behavior, and mushroom body defects in a Drosophila model of fragile X syndrome. *Neuron* **45**, 753-64.

McKinney, B. C., Grossman, A. W., Elisseou, N. M. and Greenough, W. T. (2005). Dendritic spine abnormalities in the occipital cortex of C57BL/6 Fmr1 knockout mice. *Am J Med Genet B Neuropsychiatr Genet* **136**, 98-102.

McNaughton, C. H., Moon, J., Strawderman, M. S., Maclean, K. N., Evans, J. and Strupp, B. J. (2008). Evidence for social anxiety and impaired social cognition in a mouse model of fragile X syndrome. *Behav Neurosci* **122**, 293-300.

Menon, L. and Mihailescu, M. R. (2007). Interactions of the G quartet forming semaphorin 3F RNA with the RGG box domain of the fragile X protein family. *Nucleic Acids Res* **35**, 5379-92.

Menon, R. P., Gibson, T. J. and Pastore, A. (2004). The C terminus of fragile X mental retardation protein interacts with the multi-domain Ran-binding protein in the microtubule-organising centre. *J Mol Biol* **343**, 43-53.

Mercaldo, V., Descalzi, G. and Zhuo, M. (2009). Fragile X mental retardation protein in learning-related synaptic plasticity. *Mol Cells* **28**, 501-7.

Michel, C. I., Kraft, R. and Restifo, L. L. (2004). Defective neuronal development in the mushroom bodies of Drosophila fragile X mental retardation 1 mutants. *J Neurosci* **24**, 5798-809.

Mientjes, E. J., Willemsen, R., Kirkpatrick, L. L., Nieuwenhuizen, I. M., Hoogeveen-Westerveld, M., Verweij, M., Reis, S., Bardoni, B., Hoogeveen, A. T., Oostra, B. A. et al. (2004). Fxr1 knockout mice show a striated muscle phenotype: implications for Fxr1p function in vivo. *Hum Mol Genet* **13**, 1291-302.

Mikl, M., Vendra, G. and Kiebler, M. A. (2011). Independent localization of MAP2, CaMKIIalpha and beta-actin RNAs in low copy numbers. *EMBO Rep* **12**, 1077-84.

Miles, J. H. (2011). Autism spectrum disorders--a genetics review. *Genet Med* **13**, 278-94.

Monaco, A. P. and Bailey, A. J. (2001). Autism. The search for susceptibility genes. *Lancet* **358 Suppl**, S3.

Moore, B. C., Glover, T. W., Kaiser-McCaw, B. and Hecht, F. (1982). Fragile X-linked mental retardation of macro-orchidism. *West J Med* **137**, 278-81.

Morales, J., Hiesinger, P. R., Schroeder, A. J., Kume, K., Verstreken, P., Jackson, F. R., Nelson, D. L. and Hassan, B. A. (2002). Drosophila fragile X protein, DFXR, regulates neuronal morphology and function in the brain. *Neuron* **34**, 961-72.

Muddashetty, R. S., Nalavadi, V. C., Gross, C., Yao, X., Xing, L., Laur, O., Warren, S. T. and Bassell, G. J. (2011). Reversible inhibition of PSD-95 mRNA translation by miR-125a, FMRP phosphorylation, and mGluR signaling. *Mol Cell* **42**, 673-88.

Musumeci, S. A., Hagerman, R. J., Ferri, R., Bosco, P., Dalla Bernardina, B., Tassinari, C. A., De Sarro, G. B. and Elia, M. (1999). Epilepsy and EEG findings in males with fragile X syndrome. *Epilepsia* **40**, 1092-9.

Nakamoto, M., Nalavadi, V., Epstein, M. P., Narayanan, U., Bassell, G. J. and Warren, S. T. (2007). Fragile X mental retardation protein deficiency leads to excessive mGluR5-dependent internalization of AMPA receptors. *Proc Natl Acad Sci U S A* **104**, 15537-42.

Nakamura, M., Masuda, H., Horii, J., Kuma, K., Yokoyama, N., Ohba, T., Nishitani, H., Miyata, T., Tanaka, M. and Nishimoto, T. (1998). When overexpressed, a novel centrosomal protein, RanBPM, causes ectopic microtubule nucleation similar to gamma-tubulin. *J Cell Biol* **143**, 1041-52.

Napoli, I., Mercaldo, V., Boyl, P. P., Eleuteri, B., Zalfa, F., De Rubeis, S., Di Marino, D., Mohr, E., Massimi, M., Falconi, M. et al. (2008). The fragile X syndrome protein represses activity-dependent translation through CYFIP1, a new 4E-BP. *Cell* **134**, 1042-54.

Narayanan, U., Nalavadi, V., Nakamoto, M., Pallas, D. C., Ceman, S., Bassell, G. J. and Warren, S. T. (2007). FMRP phosphorylation reveals an immediate-early signaling pathway triggered by group I mGluR and mediated by PP2A. *J Neurosci* **27**, 14349-57.

Narayanan, U., Nalavadi, V., Nakamoto, M., Thomas, G., Ceman, S., Bassell, G. J. and Warren, S. T. (2008). S6K1 phosphorylates and regulates fragile X mental retardation protein (FMRP) with the neuronal protein synthesis-dependent mammalian target of rapamycin (mTOR) signaling cascade. *J Biol Chem* **283**, 18478-82.

Nielsen, K. B. and Tommerup, N. (1981). Macroorchidism, mental retardation, and the fragile X. *N Engl J Med* **305**, 1348.

Nimchinsky, E. A., Oberlander, A. M. and Svoboda, K. (2001). Abnormal development of dendritic spines in FMR1 knock-out mice. *J Neurosci* **21**, 5139-46.

Nistal, M., Martinez-Garcia, F., Regadera, J., Cobo, P. and Paniagua, R. (1992). Macro-orchidism: light and electron microscopic study of four cases. *Hum Pathol* **23**, 1011-8.

Nitabach, M. N. and Taghert, P. H. (2008). Organization of the Drosophila circadian control circuit. *Curr Biol* **18**, R84-93.

Nosyreva, E. D. and Huber, K. M. (2005). Developmental switch in synaptic mechanisms of hippocampal metabotropic glutamate receptor-dependent long-term depression. *J Neurosci* **25**, 2992-3001.

Oberle, I., Rousseau, F., Heitz, D., Kretz, C., Devys, D., Hanauer, A., Boue, J., Bertheas, M. F. and Mandel, J. L. (1991). Instability of a 550-base pair DNA segment and abnormal methylation in fragile X syndrome. *Science* **252**, 1097-102.

Odde, D. J., Tanaka, E. M., Hawkins, S. S. and Buettner, H. M. (1996). Stochastic dynamics of the nerve growth cone and its microtubules during neurite outgrowth. *Biotechnol Bioeng* **50**, 452-61.

Olmos-Serrano, J. L., Paluszkiewicz, S. M., Martin, B. S., Kaufmann, W. E., Corbin, J. G. and Huntsman, M. M. (2010). Defective GABAergic neurotransmission and pharmacological rescue of neuronal hyperexcitability in the amygdala in a mouse model of fragile X syndrome. *J Neurosci* **30**, 9929-38.

Pan, L., Woodruff, E., 3rd, Liang, P. and Broadie, K. (2008). Mechanistic relationships between Drosophila fragile X mental retardation protein and metabotropic glutamate receptor A signaling. *Mol Cell Neurosci* **37**, 747-60.

Pan, L., Zhang, Y. Q., Woodruff, E. and Broadie, K. (2004). The Drosophila fragile X gene negatively regulates neuronal elaboration and synaptic differentiation. *Curr Biol* **14**, 1863-70.

Park, S., Park, J. M., Kim, S., Kim, J. A., Shepherd, J. D., Smith-Hicks, C. L., Chowdhury, S., Kaufmann, W., Kuhl, D., Ryazanov, A. G. et al. (2008). Elongation factor 2 and fragile X mental retardation protein control the dynamic translation of Arc/Arg3.1 essential for mGluR-LTD. *Neuron* **59**, 70-83.

Patrick, G. N. (2006). Synapse formation and plasticity: recent insights from the perspective of the ubiquitin proteasome system. *Curr Opin Neurobiol* **16**, 90-4.

Patrick, G. N., Bingol, B., Weld, H. A. and Schuman, E. M. (2003). Ubiquitin-mediated proteasome activity is required for agonist-induced endocytosis of GluRs. *Curr Biol* **13**, 2073-81.

Penagarikano, O., Mulle, J. G. and Warren, S. T. (2007). The pathophysiology of fragile x syndrome. *Annu Rev Genomics Hum Genet* **8**, 109-29.

Pfeiffer, B. E. and Huber, K. M. (2007). Fragile X mental retardation protein induces synapse loss through acute postsynaptic translational regulation. *J Neurosci* **27**, 3120-30.

Pieretti, M., Zhang, F. P., Fu, Y. H., Warren, S. T., Oostra, B. A., Caskey, C. T. and Nelson, D. L. (1991). Absence of expression of the FMR-1 gene in fragile X syndrome. *Cell* **66**, 817-22.

Pinto, D. Pagnamenta, A. T. Klei, L. Anney, R. Merico, D. Regan, R. Conroy, J. Magalhaes, T. R. Correia, C. Abrahams, B. S. et al. (2010). Functional impact of global rare copy number variation in autism spectrum disorders. *Nature* **466**, 368-72.

Qin, M., Kang, J., Burlin, T. V., Jiang, C. and Smith, C. B. (2005). Postadolescent changes in regional cerebral protein synthesis: an in vivo study in the FMR1 null mouse. *J Neurosci* **25**, 5087-95.

Qin, M., Xia, Z., Huang, T. and Smith, C. B. (2011). Effects of chronic immobilization stress on anxiety-like behavior and basolateral amygdala morphology in Fmr1 knockout mice. *Neuroscience* **194**, 282-90.

Reeve, S. P., Bassetto, L., Genova, G. K., Kleyner, Y., Leyssen, M., Jackson, F. R. and Hassan, B. A. (2005). The Drosophila fragile X mental retardation protein controls actin dynamics by directly regulating profilin in the brain. *Curr Biol* **15**, 1156-63.

Reeve, S. P., Lin, X., Sahin, B. H., Jiang, F., Yao, A., Liu, Z., Zhi, H., Broadie, K., Li, W., Giangrande, A. et al. (2008). Mutational analysis establishes a critical role for the N terminus of fragile X mental retardation protein FMRP. *J Neurosci* **28**, 3221-6.

Renn, S. C., Park, J. H., Rosbash, M., Hall, J. C. and Taghert, P. H. (1999). A pdf neuropeptide gene mutation and ablation of PDF neurons each cause severe abnormalities of behavioral circadian rhythms in Drosophila. *Cell* **99**, 791-802.

Repicky, S. and Broadie, K. (2009). Metabotropic glutamate receptor-mediated use-dependent down-regulation of synaptic excitability involves the fragile X mental retardation protein. *J Neurophysiol* **101**, 672-87.

Richardson, S. A., Katz, M. and Koller, H. (1986). Sex differences in number of children administratively classified as mildly mentally retarded: an epidemiological review. *Am J Ment Defic* **91**, 250-6.

Richter, J. D. and Klann, E. (2009). Making synaptic plasticity and memory last: mechanisms of translational regulation. *Genes Dev* **23**, 1-11.

Rogers, S. J., Wehner, D. E. and Hagerman, R. (2001). The behavioral phenotype in fragile X: symptoms of autism in very young children with fragile X syndrome, idiopathic autism, and other developmental disorders. *J Dev Behav Pediatr* **22**, 409-17.

Roos, J., Hummel, T., Ng, N., Klambt, C. and Davis, G. W. (2000). Drosophila Futsch regulates synaptic microtubule organization and is necessary for synaptic growth. *Neuron* **26**, 371-82.

Ropers, H. H. (2006). X-linked mental retardation: many genes for a complex disorder. *Curr Opin Genet Dev* **16**, 260-9.

Ropers, H. H. and Hamel, B. C. (2005). X-linked mental retardation. *Nat Rev Genet* **6**, 46-57.

Rousseau, F., Heitz, D., Tarleton, J., MacPherson, J., Malmgren, H., Dahl, N., Barnicoat, A., Mathew, C., Mornet, E., Tejada, I. et al. (1994). A multicenter study on genotype-phenotype correlations in the fragile X syndrome, using direct diagnosis with probe StB12.3: the first 2,253 cases. *Am J Hum Genet* **55**, 225-37.

Routtenberg, A. and Rekart, J. L. (2005). Post-translational protein modification as the substrate for long-lasting memory. *Trends Neurosci* **28**, 12-9.

Ruiz-Canada, C., Ashley, J., Moeckel-Cole, S., Drier, E., Yin, J. and Budnik, V. (2004). New synaptic bouton formation is disrupted by misregulation of microtubule stability in aPKC mutants. *Neuron* **42**, 567-80.

Rutter, M. L. Progress in understanding autism: 2007-2010. *J Autism Dev Disord* **41**, 395-404.

Sabaratnam, M., Vroegop, P. G. and Gangadharan, S. K. (2001). Epilepsy and EEG findings in 18 males with fragile X syndrome. *Seizure* **10**, 60-3.

Schaefer, G. B. and Mendelsohn, N. J. (2008). Clinical genetics evaluation in identifying the etiology of autism spectrum disorders. *Genet Med* **10**, 301-5.

Schaeffer, C., Bardoni, B., Mandel, J. L., Ehresmann, B., Ehresmann, C. and Moine, H. (2001). The fragile X mental retardation protein binds specifically to its mRNA via a purine quartet motif. *Embo J* **20**, 4803-13.

Schenck, A., Bardoni, B., Langmann, C., Harden, N., Mandel, J. L. and Giangrande, A. (2003). CYFIP/Sra-1 controls neuronal connectivity in Drosophila and links the Rac1 GTPase pathway to the fragile X protein. *Neuron* **38**, 887-98.

Schenck, A., Bardoni, B., Moro, A., Bagni, C. and Mandel, J. L. (2001). A highly conserved protein family interacting with the fragile X mental retardation protein (FMRP) and displaying selective interactions with FMRP-related proteins FXR1P and FXR2P. *Proc Natl Acad Sci U S A* **98**, 8844-9.

Schenck, A., Van de Bor, V., Bardoni, B. and Giangrande, A. (2002). Novel features of dFMR1, the Drosophila orthologue of the fragile X mental retardation protein. *Neurobiol Dis* **11**, 53-63.

Schulz, C., Kiger, A. A., Tazuke, S. I., Yamashita, Y. M., Pantalena-Filho, L. C., Jones, D. L., Wood, C. G. and Fuller, M. T. (2004). A misexpression screen reveals effects of bag-of-marbles and TGF beta class signaling on the Drosophila male germ-line stem cell lineage. *Genetics* **167**, 707-23.

Schuman, E. M. (1999). mRNA trafficking and local protein synthesis at the synapse. *Neuron* **23**, 645-8.

Schutt, J., Falley, K., Richter, D., Kreienkamp, H. J. and Kindler, S. (2009). Fragile X mental retardation protein regulates the levels of scaffold proteins and glutamate receptors in postsynaptic densities. *J Biol Chem* **284**, 25479-87.

Scully, C. (2002). Fragile X (Martin Bell) syndrome. *Dent Update* **29**, 196-8.

Sekine, T., Yamaguchi, T., Hamano, K., Siomi, H., Saez, L., Ishida, N. and Shimoda, M. (2008). Circadian phenotypes of Drosophila fragile x mutants in alternative genetic backgrounds. *Zoolog Sci* **25**, 561-71.

Seltzer, M. M., Shattuck, P., Abbeduto, L. and Greenberg, J. S. (2004). Trajectory of development in adolescents and adults with autism. *Ment Retard Dev Disabil Res Rev* **10**, 234-47.

Shattuck, P. T. (2006a). Diagnostic substitution and changing autism prevalence. *Pediatrics* **117**, 1438-9.

Shattuck, P. T. (2006b). The contribution of diagnostic substitution to the growing administrative prevalence of autism in US special education. *Pediatrics* **117**, 1028-37.

Sherman, S. L., Jacobs, P. A., Morton, N. E., Froster-Iskenius, U., Howard-Peebles, P. N., Nielsen, K. B., Partington, M. W., Sutherland, G. R., Turner, G. and Watson, M. (1985). Further segregation analysis of the fragile X syndrome with special reference to transmitting males. *Hum Genet* **69**, 289-99.

Shinawi, M., Liu, P., Kang, S. H., Shen, J., Belmont, J. W., Scott, D. A., Probst, F. J., Craigen, W. J., Graham, B. H., Pursley, A. et al. (2010). Recurrent reciprocal 16p11.2 rearrangements associated with global developmental delay, behavioural problems, dysmorphism, epilepsy, and abnormal head size. *J Med Genet* **47**, 332-41.

Siller, S. S. and Broadie, K. (2011). Neural circuit architecture defects in a Drosophila model of Fragile X syndrome are alleviated by minocycline treatment and genetic removal of matrix metalloproteinase. *Dis Model Mech* **4**.

Siomi, H., Choi, M., Siomi, M. C., Nussbaum, R. L. and Dreyfuss, G. (1994). Essential role for KH domains in RNA binding: impaired RNA binding by a mutation in the KH domain of FMR1 that causes fragile X syndrome. *Cell* **77**, 33-9.

Siomi, H., Siomi, M. C., Nussbaum, R. L. and Dreyfuss, G. (1993). The protein product of the fragile X gene, FMR1, has characteristics of an RNA-binding protein. *Cell* **74**, 291-8.

Siomi, M. C., Higashijima, K., Ishizuka, A. and Siomi, H. (2002). Casein kinase II phosphorylates the fragile X mental retardation protein and modulates its biological properties. *Mol Cell Biol* **22**, 8438-47.

Siomi, M. C., Zhang, Y., Siomi, H. and Dreyfuss, G. (1996). Specific sequences in the fragile X syndrome protein FMR1 and the FXR proteins mediate their binding to 60S ribosomal subunits and the interactions among them. *Mol Cell Biol* **16**, 3825-32.

Sittler, A., Devys, D., Weber, C. and Mandel, J. L. (1996). Alternative splicing of exon 14 determines nuclear or cytoplasmic localisation of fmr1 protein isoforms. *Hum Mol Genet* **5**, 95-102.

Slegtenhorst-Eegdeman, K. E., de Rooij, D. G., Verhoef-Post, M., van de Kant, H. J., Bakker, C. E., Oostra, B. A., Grootegoed, J. A. and Themmen, A. P. (1998). Macroorchidism in FMR1 knockout mice is caused by increased Sertoli cell proliferation during testicular development. *Endocrinology* **139**, 156-62.

Smalley, S. L., Asarnow, R. F. and Spence, M. A. (1988). Autism and genetics. A decade of research. *Arch Gen Psychiatry* **45**, 953-61.

Sofocleous, C., Kolialexi, A. and Mavrou, A. (2009). Molecular diagnosis of Fragile X syndrome. *Expert Rev Mol Diagn* **9**, 23-30.

Sofola, O., Sundram, V., Ng, F., Kleyner, Y., Morales, J., Botas, J., Jackson, F. R. and Nelson, D. L. (2008). The Drosophila FMRP and LARK RNA-binding proteins function together to regulate eye development and circadian behavior. *J Neurosci* **28**, 10200-5.

Song, H. J. and Taylor, B. J. (2003). fruitless gene is required to maintain neuronal identity in evenskipped-expressing neurons in the embryonic CNS of Drosophila. *J Neurobiol* **55**, 115-33.

Spencer, C. M., Graham, D. F., Yuva-Paylor, L. A., Nelson, D. L. and Paylor, R. (2008). Social behavior in Fmr1 knockout mice carrying a human FMR1 transgene. *Behav Neurosci* **122**, 710-5.

Spencer, C. M., Serysheva, E., Yuva-Paylor, L. A., Oostra, B. A., Nelson, D. L. and Paylor, R. (2006). Exaggerated behavioral phenotypes in Fmr1/Fxr2 double knockout mice reveal a functional genetic interaction between Fragile X-related proteins. *Hum Mol Genet* **15**, 1984-94.

Splawski, I., Timothy, K. W., Sharpe, L. M., Decher, N., Kumar, P., Bloise, R., Napolitano, C., Schwartz, P. J., Joseph, R. M., Condouris, K. et al. (2004). Ca(V)1.2 calcium channel dysfunction causes a multisystem disorder including arrhythmia and autism. *Cell* **119**, 19-31.

Stefanatos, G. A. (2008). Regression in autistic spectrum disorders. *Neuropsychol Rev* **18**, 305-19.

Stefani, G., Fraser, C. E., Darnell, J. C. and Darnell, R. B. (2004). Fragile X mental retardation protein is associated with translating polyribosomes in neuronal cells. *J Neurosci* **24**, 7272-6.

Stetler, A., Winograd, C., Sayegh, J., Cheever, A., Patton, E., Zhang, X., Clarke, S. and Ceman, S. (2006). Identification and characterization of the methyl arginines in the fragile X mental retardation protein Fmrp. *Hum Mol Genet* **15**, 87-96.

Steward, O. and Schuman, E. M. (2001). Protein synthesis at synaptic sites on dendrites. *Annu Rev Neurosci* **24**, 299-325.

Steward, O. and Schuman, E. M. (2003). Compartmentalized synthesis and degradation of proteins in neurons. *Neuron* **40**, 347-59.

Stoleru, D., Peng, Y., Agosto, J. and Rosbash, M. (2004). Coupled oscillators control morning and evening locomotor behaviour of Drosophila. *Nature* **431**, 862-8.

Sung, Y. J., Dolzhanskaya, N., Nolin, S. L., Brown, T., Currie, J. R. and Denman, R. B. (2003). The fragile X mental retardation protein FMRP binds elongation factor 1A mRNA and negatively regulates its translation in vivo. *J Biol Chem* **278**, 15669-78.

Sutherland, G. R. (1977). Fragile sites on human chromosomes: demonstration of their dependence on the type of tissue culture medium. *Science* **197**, 265-6.

Sutton, M. A., Taylor, A. M., Ito, H. T., Pham, A. and Schuman, E. M. (2007). Postsynaptic decoding of neural activity: eEF2 as a biochemical sensor coupling miniature synaptic transmission to local protein synthesis. *Neuron* **55**, 648-61.

Szebenyi, G., Dent, E. W., Callaway, J. L., Seys, C., Lueth, H. and Kalil, K. (2001). Fibroblast growth factor-2 promotes axon branching of cortical neurons by influencing morphology and behavior of the primary growth cone. *J Neurosci* **21**, 3932-41.

Tamanini, F., Bontekoe, C., Bakker, C. E., van Unen, L., Anar, B., Willemsen, R., Yoshida, M., Galjaard, H., Oostra, B. A. and Hoogeveen, A. T. (1999a). Different targets for the fragile X-related proteins revealed by their distinct nuclear localizations. *Hum Mol Genet* **8**, 863-9.

Tamanini, F., Meijer, N., Verheij, C., Willems, P. J., Galjaard, H., Oostra, B. A. and Hoogeveen, A. T. (1996). FMRP is associated to the ribosomes via RNA. *Hum Mol Genet* **5**, 809-13.

Tamanini, F., Van Unen, L., Bakker, C., Sacchi, N., Galjaard, H., Oostra, B. A. and Hoogeveen, A. T. (1999b). Oligomerization properties of fragile-X mental-retardation protein (FMRP) and the fragile-X-related proteins FXR1P and FXR2P. *Biochem J* **343 Pt 3**, 517-23.

Tamanini, F., Willemsen, R., van Unen, L., Bontekoe, C., Galjaard, H., Oostra, B. A. and Hoogeveen, A. T. (1997). Differential expression of FMR1, FXR1 and FXR2 proteins in human brain and testis. *Hum Mol Genet* **6**, 1315-22.

Tanaka, E. M. and Kirschner, M. W. (1991). Microtubule behavior in the growth cones of living neurons during axon elongation. *J Cell Biol* **115**, 345-63.

Terracciano, A., Chiurazzi, P. and Neri, G. (2005). Fragile X syndrome. *Am J Med Genet C Semin Med Genet* **137C**, 32-7.

Tessier, C. R. and Broadie, K. (2008). Drosophila fragile X mental retardation protein developmentally regulates activity-dependent axon pruning. *Development* **135**, 1547-57.

Tessier, C. R. and Broadie, K. (2009). Activity-dependent modulation of neural circuit synaptic connectivity. *Front Mol Neurosci* **2**, 8.

Tessier, C. R. and Broadie, K. (2011). The fragile X mental retardation protein developmentally regulates the strength and fidelity of calcium signaling in Drosophila mushroom body neurons. *Neurobiol Dis* **41**, 147-59.

Torrioli, M. G., Vernacotola, S., Peruzzi, L., Tabolacci, E., Mila, M., Militerni, R., Musumeci, S., Ramos, F. J., Frontera, M., Sorge, G. et al. (2008). A double-blind, parallel, multicenter comparison of L-acetylcarnitine with placebo on the attention deficit hyperactivity disorder in fragile X syndrome boys. *Am J Med Genet A* **146**, 803-12.

Torroja, L., Packard, M., Gorczyca, M., White, K. and Budnik, V. (1999). The Drosophila beta-amyloid precursor protein homolog promotes synapse differentiation at the neuromuscular junction. *J Neurosci* **19**, 7793-803.

Tucker, B., Richards, R. and Lardelli, M. (2004). Expression of three zebrafish orthologs of human FMR1-related genes and their phylogenetic relationships. *Dev Genes Evol* **214**, 567-74.

Tully, T., Preat, T., Boynton, S. C. and Del Vecchio, M. (1994). Genetic dissection of consolidated memory in Drosophila. *Cell* **79**, 35-47.

Tully, T. and Quinn, W. G. (1985). Classical conditioning and retention in normal and mutant Drosophila melanogaster. *J Comp Physiol A* **157**, 263-77.

Turleau, C., Czernichow, P., Gorin, R., Royer, P. and de Grouchy, J. (1979). [Sex linked mental deficiency, unusual facies, macroorchidism and fragile site on chromosome X (author's transl)]. *Ann Genet* **22**, 205-9.

Turner, G., Daniel, A. and Frost, M. (1980). X-linked mental retardation, macro-orchidism, and the Xq27 fragile site. *J Pediatr* **96**, 837-41.

van 't Padje, S., Engels, B., Blonden, L., Severijnen, L. A., Verheijen, F., Oostra, B. A. and Willemsen, R. (2005). Characterisation of Fmrp in zebrafish: evolutionary dynamics of the fmr1 gene. *Dev Genes Evol* **215**, 198-206.

Van't Padje, S., Chaudhry, B., Severijnen, L. A., van der Linde, H. C., Mientjes, E. J., Oostra, B. A. and Willemsen, R. (2009). Reduction in fragile X related 1 protein causes cardiomyopathy and muscular dystrophy in zebrafish. *J Exp Biol* **212**, 2564-70.

Verheij, C., Bakker, C. E., de Graaff, E., Keulemans, J., Willemsen, R., Verkerk, A. J., Galjaard, H., Reuser, A. J., Hoogeveen, A. T. and Oostra, B. A. (1993). Characterization and localization of the FMR-1 gene product associated with fragile X syndrome. *Nature* **363**, 722-4.

Verkerk, A. J., Pieretti, M., Sutcliffe, J. S., Fu, Y. H., Kuhl, D. P., Pizzuti, A., Reiner, O., Richards, S., Victoria, M. F., Zhang, F. P. et al. (1991). Identification of a gene (FMR-1) containing a CGG repeat coincident with a breakpoint cluster region exhibiting length variation in fragile X syndrome. *Cell* **65**, 905-14.

Vianna-Morgante, A. M., Costa, S. S., Pares, A. S. and Verreschi, I. T. (1996). FRAXA premutation associated with premature ovarian failure. *Am J Med Genet* **64**, 373-5.

Visootsak, J., Warren, S. T., Anido, A. and Graham, J. M., Jr. (2005). Fragile X syndrome: an update and review for the primary pediatrician. *Clin Pediatr (Phila)* **44**, 371-81.

Wan, H. I., DiAntonio, A., Fetter, R. D., Bergstrom, K., Strauss, R. and Goodman, C. S. (2000a). Highwire regulates synaptic growth in Drosophila. *Neuron* **26**, 313-29.

Wan, L., Dockendorff, T. C., Jongens, T. A. and Dreyfuss, G. (2000b). Characterization of dFMR1, a Drosophila melanogaster homolog of the fragile X mental retardation protein. *Mol Cell Biol* **20**, 8536-47.

Wang, H., Dictenberg, J. B., Ku, L., Li, W., Bassell, G. J. and Feng, Y. (2008a). Dynamic association of the fragile X mental retardation protein as a messenger ribonucleoprotein between microtubules and polyribosomes. *Mol Biol Cell* **19**, 105-14.

Wang, N. J., Parokonny, A. S., Thatcher, K. N., Driscoll, J., Malone, B. M., Dorrani, N., Sigman, M., LaSalle, J. M. and Schanen, N. C. (2008b). Multiple forms of atypical rearrangements generating supernumerary derivative chromosome 15. *BMC Genet* **9**, 2.

Weiler, I. J., Irwin, S. A., Klintsova, A. Y., Spencer, C. M., Brazelton, A. D., Miyashiro, K., Comery, T. A., Patel, B., Eberwine, J. and Greenough, W. T. (1997). Fragile X mental retardation protein is translated near synapses in response to neurotransmitter activation. *Proc Natl Acad Sci U S A* **94**, 5395-400.

Weiskop, S., Richdale, A. and Matthews, J. (2005). Behavioural treatment to reduce sleep problems in children with autism or fragile X syndrome. *Dev Med Child Neurol* **47**, 94-104.

Wilson, B. M. and Cox, C. L. (2007). Absence of metabotropic glutamate receptor-mediated plasticity in the neocortex of fragile X mice. *Proc Natl Acad Sci U S A* **104**, 2454-9.

Wohrle, D. and Steinbach, P. (1991). Fragile X expression and X inactivation. II. The fragile site at Xq27.3 has a basic function in the pathogenesis of fragile X-linked mental retardation. *Hum Genet* **87**, 421-4.

Xie, W., Dolzhanskaya, N., LaFauci, G., Dobkin, C. and Denman, R. B. (2009). Tissue and developmental regulation of fragile X mental retardation 1 exon 12 and 15 isoforms. *Neurobiol Dis* **35**, 52-62.

Xu, K., Bogert, B. A., Li, W., Su, K., Lee, A. and Gao, F. B. (2004). The fragile X-related gene affects the crawling behavior of Drosophila larvae by regulating the mRNA level of the DEG/ENaC protein pickpocket1. *Curr Biol* **14**, 1025-34.

Yan, Q. J., Rammal, M., Tranfaglia, M. and Bauchwitz, R. P. (2005). Suppression of two major Fragile X Syndrome mouse model phenotypes by the mGluR5 antagonist MPEP. *Neuropharmacology* **49**, 1053-66.

Yang, Y., Xu, S., Xia, L., Wang, J., Wen, S., Jin, P. and Chen, D. (2009). The bantam microRNA is associated with drosophila fragile X mental retardation protein and regulates the fate of germline stem cells. *PLoS Genet* **5**, e1000444.

Yu, S., Mulley, J., Loesch, D., Turner, G., Donnelly, A., Gedeon, A., Hillen, D., Kremer, E., Lynch, M., Pritchard, M. et al. (1992). Fragile-X syndrome: unique genetics of the heritable unstable element. *Am J Hum Genet* **50**, 968-80.

Zalfa, F., Achsel, T. and Bagni, C. (2006). mRNPs, polysomes or granules: FMRP in neuronal protein synthesis. *Curr Opin Neurobiol* **16**, 265-9.

Zalfa, F., Adinolfi, S., Napoli, I., Kuhn-Holsken, E., Urlaub, H., Achsel, T., Pastore, A. and Bagni, C. (2005). Fragile X mental retardation protein (FMRP) binds specifically to the brain cytoplasmic RNAs BC1/BC200 via a novel RNA-binding motif. *J Biol Chem* **280**, 33403-10.

Zalfa, F., Giorgi, M., Primerano, B., Moro, A., Di Penta, A., Reis, S., Oostra, B. and Bagni, C. (2003). The fragile X syndrome protein FMRP associates with BC1 RNA and regulates the translation of specific mRNAs at synapses. *Cell* **112**, 317-27.

Zanotti, K. J., Lackey, P. E., Evans, G. L. and Mihailescu, M. R. (2006). Thermodynamics of the fragile X mental retardation protein RGG box interactions with G quartet forming RNA. *Biochemistry* **45**, 8319-30.

Zhang, H. L., Eom, T., Oleynikov, Y., Shenoy, S. M., Liebelt, D. A., Dictenberg, J. B., Singer, R. H. and Bassell, G. J. (2001a). Neurotrophin-induced transport of a beta-actin mRNP complex increases beta-actin levels and stimulates growth cone motility. *Neuron* **31**, 261-75.

Zhang, J., Fang, Z., Jud, C., Vansteensel, M. J., Kaasik, K., Lee, C. C., Albrecht, U., Tamanini, F., Meijer, J. H., Oostra, B. A. et al. (2008). Fragile X-related proteins regulate mammalian circadian behavioral rhythms. *Am J Hum Genet* **83**, 43-52.

Zhang, J., Hou, L., Klann, E. and Nelson, D. L. (2009). Altered hippocampal synaptic plasticity in the FMR1 gene family knockout mouse models. *J Neurophysiol* **101**, 2572-80.

Zhang, Y., O'Connor, J. P., Siomi, M. C., Srinivasan, S., Dutra, A., Nussbaum, R. L. and Dreyfuss, G. (1995). The fragile X mental retardation syndrome protein interacts with novel homologs FXR1 and FXR2. *Embo J* **14**, 5358-66.

Zhang, Y. Q., Bailey, A. M., Matthies, H. J., Renden, R. B., Smith, M. A., Speese, S. D., Rubin, G. M. and Broadie, K. (2001b). Drosophila fragile X-related gene regulates the MAP1B homolog Futsch to control synaptic structure and function. *Cell* **107**, 591-603.

Zhang, Y. Q. and Broadie, K. (2005). Fathoming fragile X in fruit flies. *Trends Genet* **21**, 37-45.

Zhang, Y. Q., Friedman, D. B., Wang, Z., Woodruff, E., 3rd, Pan, L., O'Donnell, J. and Broadie, K. (2005). Protein expression profiling of the drosophila fragile X mutant brain reveals up-regulation of monoamine synthesis. *Mol Cell Proteomics* **4**, 278-90.

Zhang, Y. Q., Matthies, H. J., Mancuso, J., Andrews, H. K., Woodruff, E., 3rd, Friedman, D. and Broadie, K. (2004). The Drosophila fragile X-related gene regulates axoneme differentiation during spermatogenesis. *Dev Biol* **270**, 290-307.

Zordan, M. A., Cisotto, P., Benna, C., Agostino, A., Rizzo, G., Piccin, A., Pegoraro, M., Sandrelli, F., Perini, G., Tognon, G. et al. (2006). Post-transcriptional silencing and functional characterization of the Drosophila melanogaster homolog of human Surf1. *Genetics* **172**, 229-41.

Zou, K., Liu, J., Zhu, N., Lin, J., Liang, Q., Brown, W. T., Shen, Y. and Zhong, N. (2008). Identification of FMRP-associated mRNAs using yeast three-hybrid system. *Am J Med Genet B Neuropsychiatr Genet* **147B**, 769-77.